EMPIRICAL MODELING AND SIMULATION OF EDGEWATER CUSPING AND CONING

A Dissertation

by

KOLAWOLE BABAJIDE AYENI

Submitted to the Office of Graduate Studies of
Texas A&M University
in partial fulfillment of the requirements for the degree of

DOCTOR OF PHILOSOPHY

May 2008

Major Subject: Petroleum Engineering

EMPIRICAL MODELING AND SIMULATION OF EDGEWATER CUSPING AND CONING

A Dissertation

by

KOLAWOLE BABAJIDE AYENI

Submitted to the Office of Graduate Studies of
Texas A&M University
in partial fulfillment of the requirements for the degree of

DOCTOR OF PHILOSOPHY

Approved by:

Chair of Committee,	Robert A. Wattenbarger
Committee Members,	Mark Burris
	Christine Ehlig-Economides
	Bryan Maggard
Head of Department,	Steve Holditch

May 2008

Major Subject: Petroleum Engineering

ABSTRACT

Empirical Modeling and Simulation of Edgewater Cusping and Coning.

(May 2008)

Kolawole Babajide Ayeni, B.S., University of Ibadan, Nigeria;

M.S., University of Oklahoma

Chair of Advisory Committee: Dr. Robert Wattenbarger

In many cases, it is important to predict water production performance of oil wells early in, or maybe before, their production life. In as much as oil field water is important for pressure maintenance purposes and displacement of oil towards the perforation of the producing well, excessive water production leads to increased cost. In the case when no provision is made, it represents a significant liability. The case considered here is a well producing from a monocline with an edge-water aquifer. Although such problems can be computed with reservoir simulation, the objective of this work was to develop an empirical method of making water production predictions.

The reservoir model was described as a single well producing from the top of a monocline drainage block with water drive from an infinite-acting aquifer. During the reservoir simulation runs, water would cusp and cone into the well, increasing water production and decreasing oil production. A number of simulation runs were made, varying eleven model variables. Typical model variables include dip angle, formation thickness and production rate. For each run a modified Addington-style plot was made.

The relationship between each model parameter and three graphical variables was used to develop the set of empirical correlations. The empirical correlations developed were integrated with some derived equations that relate important reservoir parameters and incorporated into a computer program.

The developed correlations and program can be used to carry out sensitivity analysis to evaluate various scenarios at the early planning stages when available reservoir data are limited. This gives a quick and easy method for forecasting production performance with an active edge-water drive. Furthermore, the approach developed in the research can be applied to other water production problems in other fields/reservoirs. The developed program was validated and used to evaluate synthetic and field cases. Overall, a good match was achieved.

DEDICATION

This Dissertation is dedicated to the Almighty God, for the love, wisdom, and protection he has granted me up until this moment in my life. It is dedicated to my loving, caring, and supportive family and friends, for all their prayers and support needed to complete this work.

ACKNOWLEDGEMENTS

The author wishes to express his sincere gratitude and appreciation to the following people who greatly contributed in no small measure to this work: Dr. Robert Wattenbarger, Professor of Petroleum Engineering, who served as the chair of my graduate committee. His patience, dedication and support guided me to the completion of this work. It has being a real pleasure and privilege to work under such supervision. I also wish to thank Dr. Christine Ehlig-Economides, Dr. Bryan Maggard and Dr. Mark Burris, for their active contribution.

Thanks to the Harold Vance Department of Petroleum Engineering for financial support in the form of assistantship. My sincere regards to all my professors and other members of staff of the school for their dedication to duty and willingness to assist at all times.

I am also grateful to my colleagues and friends who offered help while the work lasted and to many who were a source of blessing to me through my stay in College Station: Omole, KP Ojo, Segun, Efe, Deji Nuc, Naga, Oyerokun, Buki, Jerome, Ajayi family and others whom space will not permit me to mention.

Finally, I am eternally grateful to God the giver of life who has kept me thus far.

TABLE OF CONTENTS

Page

ABSTRACT iii

DEDICATION v

ACKNOWLEDGEMENTS vi

TABLE OF CONTENTS vii

LIST OF FIGURES x

LIST OF TABLES xiv

CHAPTER

I INTRODUCTION 1

- Problem Description 1
- Value to Industry 2
- Objective and Procedure 3
- Organization of This Dissertation 4

II LITERATURE REVIEW 6

- Introduction 6
- Steady State Solutions 6
- Unsteady State Solutions 7
- Critical Rate Solutions 7
- Water Breakthrough Time Prediction 11
- Water-Oil Ratio after Water Breakthrough 14
- Dipping Reservoirs 17

III ASPECTS OF WATER ENCROACHMENT 20

- Overview 20
- Mechanics of Fluid Displacement 20
- Reservoir Flow Forces 26
- Summary 28

CHAPTER Page

IV EDGEWATER CUSPING & CONING MODEL DEVELOPMENT 29

Overview 29
Model Assumptions 29
Model Description 30
Aquifer Modeling 34
Quiescence 35
Pseudo Capillary Pressure 36
Stratified Flow Model 37
Modeling Vertical Heterogeneity 38
Relative Permeability Characterization 40
Plotting Style 43

V DEVELOPMENT OF EMPIRICAL CORRELATIONS 47

Overview 47
Model Parameters 47
Sensitivity of Model Parameters 49
Generalized Correlations and Parameter Groups 71
Parameter Group Experimental Range 72
Basic Equations 74
Summary 76

VI COMPUTER PROGRAM AND APPLICATION 77

Overview 77
Program Layout 79
Program Description 80
Program Calculation Procedure 82
Model Validation 83
Application and Prediction – Synthetic Case 93
Field Case Application 99
Chapter Summary 101

VII CONCLUSIONS AND RECOMMENDATIONS 102

Conclusions 102
Recommendations for Future Work 104

Page

NOMENCLATURE 105
REFERENCES 108
APPENDIX A 118
APPENDIX B 121
APPENDIX C 123
APPENDIX D 125
APPENDIX E 128
APPENDIX F 132
VITA 140

LIST OF FIGURES

FIGURE Page

3.1 Stable: G>M-1; M>1, $\beta < \theta$ 21

3.2 Stable: G>M-1; M<1, $\beta > \theta$ 22

3.3 Unstable: G<M-1 23

3.4 Water Coning 25

3.5 Aerial View Showing Water Cusping 26

4.1 Oil-Water Front with No Modification 31

4.2 Oil-Water Front with the Use of Eclipse Quiescence Option and Pseudo Capillary Pressure 32

4.3 Oil-Water Front with the Use of Quiescence, Pseudo Capillary Pressure and Pseudo Relative Permeability 32

4.4 Side View of Simulation Model at Water Breakthrough Showing Water Coning into the Perforations 33

4.5 Top View of Simulation Model at Water Breakthrough Showing Water Cusping Towards the Well for Left Half of the Simulation Model 33

4.6 Stratified Reservoir Model 37

4.7 Comparison of Pseudo Relative Permeability Curve with With Its Corresponding Rock Curve 40

4.8 Probability Density Function Plot - Approximating Log-normal Distribution with a Triangular Distribution 42

4.9 Addington Log (GOR) vs. h_{ap} Relationship 43

4.10 Yang-Wattenbarger Method 44

4.11 Simulation Results for Different Mobility Ratios, M, Using the Yang-Wattenbarger Method of Adding a Constant 0.02 to WOR 46

FIGURE Page

4.12 Simulation Results From Fig.4.11 Using the New Method, with (WOR+C)/C as y Axis. Note the Horizontal Asymptote of 1 and All Lines are Straight 46

5.1 Top and Side View Sketch of Model at Initial Conditions 48

5.2 Sketch of the Tank or Material Balance Model Showing Relationship between N_p (Simulation Model) and h_{bp} (Material Balance Model) 48

5.3a Effect of Total Liquid Flow Rate – Log (WOR+C)/C vs. h_{bp} 51

5.3b Effect of Total Liquid Flow Rate – WOR vs. N_p/N 52

5.3c Incremental Ultimate Recovery– WOR vs. N_p/N 54

5.4 Rate Sensitivity 54

5.5a Effect of End Point Mobility Ratio – Log (WOR+C)/C vs. h_{bp} 55

5.5b Effect of End Point Mobility Ratio – WOR vs. N_p/N 56

5.6a Effect of Horizontal Permeability – Log (WOR+C)/C vs. h_{bp} 57

5.6b Effect of Horizontal Permeability – WOR vs. N_p/N 57

5.7a Effect of Vertical Permeability – Log (WOR+C)/C vs. h_{bp} 58

5.7b Effect of Vertical Permeability – WOR vs. N_p/N 59

5.8a Effect of Perforation Thickness – Log (WOR+C)/C vs. h_{bp} 60

5.8b Effect of Perforation Thickness – WOR vs. N_p/N 60

5.9a Effect of Water-Oil Gravity Gradient – Log (WOR+C)/C vs. h_{bp} 61

5.9b Effect of Water-Oil Gravity Gradient – WOR vs. N_p/N 62

5.10a Effect of k_{ml}/k_{max} Ratio – Log (WOR+C)/C vs. h_{bp} 63

5.10b Effect of k_{ml}/k_{max} Ratio – WOR vs. N_p/N 63

FIGURE Page

5.11a Effect of Reservoir Length – Log (WOR+C)/C vs. h_{bp} 64

5.11b Effect of Reservoir Length – WOR vs. N_p/N 65

5.12a Effect of Formation Thickness – Log (WOR+C)/C vs. h_{bp} 66

5.12b Effect of Formation Thickness – WOR vs. N_p/N 66

5.13a Effect of Dip Angle – Log (WOR+C)/C vs. h_{bp} 67

5.13b Effect of Dip Angle – WOR vs. N_p/N 68

5.13c WOR vs. Time - Dip Angle 68

5.14a Effect of Vertical Distance – Log (WOR+C)/C vs. h_{bp} 69

5.14b Effect of Vertical Distance – WOR vs. N_p/N 70

5.14c WOR vs. Time – Vertical Distance 70

5.15 Comparison of h_{wb} Observed and h_{wb} Obtained From Eq. 5.4
Within the Experimental Range 73

5.16 Comparison of m Observed and m Obtained From Eq. 5.5
Within the Experimental Range 73

5.17 Comparison of C Observed and C Obtained From Eq. 5.6
Within the Experimental Range 74

6.1 Edgewater Program Front Page 78

6.2 Edgewater Program Flow Chart 79

6.3 Input Form 81

6.4 Total Liquid Flow Rate Match 84

6.5 End Point Mobility Ratio Match 85

6.6 Horizontal Permeability Match 86

6.7 Vertical Permeability Match 87

FIGURE Page

6.8 Perforation Thickness Match 88

6.9 Water-Oil Gravity Gradient Match 89

6.10 k_{ml}/k_{max} Match 89

6.11 Reservoir Length Match.. 90

6.12 Formation Thickness Match... 91

6.13 Dip Angle Match.. 92

6.14 Vertical Distance Match... 93

6.15 Oil Rate Match and Prediction-Simulation and Correlation Comparison.. 95

6.16 Water Rate Match and Prediction-Simulation and Correlation Comparison 95

6.17 WOR Match and Prediction-Simulation and Correlation Comparison...... 96

6.18 Water-Cut Match and Prediction-Simulation and Correlation Comparison 96

6.19 Cumulative Oil Production Match and Prediction-Simulation and Correlation Comparison 97

6.20 Rate Change before Water Breakthrough 98

6.21 Rate Change after Water Breakthrough 99

6.22 Field Plot Match.. 101

LIST OF TABLES

TABLE Page

5.1 Base Case Model Parameters 50

5.2 Experimental Range 50

6.1 Synthetic Case Model Parameters 94

6.2 Field Data Model Parameters 100

CHAPTER I

INTRODUCTION

Problem Description

A major problem in hydrocarbon depletion is the accompanying water production. Water production, especially in a deep offshore aquifer driven reservoir, is inevitable. Water production may come in the form of a tongue, cone, cusp or a combination of all depending on the location, magnitude and direction of water movement. Some of the drawbacks include decrease in oil flow rate, increase in the volume of water to be handled thereby increasing the cost of surface installations, reduced efficiency in the depletion mechanism, increase in water disposal cost because produced water is often corrosive, early abandonment of affected well and loss of field total overall recovery.

The situation is not different in a monocline reservoir. Edgewater cusping and coning presents huge challenges especially when it is unanticipated. Edgewater cusping and coning is different from bottom water coning because water encroaches in a sloping bed. Some of the challenges encountered in a monocline reservoir include difficulty in predicting water breakthrough time and Water-oil ratio (WOR) performance after breakthrough.

Most of the work related to water production in oil wells available in the literature deals with bottom water coning. This study focuses on edgewater cusping and

---

This dissertation follows the style of *Society of Petroleum Engineers Journal*.

coning behavior in a deep offshore monocline reservoir with strong aquifer support. The approach employed in this study is to construct a model and perform an extensive parameter study using reservoir simulation. The research modifies the Addington/Yang[1,2] procedure and also introduces a new plotting method. The resulting correlations obtained are coupled with the derived equations to obtain a model for describing edgewater cusping performance. The emphasis was on breakthrough time prediction and post-breakthrough performance because of their practical application.

It is also important to distinguish between coning and cusping. Coning of water and/or gas in an oil well or water in a gas well is the phenomenon related to the vertical movement of water from the underlying water zone or gas from the overlying gas zone towards the completion interval of the production well[3]. Cusping[4] of water is the lateral breakthrough of water from a down-dip aquifer.

Value to Industry

During the well planning stage, the reservoir engineer wants to know the maximum oil production rate at which a well can be produced without concurrent production of the displacing phase. This is referred to as the critical rate. If economic conditions dictate production above this 'critical rate', the engineer wants to know two additional things: time of water breakthrough and WOR following breakthrough. At this stage, the available reservoir parameters or data are at a minimum and the dollar value of an accurate forecast is critical and at the highest.

The importance of a simple predictive tool at this stage of field development cannot be over emphasized. The objective is to be able to make an accurate forecast when we have little data. This stresses the benefits of a predictive tool that can be used to carry out sensitivity analysis to evaluate various scenarios. For the current problem encountered by the operator/research sponsor, the predictive tool can explain the early water breakthrough; give guidance regarding proposed future wells and recommend optimum rates at the initial planning stage.

The goal of this research is to develop a simple and practical tool that will assist the reservoir/planning engineer to make an accurate forecast at the early planning stages when available reservoir data are limited. The developed correlation can be used to predict breakthrough time and WOR performance after water breakthrough. It will also permit preliminary studies without a full simulation. Furthermore, the developed correlation can be used as a planning tool for quick approximations, screening and comparison of alternatives.

Objectives and Procedure

The objectives of this research are:

(1) To present a new method for describing edgewater cusping and coning performance in a monocline reservoir with strong aquifer drive.

(2) To develop an empirical model that can predict water breakthrough time and WOR for new wells given available reservoir data.

(3) To develop an empirical model that can be used to match WOR for existing wells (calibrating parameters).

(4) To present a computer based program that incorporates the developed correlations and equations to determine WOR performance for vertical wells.

Reservoir simulation techniques are used in combination with analytical and field data to achieve our objectives.

Organization of this Dissertation

The study is divided into seven chapters. The outline and organization of this dissertation are as follows:

Chapter I presents an overview of the problem of edgewater cusping and coning and the challenges associated with the undesirable phenomena. The relevance of the research, approach, objectives and deliverables of the research are concisely stated.

Chapter II presents an extensive literature review describing the previous approach to cusping and coning problems. A review of some papers relevant to dipping reservoirs was carried out. Chapter III gives an overview of the various displacement mechanisms encountered in the displacement of one fluid by another fluid in a dipping reservoir.

Chapter IV gives a qualitative analysis of the various stages of the development of the simulation model. Chapter V discusses the development of the empirical correlations.

Chapter VI presents the computer program and application of the developed model to synthetic and field data. Chapter VII provides conclusions from this research work and recommendations for future research work.

CHAPTER II

LITERATURE REVIEW

Introduction

From an extensive literature review, the solution to the coning problem as been addressed along two main lines[5, 6]:

- Steady State Solutions
- Unsteady State Solutions

This chapter reviews the previous approach to cusping and coning problems in general.

Steady State Solutions

Most steady state solutions determine the critical oil flow rate which is defined as the maximum rate of oil production without concurrent production of the displacing phase by coning. A steady state condition is achieved when the outer drainage boundary is at a constant pressure. This makes the potential at the lateral boundary constant thereby creating a steady state flow condition. In this case, the critical coning rate obtained doesn't change with time or cumulative oil production.

The critical rate solution can be divided into 2 parts:

1. Analytical solution based on the equilibrium conditions of viscous and gravity forces.
2. Empirical correlations. This involves laboratory experiments and recently the use of numerical simulation.

Unsteady State Solutions

This category of solution uses numerical simulation to obtain correlations for break through time and post break through behavior. Here, a closed boundary problem is encountered. The critical rate obtained decreases with time or cumulative oil production. The approaches and solutions developed by Addington[1], and Yang-Wattenbarger[2] fall into this category.

Three parameters are used to characterize coning solutions: critical coning rate, water breakthrough time and WOR after water breakthrough.

Critical Rate Solutions

A number of methods have been developed for determining critical coning rate. The pioneering work was done by Muskat and Wyckoff[7]. They presented an approximate analytical solution by solving the gravity equilibrium equation for the total pressure drop using a graphical method to obtain the critical coning rate. Their assumption was based on single phase (oil) potential distribution around the well at steady state conditions whose solution is given by the solution of Laplace equation for incompressible fluid. It was also assumed that a uniform flux boundary condition exists at the well, giving a varying well potential with depth and the potential distribution in the oil phase is not influenced by the cone shape.

From the continuity equation and Darcy's law, the expression for critical coning rate was derived by Meyer and Garder.[8] They simplified the analytical derivation by assuming radial flow and the critical rate is determined when the water cone touches the bottom of the well.

Chaney, *et al*[9] and Chierici, *et al*[10] used potentiometric techniques to determine critical rate. Chaney *et al* determined the oil potential using both mathematical equations and potentiometric analyzer. They assumed that critical rate obtained for a given geometry, fluid and rock properties can be corrected for other fluid and rock properties as long as the geometry don't change. Following this assumption, they developed a set of curves for predicting critical coning rate for various lengths of perforations. The Chierici et al model included both gas and water coning. The results were presented in dimensionless graphs that take into account reservoir anisotropy.

Schols[11] derived an empirical relationship for the critical rate for water coning based on Experimental study using a Hele-shaw model.

Wheatley[12] determined critical oil production rate for a water coning problem in a partially penetrating oil well. The problem was formulated in terms of the fluid potential, Φ in the oil phase and the presence of the cone was taken into consideration in the problem formulation. A potential function for the radial flow problem was formulated with a set of boundary conditions. The Laplace equation was solved and the resulting function modified subject to the stated boundary conditions. The solution of the Laplace equation in terms of the steady state flow potential was used to obtain the dimensionless source strength q_D in terms of the position of the apex of the cone. An iterative algorithm is then used to solve the derived equations for the critical rate.

Arbabi and Fayers[13] examined the accuracies of various analytical equations for calculating critical coning rates in vertical wells and horizontal wells and found out that there were uncertainties by a factor of 20 in the results for horizontal wells. Five equations for evaluating critical cresting rates were applied to a horizontal well gas cresting problem. The results from the approximating equations were compared to results from numerical simulation to determine which of the methods were accurate. Comparison of critical rates between simulation and analytical solution for a vertical well at various completion penetration fractions revealed that the Wheatley analysis is the only vertical well coning prediction method with good accuracy for vertical wells. Thus, following Wheatley's approach for deriving the equations for vertical wells, a new semi-analytic solution for critical cresting rates for horizontal well was derived for investigating critical cresting rates for a horizontal well located at any depth or level in the reservoir. It was modeled as an infinite line sink thus the 3D flow problem was reduced to 2D flow geometry in Cartesian coordinate.

Hoyland et al[14] employed an analytical and simulation approach to predict critical oil rate for bottom water coning in an anisotropic, homogeneous formation with the well completed from the top of the formation. The analytical solution uses the general solution of the time independent diffusivity equation for compressible, single phase flow in the steady state limit with the replacement of Muskat's assumption of uniform flux at the well bore with that of an infinitely conductive well bore. The simulation approach was based on large number of simulation runs with more than 50 critical rates determined. The result of the analytical solution was presented as a plot of dimensionless critical rate q_{CD} vs. dimensionless r_D for five fractional well penetrations L_p/h_t. For the simulation, regression analysis was used to analyze the simulation runs. A relationship was derived for q_c for the isotropic reservoir case and for the anisotropic reservoir case. The simulation results could not be correlated into an equation but summarized in graphical form.

Giger[15] used the hodograph method to derive equations for the shape of the water cone. Water cresting problem in horizontal wells was solved analytically for lateral edge drive, gas-cap drive and bottom water drive. The critical flow rate for the three production mechanisms as a function of the coordinates was used to obtain the shape of the WOC.

Menouar and Hakim[16] used numerical approach to analyze water coning for vertical wells and water cresting for horizontal wells. A method to estimate critical rate was presented and the influence of some of the most relevant reservoir parameters on critical rate was investigated. The parameters include well length, mobility ratio, anisotropy ratio, well position and reservoir geometry. The solution developed by the authors was based on the observation of the variation of the saturation gradient in the reservoir. An expression that relates the saturation function f_s to water saturation at two coordinate points as a function of oil column thickness was written.

Kidder[17] determined the maximum water free production rate for the cusping problem by the solution of the free boundary problem using the methods of complex variable theory and the hodograph method. The dipping permeable stratum within which the flow of oil takes place is assumed to be of uniform thickness and sufficiently thin that the flow may be treated as a 2-D taking place in the plane of the dipping stratum.

Water Breakthrough Time Prediction

Most prediction methods for coning give a "critical rate" at which a stable cone can exist from the fluid contact to the nearest perforations. The theory is that, at rates below the critical rate, the cone will not reach the perforations and the well will produce the desired single phase. At rates equal to or greater than the critical rate, the second fluid will eventually be produced and will increase in amount with time. However, these theories based on critical rates do not predict when breakthrough will occur nor do they predict water/oil ratio or gas/oil ratio after breakthrough.

Sobocinski and Cornelius[18] developed a correlation for predicting water coning time based on laboratory experimental data and computer program results. The method is a correlation of dimensionless cone height, Z_D versus dimensionless time, t_D. It is based partly on experimental work done on a single sand–packed laboratory model and partly on results from a 2-D computer program for 2-phase, incompressible fluid flow. The groups were developed from the scaling criteria for the immiscible displacement of oil by water using the equations below to obtain the dimensionless groups

$$Z_D = \frac{0.00307 \Delta\rho k_h h h r}{\mu_o q_o B_o} \quad \text{.. (2.1)}$$

$$t_D = \frac{0.00137 \Delta\rho k_h (1 + M^{\alpha}) t}{\mu_o \phi h F_k} \quad \text{.. (2.2)}$$

Using the build-up and departure curves on the Z_D vs. t_D plot, coning situations can be predicted.

Bournazel and Jeanson[19] modified Sobocinski and Cornelius equation for the dimensionless height of the water cone with results from experimental research. A simple analytic equation was found that relates dimensionless height to dimensionless time.

$$t_D = \frac{Z_D}{3 - 0.7 Z_D} \quad \text{.... ....} \quad (2.3)$$

Thus, breakthrough time can be calculated with the equation above without using the plot Sobocinski and Cornelius proposed earlier.

Ozkan and Raghavan[20] investigated the behavior of water or a gas cone in a horizontal well and derived an approximate analytical equation to predict breakthrough time in horizontal wells. By assuming steady state flow, same mobility for oil and water, constant pressure at the water-oil interface etc and using dimensionless variables, the equation for calculating breakthrough time was derived to be:

$$t_{DBT} = \int_0^{z_D} \frac{dz_D}{(\partial \phi_D / \partial Z_D) r_D} = 0 \quad \text{...} \quad (2.4)$$

The dimensionless production rate q_D and time t_D are defined as:

$$q_D = \frac{q \mu_o B_o}{2\pi k r h^2 \Delta \rho g} \quad \text{...} \quad (2.5)$$

$$t_D = \frac{k_z \Delta \rho g t}{\phi \mu_o h} \quad \text{...} \quad (2.6)$$

The behavior of the cone was correlated as a function of dimensionless parameters when $r_{ed} \geq 3.3$ & $L_D \geq 2.3$.

Papatzacos[21] et al derived a semi-analytical solution for time development of a gas or water cone and of simultaneous gas and water cones in an anisotropic infinite reservoir with a horizontal well placed in the oil column. The solution was derived using the moving boundary method with gravity equilibrium assumed in the cones. A numerical simulation model was used to validate the accuracy of the semi-analytical solution. For the gas cone case, the semi-analytical results were presented as a single dimensionless curve (time to breakthrough versus rate). For the simultaneous gas and water-cone case, the results were given in 2D sets of curve – one for the optimum vertical well placement and one for the corresponding time to breakthrough as functions of rate with the density contrast as a parameter. For the single cone solution, the breakthrough time is given by:

$$\ln(t_{BtD}) = -1.7179 - 1.1633U + 0.16308U^2 - 0.046508U^3 \quad where U = \ln(\mathrm{q_D}) \qquad \text{…… (2.7)}$$

Zamonsky[22] et al used a numerical simulation model to study the behavior of water production as a function of reservoir parameters. The water cut versus time plot was the variable used for characterization. A database consisting of almost 20,000 cases was built. From analyzing the data, a formula for calculating break through time was proposed.

Water-Oil Ratio after Water Breakthrough

In addition to developing an equation to obtain breakthrough time, Bournazel and Jeanson[19] developed a correlation for the Water-Oil Ratio (WOR) evolution after breakthrough. They combined experimental correlations using dimensionless numbers with a simplified analytical approach based on the assumption that the front shape behaves like a current line in an equivalent model of different shape to determine WOR performance after breakthrough.

Chappelear and Hirasaki[23] developed a theoretical model that can be installed in a finite-difference reservoir simulator. The model was for oil-water coning in a partially perforated well. The derived coning model was expressed as an equation that relates the water cut, f_w, the average oil column thickness, h_o and the total rate q_t.

Addington[1] used a 2-D fully implicit radial simulator to model coning. The correlation developed by simulating numerous one well models at a constant total fluid production rate for a variety of well parameters can be used to predict critical coning rate and gas-oil ratio of a well after gas coning. The gas coning behavior was correlated to the average oil column height above the perforated interval of the well. Three regions were modeled around the well – the gas cap, the gas invaded region and the oil column. By writing an oil material balance around the 3 regions of the well, the average oil column height above the perforation was calculated. The results were represented by the plot of the log of the Gas liquid Ratio (GLR) vs. the average oil column height above perforations (h_{ap}). Therefore, it was observed that gas coning behavior of any well could be established if the GLR slope and the oil column height above the perforation at gas breakthrough are determined. Two generalized correlations were developed. The effects of the variables on h_{ap} and m were used to develop the correlations.

Kuo and DesBrisay[24] presented a simplified correlation that can be used to predict water cut performance. Using numerical simulation, the sensitivity of four reservoir parameters was investigated. Generalized correlations between water cut performance and these parameters were then developed by normalizing the simulation results using two dimensionless equations – dimensionless time and dimensionless water cut. The normalized results were plotted as dimensionless water cut versus dimensionless time, and a simple correlation was drawn to fit the data.

Lee and Tung[25] modeled the average cone development velocity which is the reciprocal of water breakthrough time. Correlations for water breakthrough time were first developed based on three key controlling parameters: q (flow rate), C_g (gravitational force due to density difference) and m (mobility ratio). Then the effects of aquifer thickness, h_a and perforation interval h_p were added to the correlations. Correlation for water cut prediction after water breakthrough was developed. A single functional form with an independent variable time and three coefficients was devised to represent water cut performance. The three coefficients are dependent on the controlling parameters.

Yang and Wattenbarger[2,5] developed a method suitable for either hand calculation or simulation to predict critical rate, breakthrough time and WOR after breakthrough in both vertical and horizontal wells. Following the Addington approach, a one well model was simulated at constant total production rate and a number of simulation runs were made to investigate coning performance at different reservoir and fluid properties for both vertical and horizontal wells. For each simulation run, a plot of WOR plus a constant C versus average oil column height below perforation h_{bp} was made on a semi-log scale from which the slope of the water-oil ratio plot m, and the breakthrough height h_{wb} was determined. Regression analysis was then used to define the relationship between m, $\mathrm{h_{wb}}$ and various reservoir and fluid properties. The procedure was followed and coning correlation for both vertical and horizontal wells was developed.

De Souza, Arbabi and Aziz[6,26] analyzed simulation runs coupled with appropriate set of dimensionless variables and obtained correlations for approximating breakthrough time, post breakthrough behavior, optimum grid, cumulative oil recovery, maximum rate and pseudo functions for horizontal wells.

Other authors have looked at coning from other perspectives[27-43]. In a bid to study water coning challenges in a bottom water drive reservoir, Kabir[44] et al used a single well model to study the various parameters influencing coning. Alternative completions using single and dual lateral wells and cone reversal techniques were also explored. The effect of grid refinement, size of drainage area, anisotropy was also studied. It was observed that k_v/k_h ratio is a very important parameter in coning assessment. Dual completion for cone reversal appears promising for thin pays, even in a favorable mobility situation.

Dipping Reservoirs

Displacement of a fluid by another fluid in a dipping reservoir creates an interface. The tilted interface problem is a fundamental reservoir engineering challenge. It defines the water under-running and gas over-running phenomena associated with water drives, gas drives and secondary recovery operations.

The first work on edgewater coning was carried out by Dietz[45]. He presented a theoretical approach to the problem of encroaching and by-passing edgewater using a 2-D mathematical analysis. Equations were derived to determine the value of the critical rate and to predict the development of a water tongue when the critical rate was exceeded.

Sheldon and Fayers[46] presented an approximate equation of motion to describe the behavior of the interface between two fluids of different physical properties when displacement occurs along a thin tilted bed. Conditions for which steady state solutions are valid and a transient solution were shown. The developed equations were applied to a favorable and unfavorable mobility ratio water drive problem to demonstrate the importance of mobility ratio in under-running and over-running situation.

The simulation of segregated flow poses significant problem with present black oil simulators because the thickness of transition zone between the oil and gas is generally thin compared with the dimensions of the grid blocks typically used in the solution.

Fayers and Muggeridge[47] extended Dietz equation to study the behavior of gravity tongues in slightly tilted reservoirs. The Dietz equation was modified by the addition of a curvature term to account for strongly unstable flow. The results obtained from the Dietz equation and modified Dietz equation were compared to an already established accurate procedure for solving the general 2D, 2-phase flow miscible displacement equation that incorporates flux corrected transport techniques. Both equations were used to investigate the importance of physical and numerical dispersion effects by simulating the vertical-section miscible experiments already reported in the literature. It was observed that the extended Dietz method compared well to the high resolution model. The limitation of the extended Dietz method was also stated.

Recently, numerical simulation models were used to study the effect of water invasion in edgewater reservoirs. Hernandez, Wojtanowicz and White[48] developed a regression model that was used to evaluate the effect of anisotropy on water invasion and determine the percentage of oil by-passed at abandonment conditions. Inspectional analysis was used to select a complete set of dimensionless groups for 3D immiscible displacement of oil by water in an anisotropic reservoir. The five dimensionless groups were then validated using numerical simulation. The relative effects of the five dimensionless groups on the oil by-passed at well abandonment were analyzed using a statistical package. The selected dimensionless groups were used to develop the regression model.

Hernandez and Wojtanowicz[49] used a single well model to study the effect of oil viscosity, production rate, absolute permeability, vertical to horizontal permeability ratio, dip angle, oil density and well penetration so as to understand the mechanisms that control the bypassing of oil in water drive reservoirs. They developed a correlation to calculate the amount of un-recovered oil and to estimate breakthrough time.

In an attempt to identify causes of un-recovered oil in reservoir systems under edge water and bottom water drives, Hernandez and Wojtanowicz[50] compared breakthrough time, water cut and by-passed oil profile results from the numerical model to analytical models. They concluded that in most of the unstable displacement cases, the analytical models under estimated the water breakthrough time and over estimated the volume of by-passed oil. For stable displacement, Dake's method was accurate predicting the water breakthrough time, water cut and by-passed oil profiles. It was also observed that low dip angles, high production rates and high oil viscosities are the flow conditions that stimulate water under running and oil by-passing. Combined effect of gravity under-running and coning in dipping systems with edgewater systems could leave up to 70% of the mobile oil volume in the reservoir and water coning in bottom water could leave up to 93% of the mobile oil volume in the reservoir.

This work presents a new approach/solution to edgewater production challenges in a monocline reservoir. A single well, 3-D numerical simulation model was used to investigate coning and cusping performance at different reservoir and fluid properties. This work includes the derivation of the equation for calculating the height of the water invaded zone for each time step, the procedure for the determination of the correlation and the determination of the height at water breakthrough, slope of the WOR curve and the constant used. The work also includes the computer program that incorporates the correlations and equations.

CHAPTER III

ASPECTS OF WATER ENCROACHMENT

Overview

Different mechanisms take place in the movement of the oil-water interface during oil production. This chapter describes the various types of water encroachment mechanisms interacting in the reservoir during hydrocarbon depletion.

Mechanics of Fluid Displacement

Diffuse Flow Condition

The diffuse flow condition[51] implies that fluid saturation at any point is uniformly distributed with respect to thickness. Diffuse flow is favored under the following conditions:

- Displacement at low injection rates in reservoirs for which the capillary transition zone greatly exceeds the reservoir thickness and the vertical equilibrium condition applies.
- Displacement occurs at very high injection rates so that the effects of capillary and gravity forces are negligible. The vertical equilibrium condition is not satisfied.

The diffuse flow condition permits displacement to be described mathematically in one dimension.

Segregated Flow Condition

The segregated flow condition implies that there is a distinct interface with negligible transition zone. It also assumes that displacement is governed by vertical equilibrium. Segregated flow is a two dimensional problem unlike diffuse flow. It can be reduced to a 1-D problem by averaging the saturations and saturation dependent relative permeability over the reservoir thickness.

There are stable and unstable displacement conditions under segregated flow conditions. Stable and unstable displacement conditions can be quantified by the dimensionless gravity number *G* which is the ratio of gravity forces to viscous forces, end point mobility ratio *M* and the angle between the fluids interface β. The interaction of these three variables determines the stability of the displacement.

Three cases were considered [45, 51]. Fig. 3.1 represents a stable displacement when the gravity number is greater than the end point mobility ratio i.e. $G>M-1$, the end point

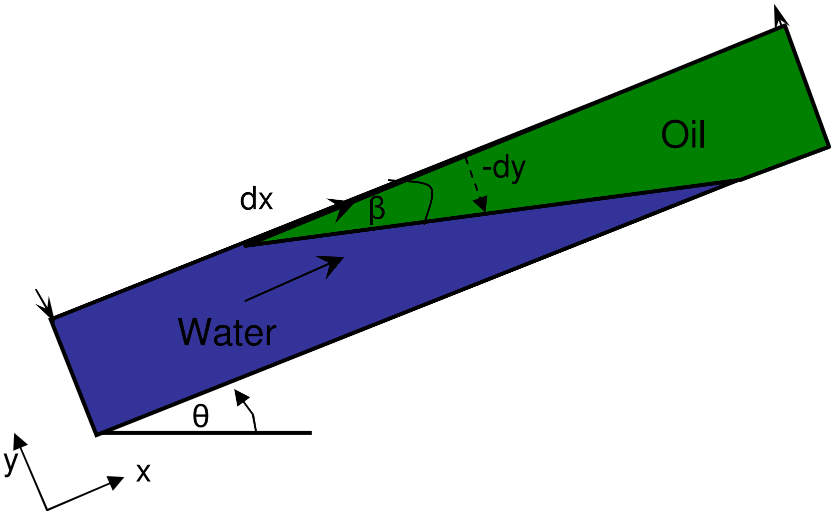

Fig. 3.1-Stable: $G>M-1$; $M>1$, $\beta < \theta$.

mobility ratio is greater than 1 (M>1) and the angle between the fluid interface β is less than the dip angle θ.

Fig. 3.2 shows another condition when stable displacement can be encountered during segregated flow conditions. The gravity number is still greater than M-1 while the end point mobility ratio is less than 1 and the angle between the fluid interface β is greater than the dip angle θ.

The two conditions above can be satisfied at low displacement rate when gravity forces due to fluid density difference, maintains the interface to be horizontal.

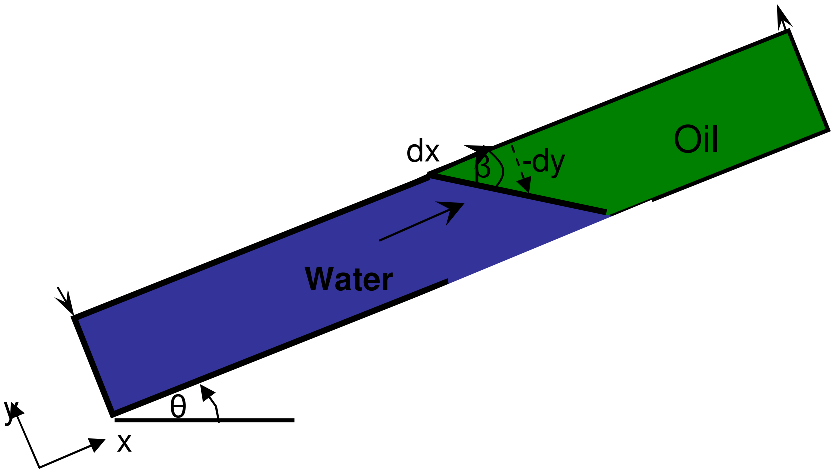

Fig. 3.2-Stable: G>M-1; M<1, β >θ.

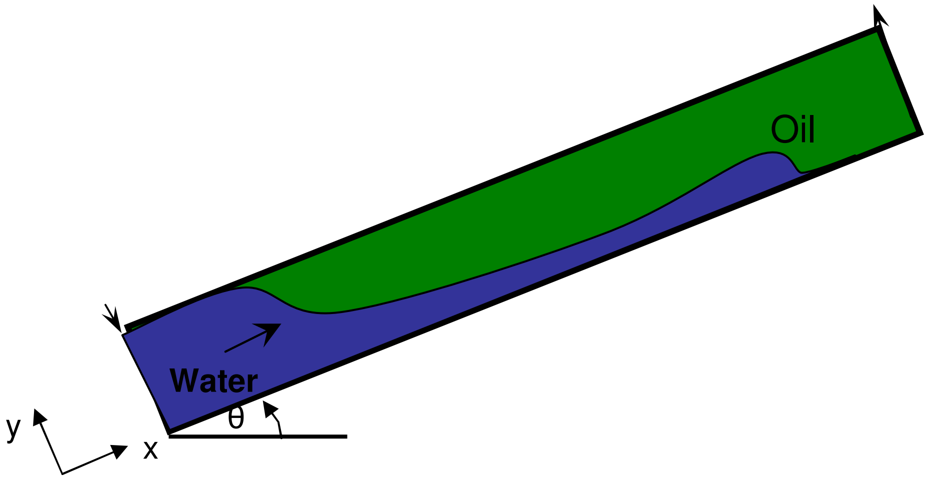

Fig. 3.3-Unstable: $G<M-1$.

Fig. 3.3 shows an unstable condition. Here, $G < M-1$. Water under-runs the oil in the form of a water tongue leading to premature water breakthrough.

Coning

Coning is the term used to describe the production of a usually unwanted second phase concurrently with a desired hydrocarbon phase. The term is referred to as coning in a vertical well because the shape of the interface resembles an upright (water coning) or inverted cone (gas coning) when the well produces the unwanted phase. In a horizontal well, the shape resembles a crest. Coning is determined by the interaction of two major forces (viscous and gravity) in the reservoir. Viscous forces due to pressure gradients caused by production from a well cause coning. The gravity force due to fluid density difference tends to retard water movement. When the viscous force is greater than the gravity force, the cone will advance further and ultimately breaks into the well.

Most prediction methods for coning estimate a “critical rate” at which a stable cone can exist from the fluid contact to the nearest perforations. Yang[5] presented a summary of equations for critical coning rate calculation. Critical rate is defined as the maximum flow rate without any gas and or water production. The theory is that, at rates below the critical rate, the cone will not reach the perforations and the well will produce the desired single phase. At rates equal to or greater than the critical rate, the second fluid will eventually be produced and will increase in amount with time. The critical rate method does not predict breakthrough time and WOR or GOR after breakthrough.

The estimated critical rate changes with time. It is only valid for a fixed distance between the fluid contact and the perforations because as production proceeds, the distance between the contact and the perforations decreases with time for a water coning case. Thus, the critical rate will tend to decrease with time, and the economics of a well with a tendency to cone will continue to deteriorate with time. Fig. 3.4 shows a three dimensional water coning example.

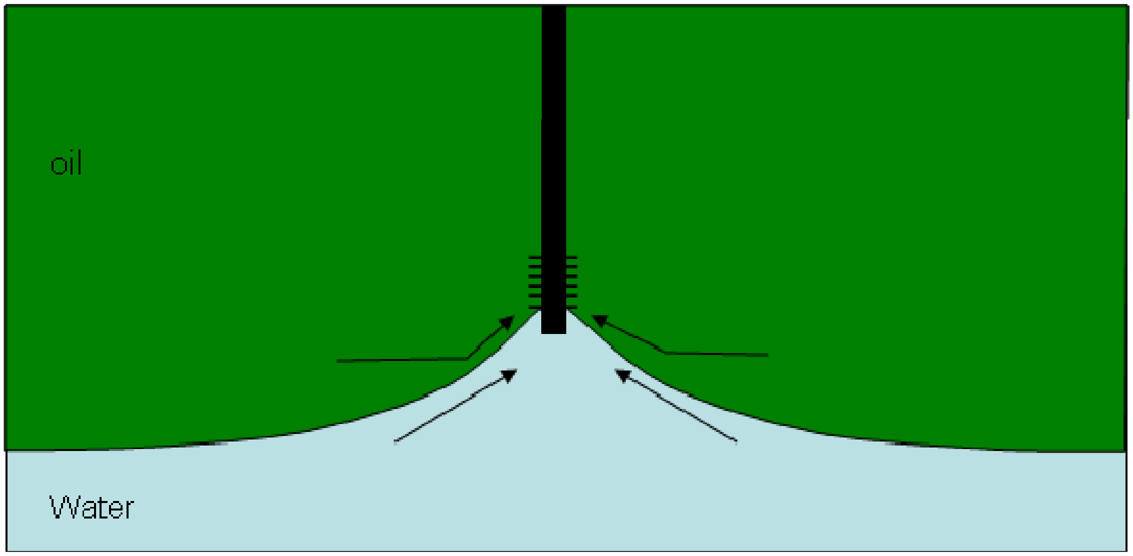

Fig. 3.4-Water Coning.

Cusping

Cusping[4] of water and/or gas in an oil well or water in a gas well is the lateral movement along a dipping reservoir of water from a down dip water zone or gas from an up dip gas zone towards a production well. Fig. 3.5 shows an aerial view of a water cusping phenomenon.

The following expression for cusping of water or gas in a 2-dimensional system (areal) was derived[4, 17].

$$\pi d_{CD} = (1+2q_{CD})\ln(1+2q_{CD}) - 2q_{CD}\ln 2q_{CD} \qquad (3.1)$$

Dimensionless distance from the well to the original contact is given by:

$$d_{CD} = \frac{2d_c}{w} \qquad (3.2)$$

For a given d_{CD}, the value of the dimensionless critical rate q_{CD} can be derived from equation 3.1. The critical oil rate $q_{sc,c}$ is given by:

$$q_{sc,c} = \frac{C_1 K_o h w \Delta\rho g \sin\alpha}{B_o \mu_o} q_{CD} \quad \text{..........} \quad (3.3)$$

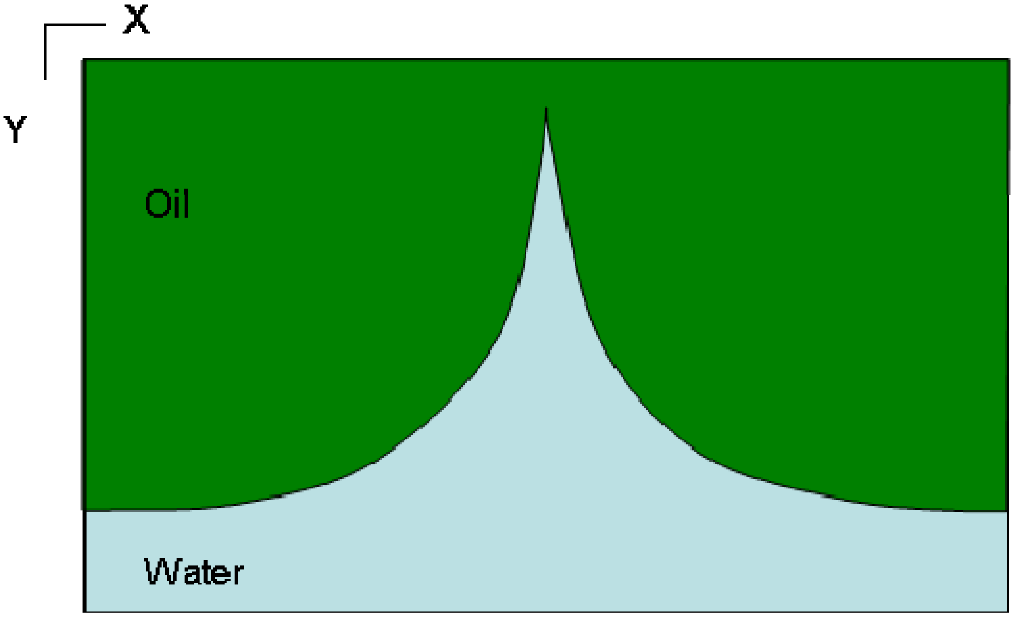

Fig. 3.5-Aerial View Showing Water Cusping.

Reservoir Flow Forces

Interaction of forces determines fluid flow in the reservoir. A combination of capillary, gravity and viscous forces affect fluid flow distribution around the wellbore. For coning problems, it's been observed that capillary forces usually have a negligible effect. Cusping and coning of water into the perforation of a producing well is caused by pressure gradients established around the wellbore by the production of fluids from the well. These pressure gradients can raise the water-oil contact near the well where gradients are most severe. Gravity forces that arise from fluid density-differences counterbalance the flowing pressure gradients and tend to keep the water out of the oil zone. Therefore, at any given time, there is balance between gravitational and viscous forces at points on and away from the completion interval. When the viscous force at the wellbore exceeds the gravitational force, a cusp and cone of water will ultimately break into the well to produce water along with the oil.

The effect of reservoir forces can be analyzed using the gravity number. The gravity number is defined as the ratio of gravity to viscous forces. Different authors have presented different forms of the gravity number[51, 52]. Shook[53] et al presented a list of various gravity number found in the literature. He observed that the equations were inconsistent due to lack of agreement about the number of dimensionless groups required to describe a specific result and a lack of consistency in the form of the groups.

Two approaches were used to obtain a representative gravity number. At very early times, the transient flow equation for under-saturated oil can be used to estimate the pressure drop due to viscous forces. The pressure drop obtained from simulation was compared to analytical equation to ensure accuracy. The pressure drop equations are given by:

$$p_i - p_{wf} = \Delta p_{viscous} = \frac{162.6 q\mu B}{kh}\left[\log(t) + \log\frac{k}{\phi\mu c_t r_w^{\,2}} - 3.23\right] \text{......................... (3.4)}$$

$$\Delta p_{Gravity} = \frac{\Delta\rho}{144} h_{bp} \text{ .... (3.5)}$$

Gravity number is a ratio of gravity forces to viscous forces. A gravity number of 0.12 was obtained after fifteen minutes of production. To obtain a more representative number, the pressure drop due to viscous forces at water breakthrough was used to estimate gravity number from simulation. Water breakthrough is defined as water-cut greater than 0.001. For this work, it is given by:

$$N_{Grav} = \frac{\Delta p_{Gravity}}{\Delta p_{viscous}} = \frac{\frac{\Delta \rho}{144} h_{bp}}{(p_i - p_{wf})_{BT}} \quad \ldots\ldots\ldots\ldots\ldots\ldots\ldots\ldots\ldots\ldots\ldots\ldots\ldots\ldots\ldots\ldots\ldots\ldots \text{(3.6)}$$

The difference between the initial pressure and the flowing bottom-hole pressure at water breakthrough $(p_i - p_{wf})_{BT}$ is obtained from simulation. The gravity number obtained for the base case is approximately 0.048. Gravity number range of 0.032 – 0.08 was obtained for the range of experimental investigation. Thus, the range of values used is viscous dominated.

The gravity number obtained explains the region of the experimental range of investigation. The gravity number is low i.e. viscous forces are greater compared to gravity forces. Thus, the insensitivity at higher rates is the result of low gravity numbers. Coning occurs when the gravity number is less than one. It is also important to note that the number changes as reservoir and fluid properties change.

Summary

This chapter reviews the various types of water encroachment mechanism interacting in the reservoir during hydrocarbon production. Reservoir forces play a huge role in fluid movement and this can be quantified using gravity number calculations.

CHAPTER IV

EDGEWATER CUSPING & CONING MODEL DEVELOPMENT

Overview

To enhance the proper understanding of a problem, models are created. The complexity of a problem can be analyzed by creating, verifying and modifying the model. A model is a representation containing the essential structure of some object or event. The representation could be physical (an architect's model of a building) or symbolic (a computer problem or a set of mathematical equations).

Different authors have used various approaches in their simulation model development[54-56]. This chapter gives a detailed breakdown of the procedure used to develop the simulation model for the edgewater coning/cusping phenomenon.

Model Assumptions

The assumptions listed below were employed in the simulation model development. This includes:

- Homogeneous media
- Constant porosity
- Anisotropic media $\frac{k_z}{k_x} = \frac{k_z}{k_y} = 0.1$
- Three dimensional flow
- Under-saturated reservoir ($S_g = 0$)
- Constant production rate

- Single well model with infinite acting properties
- Two – phase flow (oil-water)
- Specific set of rock-fluid and PVT data

Model Description

A single well, Cartesian model was developed using the Eclipse[57] commercial simulator. A 20° dipping, monocline reservoir was constructed with a computer program that calculates the tops for each grid dimension in the y-direction. This is imported to the data file. The production well was placed in the left most corner of the grid block. Data trick was employed and variable grid block spacing both in the x and y direction used. The block centered grid block approach is used.

Optimum gridblock size selection is important in numerical simulation[58,59]. Thus, it is important to test the accuracy of a grid using multiple simulation runs. This enables the determination of how the error varies because analytical determination of the amount of error from grid discretization is not feasible. By changing the grid dimensions in x, y & z directions choosing different time-steps and making successive runs, a 21x80x25 grid dimension was chosen when a convergence in water-cut match was achieved.

One of the objectives of the research is to model edgewater coning. The grid set up ensured that most of the water came from the edge. In the motion of the oil-water interface in a dipping reservoir, the two fluids are separated by a horizontal interface controlled by gravity. When production starts, the interface begins to move towards the well. For low flow rates, gravity forces tend to dominate the displacement and a stable interface occurs. When flow rates are high, the front becomes unstable and a water tongue develops from the bottom of the dipping structure. To ensure that the model correctly captures these effects, the use of the quiescence option in Eclipse, pseudo capillary pressure and Hearn relative permeability curves were employed in the model development. Fig 4.1 – 4.3 shows the importance of accurate modeling. The various stages are shown. Fig. 4.1 shows the shape of the interface without any modification.

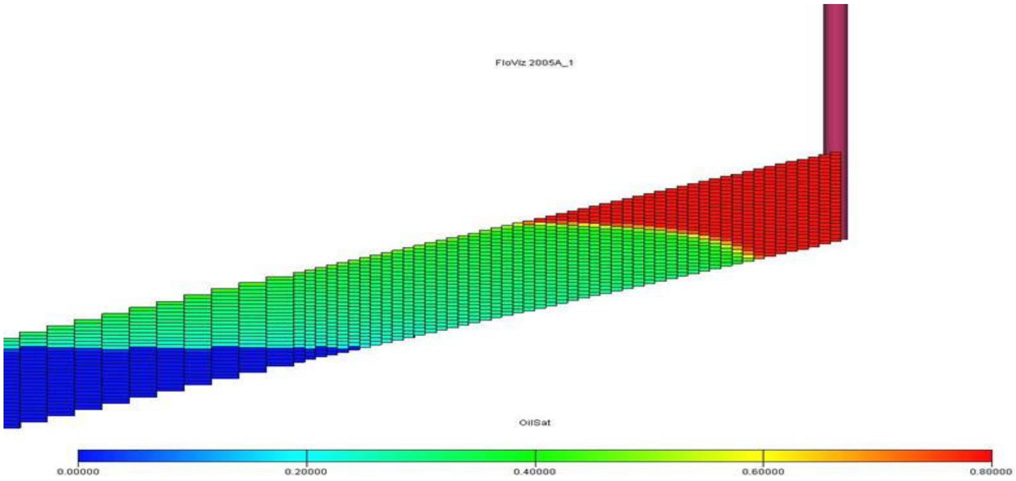

Fig. 4.1-Oil-Water Front with No Modification.

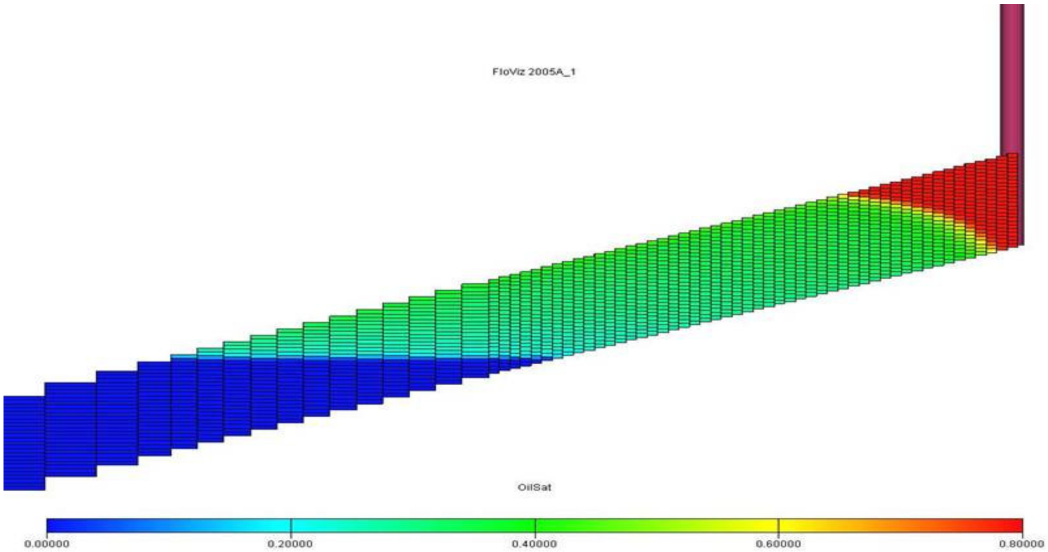
FloViz 2005A_1
OilSat
0.00000
0.20000
0.40000
0.60000
0.80000

Fig. 4.2-Oil-Water Front with the Use of Eclipse Quiescence Option and Pseudo Capillary Pressure.

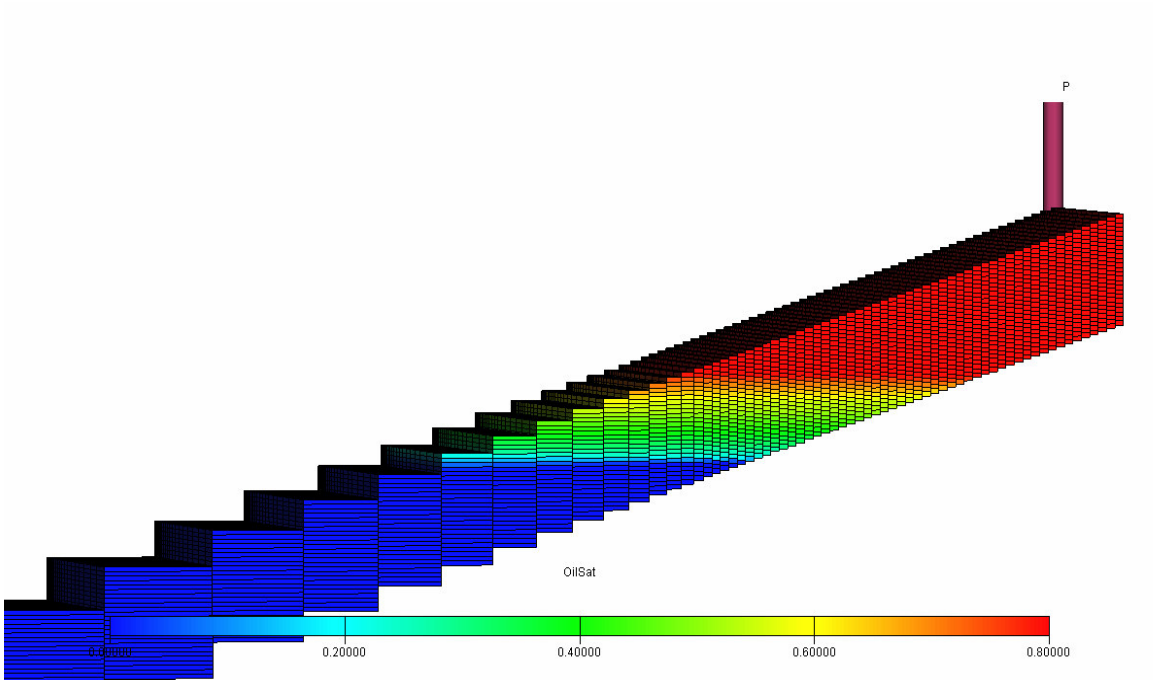
P
OilSat
0.00000
0.20000
0.40000
0.60000
0.80000

Fig. 4.3-Oil-Water Front with the Use of Quiescence, Pseudo Capillary Pressure, and Pseudo Relative Permeability.

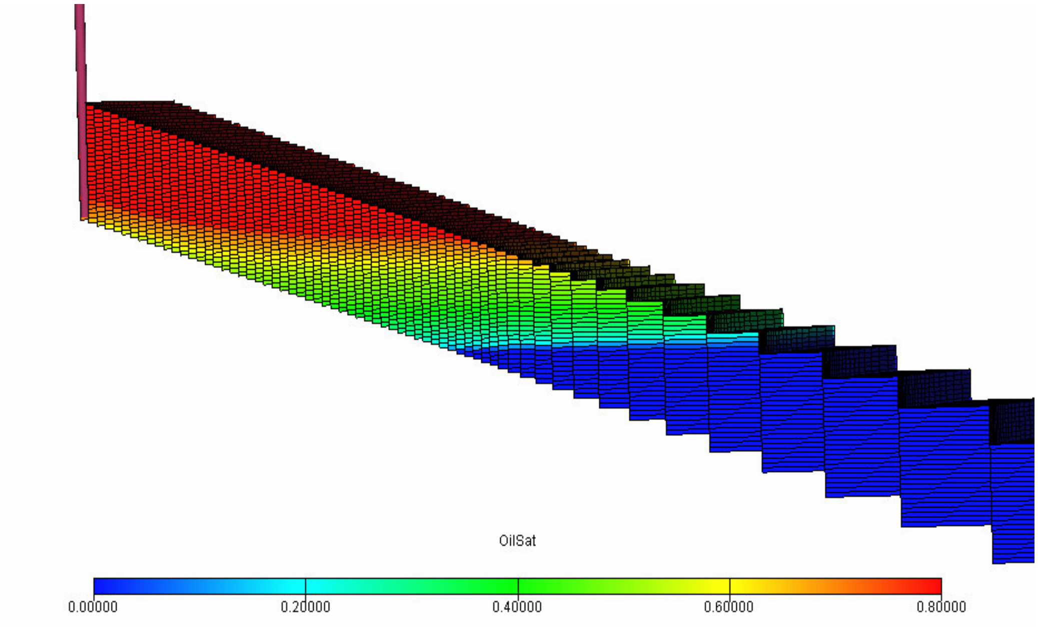
OilSat
0.00000
0.20000
0.40000
0.60000
0.80000

Fig. 4.4-Side View of Simulation Model at Water Breakthrough Showing Water Coning into the Perforations.

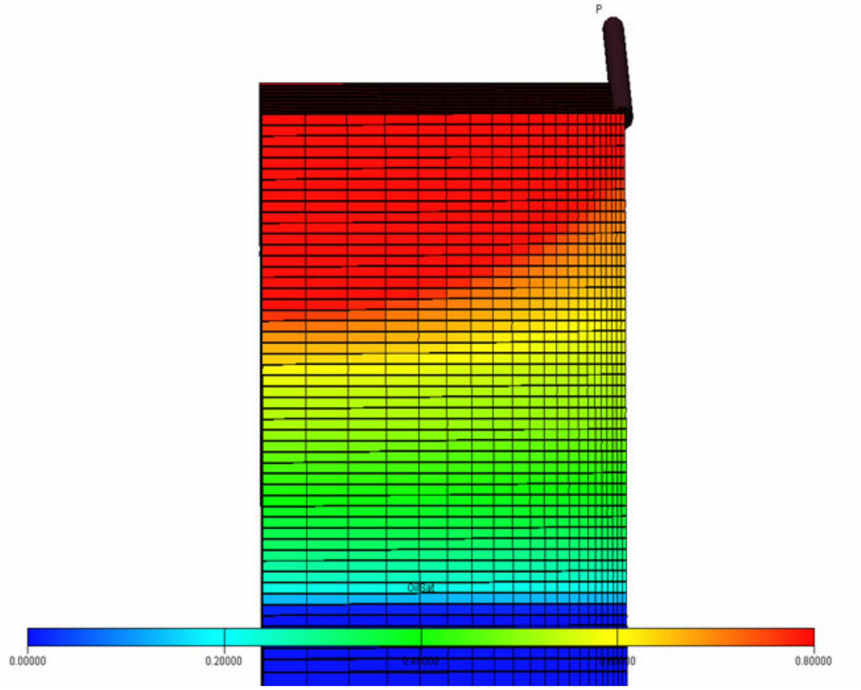
P
OilSat
0.00000
0.20000
0.40000
0.60000
0.80000

Fig. 4.5-Top View of Simulation Model at Water Breakthrough Showing Water Cusping Towards the Well for Left Half of the Simulation Model.

We can see from the first two figures that the shape of the oil-water contact bends as the interface moves. Furthermore, there was delayed water breakthrough which isn't representative of the actual situation. Fig.4.3 shows the effect of using the quiescence option, pseudo capillary pressure and Hearn relative permeability curves. Figs. 4.4 and 4.5 show water coning and cusping. The final model captured the various mechanisms modeled which includes coning, cusping and gravity under-running with early water breakthrough.

Aquifer Modeling

Aquifers supply additional energy to a connected reservoir in the form of water influx. It can be represented as a numerical aquifer (use of additional grid blocks) or analytical aquifers.[60,61] A disadvantage of analytical aquifers is that it does not properly model reservoir fluids flowing back to the aquifer. Use of additional grid blocks has the disadvantage of increasing the number of blocks which increases both the CPU time and storage. The commercial simulator supports radial aquifer. This presents us with limited choices as a radial aquifer is not appropriate for the problem being modeled. The option available is either to find a way to use a linear aquifer or add many grid block so that when the effect of pressure change is not felt at the reservoir boundary, the reservoir is infinite acting. The latter approach was taken. As a result, large grid blocks sizes were used in the water zone.

Quiescence

The use of this option[57]enables pressure modifications to achieve initial quiescence i.e. produce a true steady state solution. A redistribution of fluids takes place between grid blocks near the contacts when simulation begins with fine grid equilibration. If the redistribution of fluids produces a significant transient when the simulation is started, this can be overcome using the quiescence option. The quiescence option achieves hydrostatic equilibrium for flows of each phase. For the oil-water case, it modifies the initial (oil phase) pressure p and introduces cell dependent modifiers p_{MODW} to the water phase pressures such that

$$p_{wat} = p - P_{cow} + p_{MODW} \quad \text{...} \quad (4.1)$$

The phase pressure modifications p_{MODW} are determined to achieve quiescence at initial conditions and are then applied throughout the simulation. The quiescent pressure is constructed from the initial tables of phase pressure versus depth. The oil phase pressure in each grid block center, p is modified by

$$p = \max(p, p_{wat} - (\rho_{wat} - \rho_{oil})z/2) \quad \text{...} \quad (4.2)$$

Where z is the height of the cell and ρ denotes the phase gravity density.

The water phase pressure modification are then determined from

$$p_{MODW} = sign(p_{wat} - p + p_{cow}) * \min(|p_{wat} - p + p_{cow}|, (\rho_{wat} - \rho_{oil})z/2) \quad \text{................} \quad (4.3)$$

These phase pressure modifications are chosen such that the water phase pressure p_{wat} approximately follows the hydrostatic water pressure curve p_{wat} in the presence of mobile water.

Pseudo Capillary Pressure

The assumption of zero capillary pressure for segregated cases is valid on the field[62-64]. In other to achieve an appropriate oil-water front, it was found necessary to use pseudo capillary pressure in the fluid property model. The model requires a capillary transition zone be accounted for.

When the grid-blocks are smaller than the thickness of the capillary transition zone, the saturation of the grid-blocks can be accurately estimated from capillary pressure curve at the midpoint of the grid-block. Here, fluid distribution in the grid-block is assumed to be uniform. When the capillary pressure transition zone is smaller than grid block height, it poses a problem. Pseudo capillary pressure using the vertical equilibrium approach can be used. It involves averaging the saturations in the grid blocks. Since the transition zone is assumed to be of negligible thickness, the saturation of the block can be calculated using a linear relationship based on the distance from the specified WOC.

The final form of the equation used to generate the pseudo capillary pressure curves is shown below[1]:

$$\frac{\Delta \tilde{P}_{cow}}{\Delta \tilde{S}_w} = \frac{-h(\rho_w - \rho_o)}{(1 - S_{wc})144} \qquad (4.4)$$

---

[1] Personal communication with Robert Wattenbarger, Texas A&M U., College Station, Texas (2007)

Stratified Flow Model

Hearn [65] applied the pseudo relative permeability concept to stratified reservoirs. Here, vertical sweep is dominated by viscous flow forces rather than gravity and capillary forces due to vertical permeability variation. The stratified flow model assumes a layered system with homogeneous properties. It is applicable to only oil-water systems and assumes piston-like displacement which implies that only water flows behind the flood front and only oil flows ahead of the flood front. Capillary and gravity forces are ignored. The equations used in the stratified flow models are based on piston like displacement at some point in the reservoir. The saturation equation is a volume weighted average saturation. The relative permeability is a permeability-thickness weighted average relative permeability. The stratified flow model is applicable to reservoirs with high horizontal permeability, high fluid velocities and reservoirs where viscous forces dominate compared to gravity forces. Fig. 4.6 shows a sketch of the stratified model.

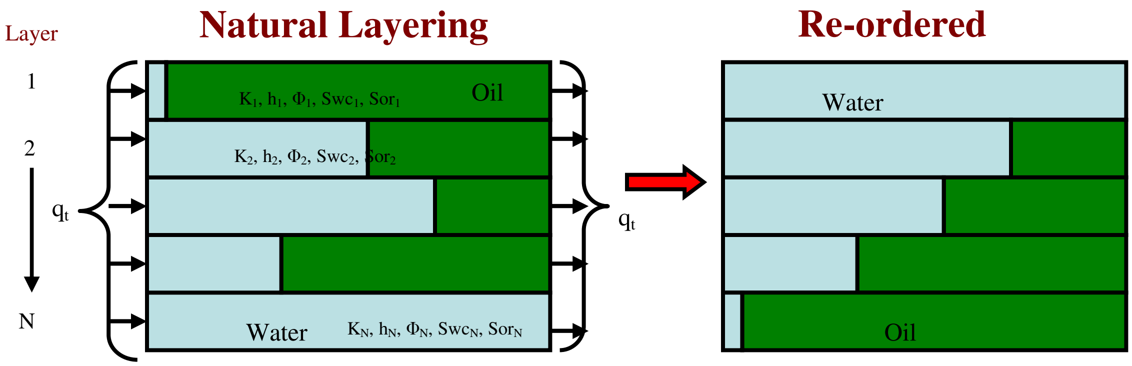
Layer
Natural Layering
Re-ordered
1
2
N
q_t
q_t
$K_1, h_1, \Phi_1, Swc_1, Sor_1$
Oil
$K_2, h_2, \Phi_2, Swc_2, Sor_2$
Water
$K_N, h_N, \Phi_N, Swc_N, Sor_N$
Water
Oil

Fig. 4.6-Stratified Reservoir Model.

Modeling Vertical Heterogeneity

Stratified models do provide a mathematical simulation of early water breakthrough or channeling present in aquifer driven reservoirs. In a layered reservoir, the displacing fluid will move more quickly through the most permeable layer. This causes a more rapid and more gradual breakthrough of the displacing fluid. Hearn[65]presented a method for developing pseudo relative permeability curves[66-71] for 2-D simulation of fluid displacement projects where vertical sweep is primarily affected by permeability variation. Here, gravity and capillary forces are neglected and the vertical fluid saturation distribution is assumed to be controlled by viscous flow forces resulting from vertical permeability variation.

The underlying assumption is based on the fact that when reservoir layers are separated by impermeable barrier, the assumption of high conductivity for vertical flow is incorrect. In this case, vertical equilibrium cannot exist. However, the geometry of most reservoirs is such that the area for cross-flow is large compared with the area for horizontal flow. This may result in a high vertical conductivity even if localized areas of low vertical permeability exist. Thus in many reservoirs, the assumption of high vertical flow conductivity may be more realistic than the assumption of barrier to flow.

The approach requires that the layers be re-ordered in order of decreasing permeability so that the relative permeability data may be calculated in order of increasing water saturation.

The resulting equations are:

For $n = 0$ (before breakthrough)

$$S_{w0} = \frac{\sum_{i=1}^{N} h_i \phi_i S_{wci}}{\sum_{i=1}^{N} h_i \phi_i} \quad \text{……………………………………………………………...} \quad (4.5)$$

$$\tilde{k}_{w0} = 0$$

$$\tilde{k}_{o0} = k_{o\,r}$$

For n = 1,2,3………..N-1,

$$S_{wn} = \frac{\sum_{i=1}^{n} h_i \phi_i (1 - S_{ori}) + \sum_{i=n+1}^{N} h_i \phi_i S_{wci}}{\sum_{i=1}^{N} h_i \phi_i} \quad \text{…………………………………………} \quad (4.6)$$

$$\tilde{k}_{wn} = \frac{k_{wr} \sum_{i=1}^{n} k_i h_i}{\sum_{i=1}^{N} k_i h_i} \quad \text{……………………………………………………………} \quad (4.7)$$

$$\tilde{k}_{on} = \frac{k_{or} \sum_{i=n+1}^{N} k_i h_i}{\sum_{i=1}^{N} k_i h_i} \quad \text{……………………………………………………………} \quad (4.8)$$

For n =N

$$S_{wN} = \frac{\sum_{i=1}^{N} h_i \phi_i (1 - S_{ori})}{\sum_{i=1}^{N} h_i \phi_i} \quad \text{………………………………………………………} \quad (4.9)$$

$$\tilde{k}_{wN} = krw$$

$$\tilde{k}_{oN} = 0$$

Fig. 4.7 shows the pseudo relative permeability curve used in comparison with a typical rock curve.

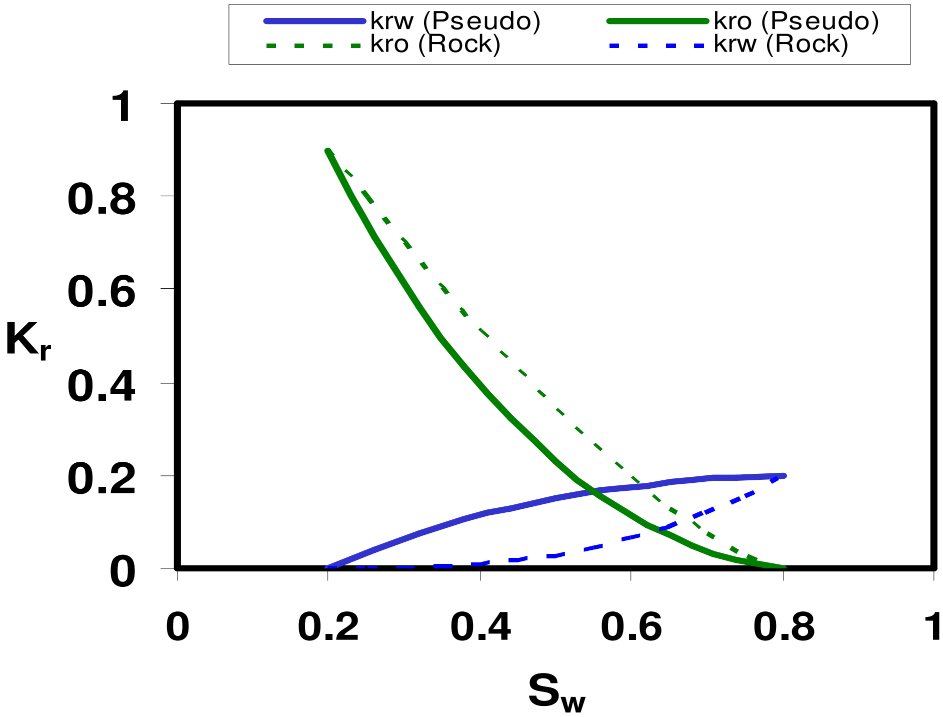

Fig. 4.7-Comparison of Pseudo Relative Permeability Curve with Its Corresponding Rock Curve.

Relative Permeability Characterization

The use of Hearn relative permeability equations enables the development of maximum bounding relative permeability curves for use in the simulation model to simulate stratified flow.

Historically, uncertainty in permeability distribution is characterized by a log-normal distribution. The triangular distribution equation is used to populate the randomly generated permeability for the pseudo relative permeability curve to obtain a log-normal distribution of the generated permeability. It has three parameters: the minimum, *a*, the maximum, *b* that defines the range, and the most likely, *c* (the peak). The distribution is skewed to the left when the peak is close to the minimum and to the right when the peak is closed to the maximum.

It is described by the equations below:

$$f(x \mid a,b,c) = \frac{2(x-a)}{(b-a)(c-a)} \qquad \text{For } a \le x \le c \text{ ……………………….. } (4.10)$$

$$f(x \mid a,b,c) = \frac{2(b-x)}{(b-a)(b-c)} \qquad \text{For } c \le x \le b \text{ ……………………… } (4.11)$$

The solutions to the equations above are given by

$$x = a + \sqrt{RND(b-a)(c-a)} \qquad \text{For } a \le x \le c \text{ ……………………..... } (4.12)$$

$$x = b - \sqrt{(1-RND)(b-a)(b-c)} \qquad \text{For } c \le x \le b \text{ ……………………..... } (4.13)$$

A VBA program was written to randomly generate permeability using the triangular distribution method described earlier. Using the equations above, we specify a minimum permeability, a maximum permeability and the most likely permeability to generate the relative permeability curves. The layers are re-ordered in order of decreasing breakthrough of the water-oil displacement front so that the first layer is flooded out first then the second layer etc. After re-ordering, pseudo relative permeability curves are generated by calculating the average water saturation at the outflow end of the system. Although Hearn resulting model was a layer, a 25 layer model was used, each layer with the same distribution. Thus, the average permeability is equal to the model permeability.

The ratio of the specified most likely permeability (k_{ml}) to the specified maximum permeability (k_{max}) assuming the minimum permeability (k_{min}) is equal to zero is used to characterize the relative permeability curve. The k_{ml}/k_{max} ratio range of 0.1 – 0.5 which implies a skewness of 0.5 – 0 is used in the parameter sensitivity analysis. Fig. 4.8 shows a log-normal representation of permeability obtained from the triangular distribution.

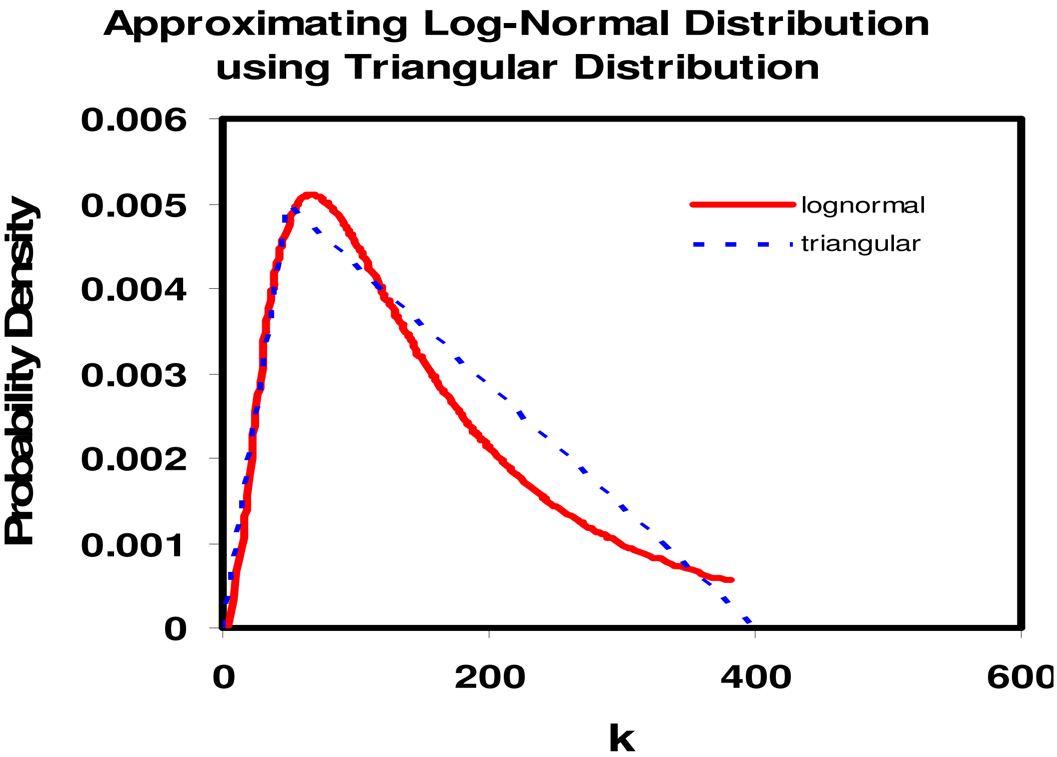

Fig.4.8-Probability Density Function Plot - Approximating Log-normal Distribution with a Triangular Distribution.

Plotting Style

Addington[1] developed a generalized gas correlation for 3-D, 5 layer large grid cell model of the Prudhoe Bay field. The developed correlation can be used to predict critical coning rate and Gas-Oil ratio (*GOR*) of a well after coning. The gas-coning correlations were developed by simulating numerous one-well models at a constant total fluid production rate for a variety of well parameters.

He observed that a linear relationship existed when the plot of GOR versus the average oil column height above the perforations on a semi-log paper is made. The linear relationship was the basis for the generalized correlations. Fig. 4.9 shows this relationship.

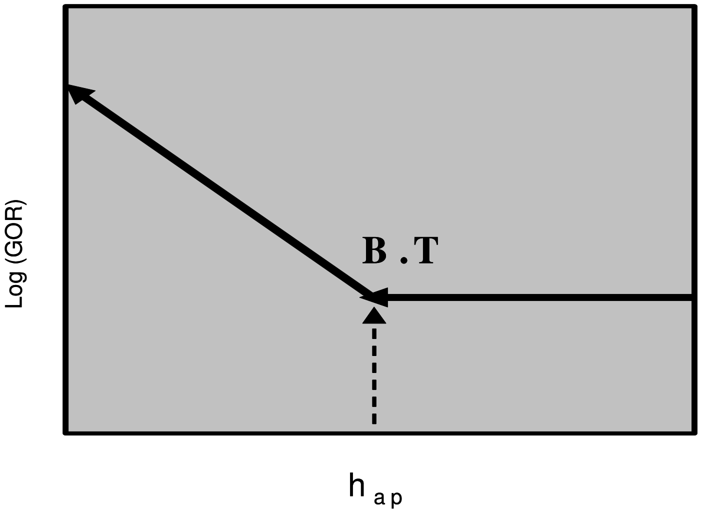

Fig. 4.9-Addington Log (GOR) vs. h_{ap} Relationship.

Yang and Wattenbarger[2,5] followed Addington's approach to develop water coning correlations for vertical and horizontal wells for water-oil problems. They developed a method that can be used for hand calculation or simulation to predict critical rate, breakthrough time and WOR after breakthrough in both vertical and horizontal well. The correlations developed were based on basic flow equations and regression analysis.

The one well model was run on a 2-D simulator. A number of simulation runs was made to investigate coning performance at different reservoir and fluid properties. For each simulation run, a plot of *WOR* plus a constant, *C*, as a function of the average oil column height below perforation is a straight line after water breakthrough on a semi log scale. Fig. 4.10 shows the Yang-Wattenbarger method. For a vertical well, the constant, *C* was found to be 0.02 to obtain the straight line. Thus, if the breakthrough height h_{wb}, and slope of the straight line *m* can be determined, the whole process of coning can be predicted.

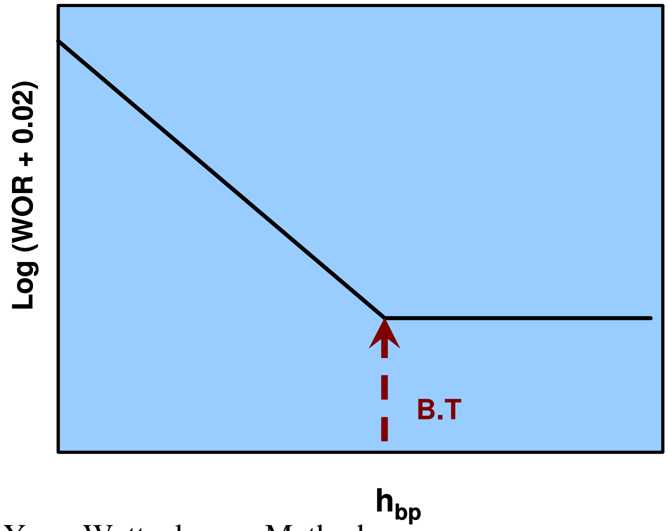

Fig. 4.10-Yang-Wattenbarger Method.

This research modifies the Addington-Yang approach to solve edgewater coning problem using a single well modeling. For the edgewater coning model, it was observed that while investigating the effect of certain model parameters, using a fixed value of *C* as Yang did might not be accurate for this study – Fig. 4.11. It was also observed that for a particular model parameter under investigation, different values of *C* might be required to give a straight line. The importance of accurately estimating *C* cannot be overemphasized. *C* affects the average oil column height at water breakthrough calculated and the slope of the *WOR* curve.

We observe that in order to be able to accommodate different values of *C* and also obtain visually determined straight lines after water breakthrough, a plot of Log ((WOR+*C*) /*C*) versus average oil column height below perforation h_{bp} should be made. This would always give a horizontal asymptote of 1, and allow the different *WOR* data sets to be plotted together without introducing bending. Fig. 4.12 shows an example sensitivity of the new approach. The new plotting technique would always give a horizontal asymptote of 1, and allow the different *WOR* data sets to be plotted together without introducing bending.

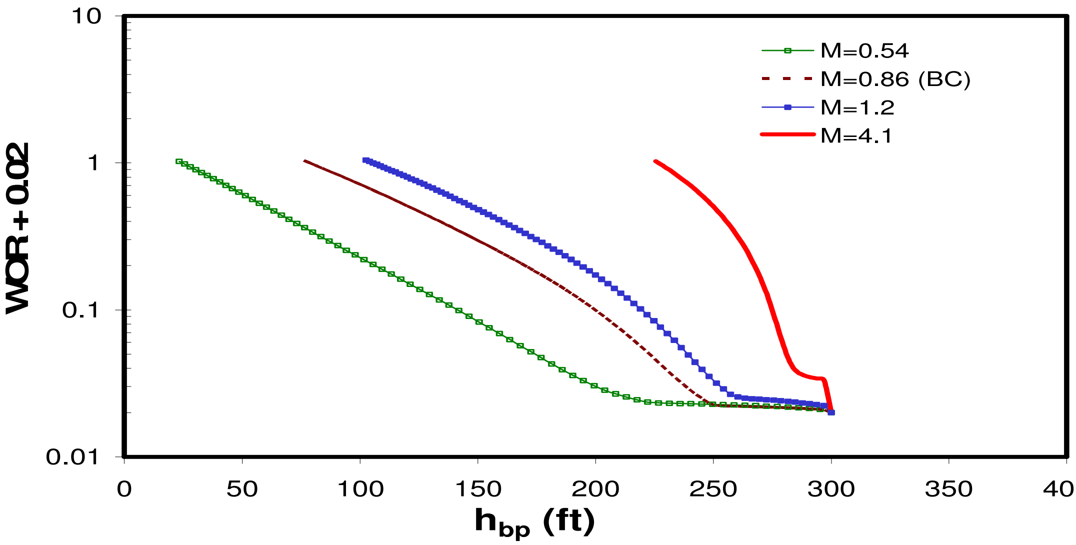

Fig. 4.11-Simulation Results for Different Mobility Ratios, M, Using the Yang-Wattenbarger[4] Method of Adding a Constant 0.02 to WOR.

Plot of Log (WOR+C)/C vs h_{bp}

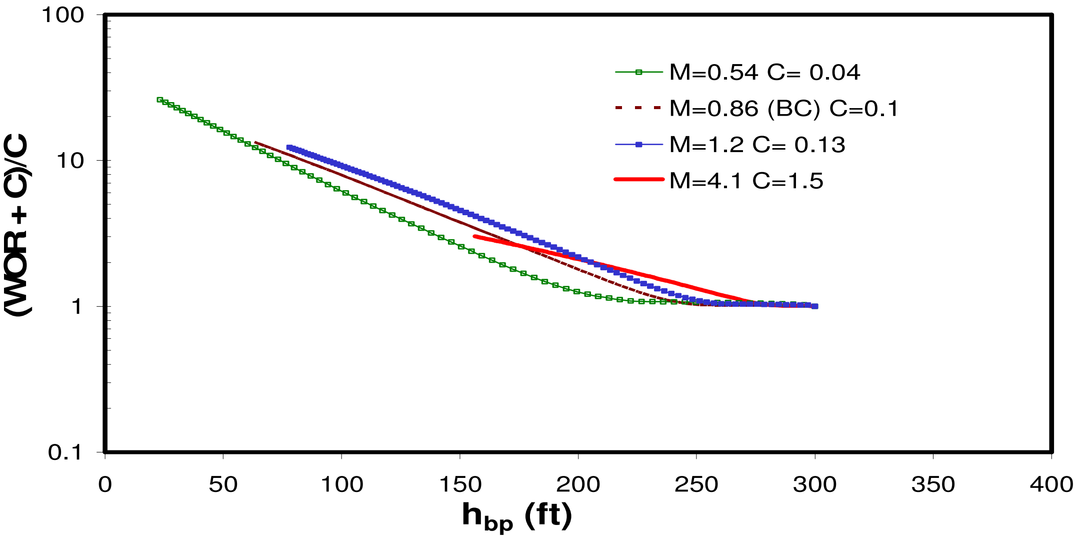

Fig. 4.12-Simulation Results From Fig.4.11 Using the New Method, with (WOR+C)/C as y Axis. Note the Horizontal Asymptote of 1 and All Lines are Straight.

CHAPTER V

DEVELOPMENT OF EMPIRICAL CORRELATIONS

Overview

This chapter deals with the development of the empirical correlations. A single well 3-D Cartesian model was developed to model edgewater production challenges in a monocline reservoir. A number of simulation runs was carried out to investigate coning performance at different reservoir and fluid properties. The effect of each variable was quantified by making a plot of Log ((WOR+C)/C) versus h_{bp} i.e. water-oil ratio plus C divided by C, versus the average oil column height below perforation, h_{bp} on a semi-log plot. The correlations were developed by correlating each variable to the average oil column height at water breakthrough, h_{wb}, slope of the water-oil ratio plot, m and constant C. To understand the importance of recovery as a function of producing rate, a plot of WOR versus the ratio of cumulative oil production to the oil in place (N_p/N) was made for all the model parameters.

Model Parameters

Fig. 5.1 shows a sketch of a monocline reservoir at initial conditions. During production, water cusps and cone towards the perforation of the producing interval. Assuming a piston-like displacement, as water moves up, Fig. 5.2, the height of the water invaded zone ΔH can be calculated. Appendix A shows the derivation of the equation that relates the height of the water invaded zone to the cumulative oil production. The distance between the bottom of the perforation and the current oil-water contact is referred to as the h_{bp}. As production proceeds, water breaks through into the wellbore and this height is referred to as the average oil column height at water breakthrough h_{wb}. After water breakthrough, the *WOR* increases as the average oil column height below perforation decreases.

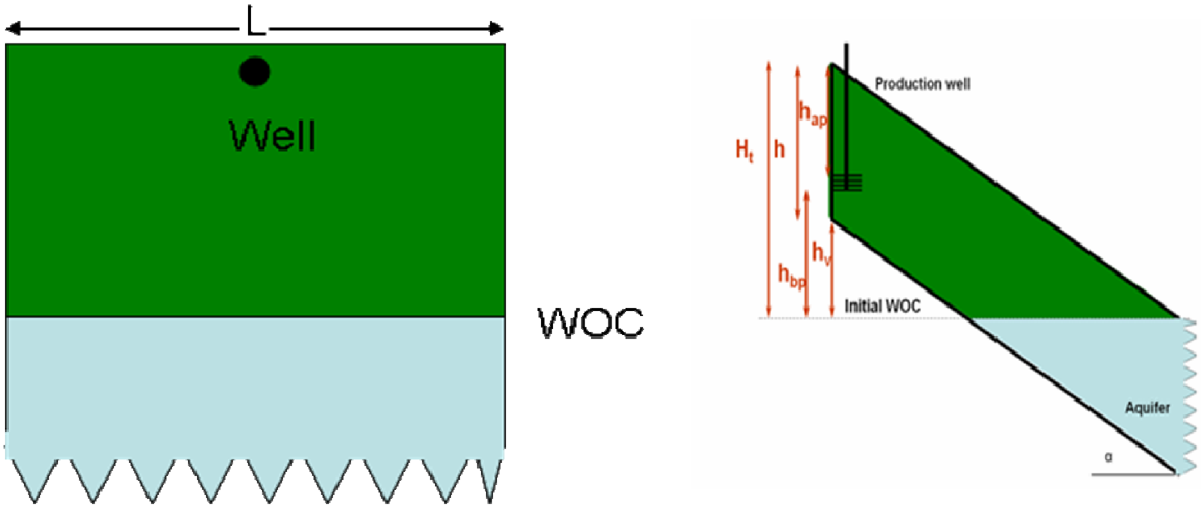
L
Well
WOC
H_t
h
h_{ap}
h_v
h_{bp}
Production well
Initial WOC
Aquifer
α

Fig. 5.1-Top and Side View Sketch of Model at Initial Conditions.

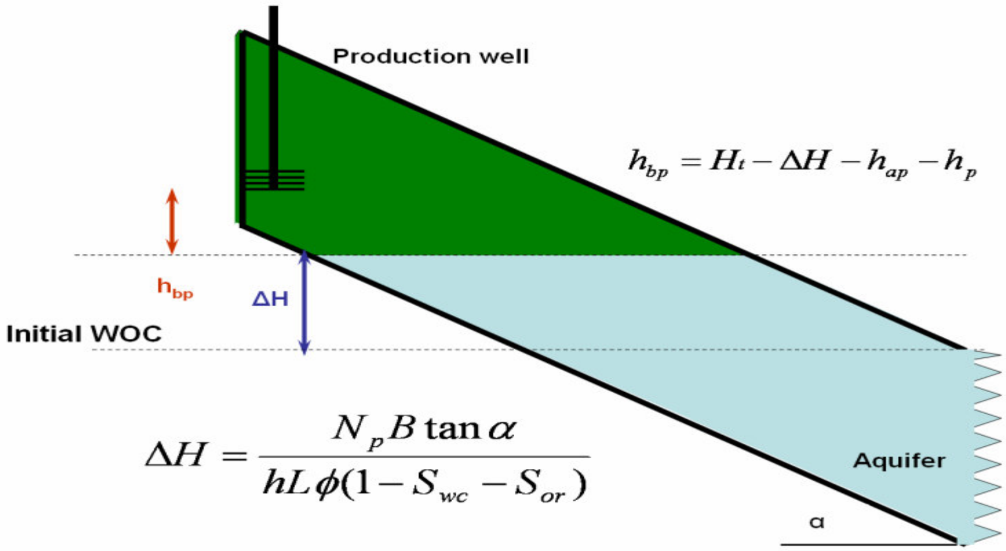
Production well
$h_{bp} = H_t - \Delta H - h_{ap} - h_p$
h_{bp}
ΔH
Initial WOC
$\Delta H = \dfrac{N_p B \tan\alpha}{hL\phi(1 - S_{wc} - S_{or})}$
Aquifer
α

Fig. 5.2-Sketch of the Tank or Material Balance Model Showing Relationship between N_p (Simulation Model) and h_{bp} (Material Balance Model).

Using a single well model, the effect of eleven model parameters on edgewater coning was investigated. This include total liquid flow rate, formation thickness, reservoir length, vertical distance (initial standoff), perforation thickness, dip angle, end point mobility ratio, water-oil gravity gradient, vertical permeability, horizontal permeability, ratio of most likely permeability to maximum permeability for Hearn relative permeability curves. Model parameters dip angle, vertical distance, reservoir length and formation thickness are not independent variables.

A number of simulation runs were carried out for different reservoir and fluid properties. For every simulation run, all other variables are kept constant while the parameter under investigation is varied for a wide variety of practical range. The emphasis is on breakthrough time prediction and post-breakthrough performance.

Sensitivity of Model Parameters

The method for determining h_{wb}, m and C was from a stepwise procedure. A base case was set-up. Table 5.1 shows the base case data. A number of simulation runs was carried out to investigate coning performance at different reservoir and fluid properties by modifying the base case model. Table 5.2 shows the experimental range. For a particular parameter under investigation, a semi-log plot of (WOR+C)/C vs. h_{bp} is made. From the plot, h_{wb}, m and C are obtained. Using the Spider plot approach, the relationship between $h_{wb,}$ m, C and model parameters are determined. Appendix B describes the Spider Plot procedure. For each plot, the constant C that gives a straight line is determined.

Table 5.1 Base Case Model Parameters

Model Parameters	Symbol	Value	Units
Total Liquid Flow Rate	q_t	2000	STB/D
End Point Mobility Ratio	M	0.86	
Vertical Distance	h_v	300	ft
Vertical Formation Thickness	h	250	ft
Reservoir Length (in x-dir)	L	800	ft
Horizontal Permeability	k_h	200	md
Vertical Permeability	k_v/k_h	0.1	
Perforation Thickness	h_p	250	ft
Dip Angle	α	20	degrees
Water-oil gravity gradient	$\Delta\gamma$	0.095	psi/ft
Ratio of k_{ml}/k_{max}	k_{ml}/k_{max}	0.1	

Table 5.2 Experimental Range

Model Parameters	Symbol	Value Range	Units
Total Liquid Flow Rate	q_t	200 - 2000	STB/D
End Point Mobility Ratio	M	0.54 – 4.1	
Vertical Distance	h_v	200 - 500	ft
Vertical Formation Thickness	h	125 - 500	ft
Reservoir Length (in x-dir)	L	400 - 3200	ft
Horizontal Permeability	k_h	100 - 2000	md
Vertical Permeability	k_v/k_h	0.001 - 1	
Perforation Thickness	h_p	50 - 250	ft
Dip Angle	α	10 - 40	deg
Water-oil gravity gradient	$\Delta\gamma$	0.095 – 0.18	psi/ft
Ratio of k_{ml}/k_{max}	k_{ml}/k_{max}	0.1 – 0.5	

Effect of Total Liquid Flow Rate - q_t

The effect of total liquid rate on edgewater cusping and coning was investigated by considering liquid flow rates from 200 – 3000 STB/D. For each rate, all the other variables were held constant and the effect observed. Fig. 5.3a shows the effect. As would be expected, the average oil column height below perforation, h_{bp} decreases as production rate decreases. An important observation is that the log of (WOR+C)/C vary linearly with the average oil column height below perforation, h_{bp} at all production rates.

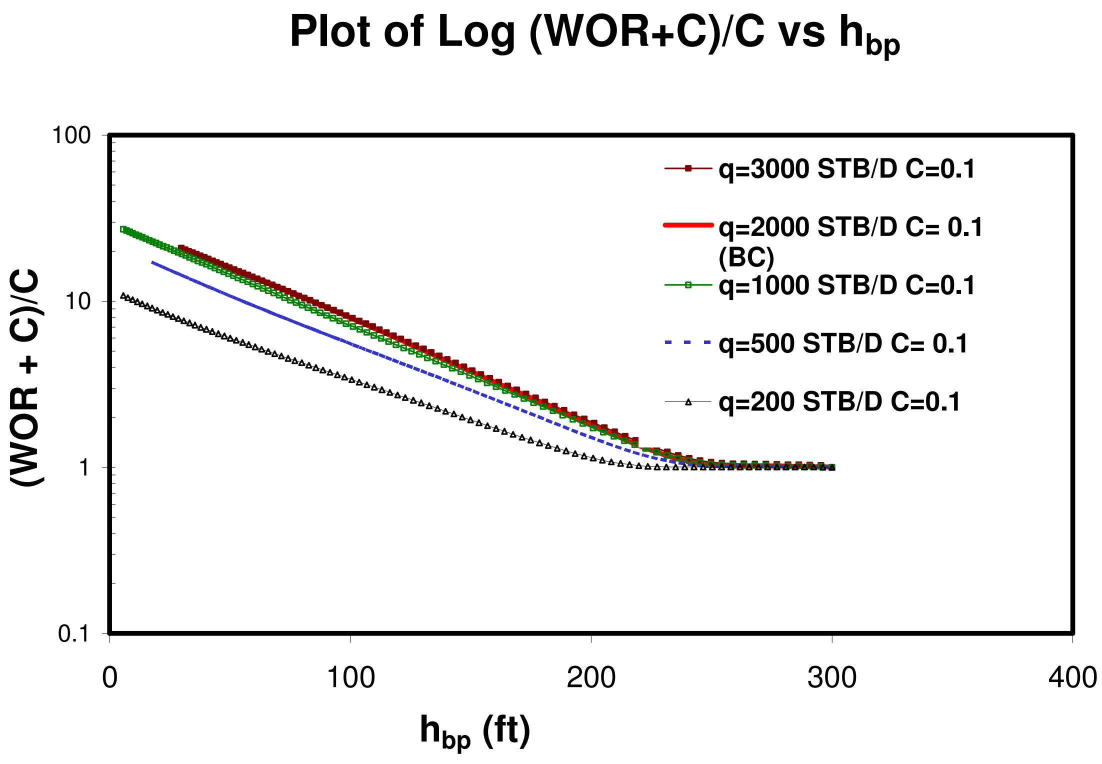

Fig. 5.3a-Effect of Total Liquid Flow Rate – Log (WOR+C)/C vs. h_{bp}.

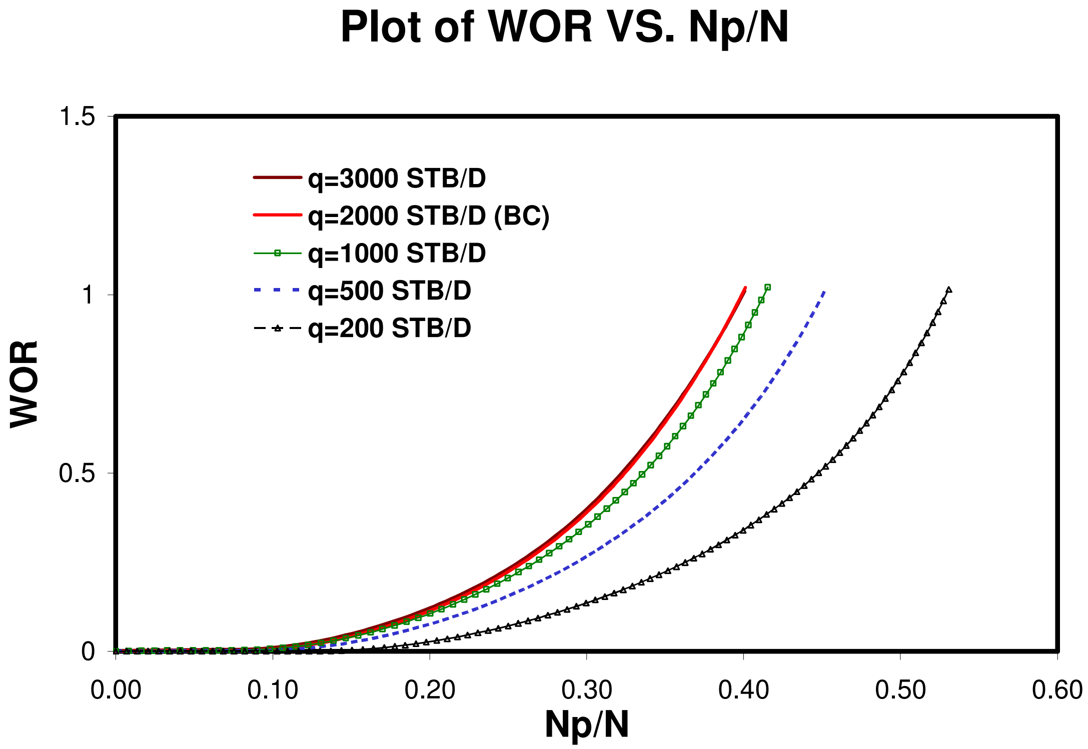

Fig. 5.3b-Effect of Total Liquid Flow Rate – *WOR* vs. N_p/N.

To quantify the effect of recovery as a function of producing rate, a plot of *WOR* vs. N_p/N was made Fig.5.3b. For rates greater than 2000 STB/D, the slope of the *WOR* plot doesn't change. This is due to rate insensitivity. This can be further explained with Fig. 5.4. The *WOR* versus Cumulative Oil Production N_p confirms that at rates greater than or equal to 2000 STB/D, *WOR* plot doesn't change. The implication of this is at a certain flow rate, it doesn't matter – the same magnitude of water is produced. It was observed that the water-oil ratio at the *WOR* economic limit of 1 increased with rate. Although recovery is higher while producing at a lower rate, the economic implication should be put into consideration. For a well in a deep offshore environment where the aim is to maximize production in the shortest possible time, there is no difference in the magnitude of water produced and recovery at rates greater than 2000 STB/D going by the simulation results. *WOR* of 1 was used as a benchmark because of the cost associated with water production in the offshore environment.

In predicting the incremental ultimate recovery with increasing rates of fluid production for the simulation model, the additional volume of oil produced was compared to the cost of water handling. To achieve the same recovery obtained at 500 STB/D for 8200 days by increasing the rate to 3000 STB/D, an approximately 507,000 STB of water is produced with 393,000 STB of oil. Comparing today's high oil prices greater than $90 per bbl and cost of water handling which includes capital and operating expenses, utilities & chemicals – lifting, separation, de-oiling, filtering, pumping and injection of about $0.578/bbl [72], incremental recovery from increased rates of production will be adequate to accommodate additional capital cost which may be required for larger water handling facilities. This is achieved in a shorter time period of 1520 days! Fig. 5.3c shows the result.

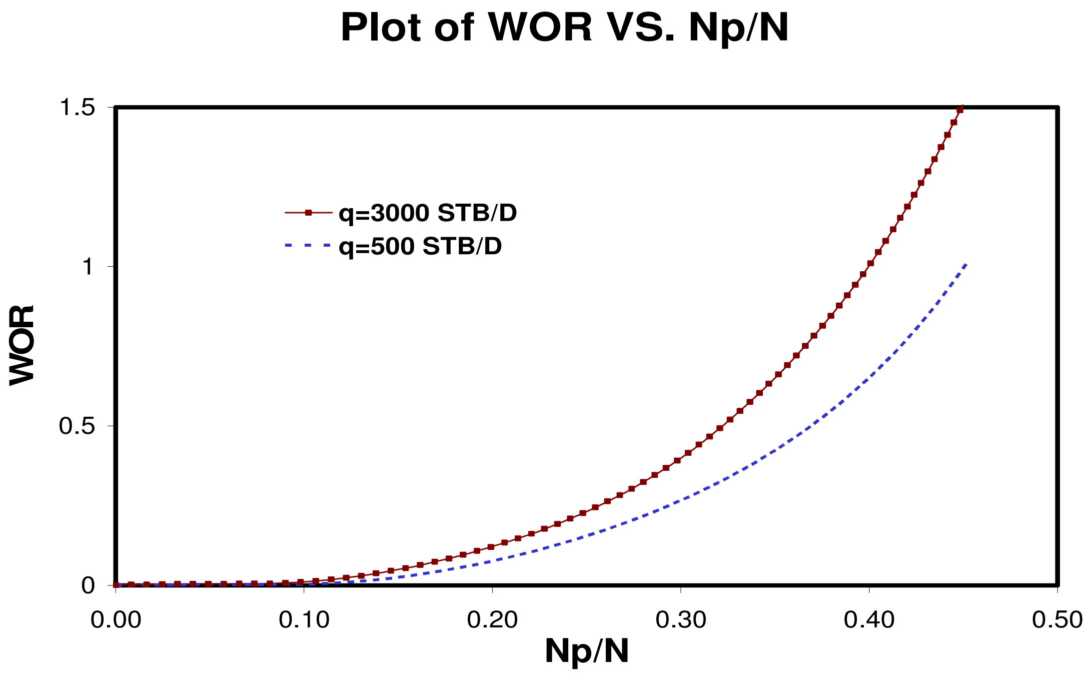

Fig. 5.3c-Incremental Ultimate Recovery – *WOR* vs. N_p/N.

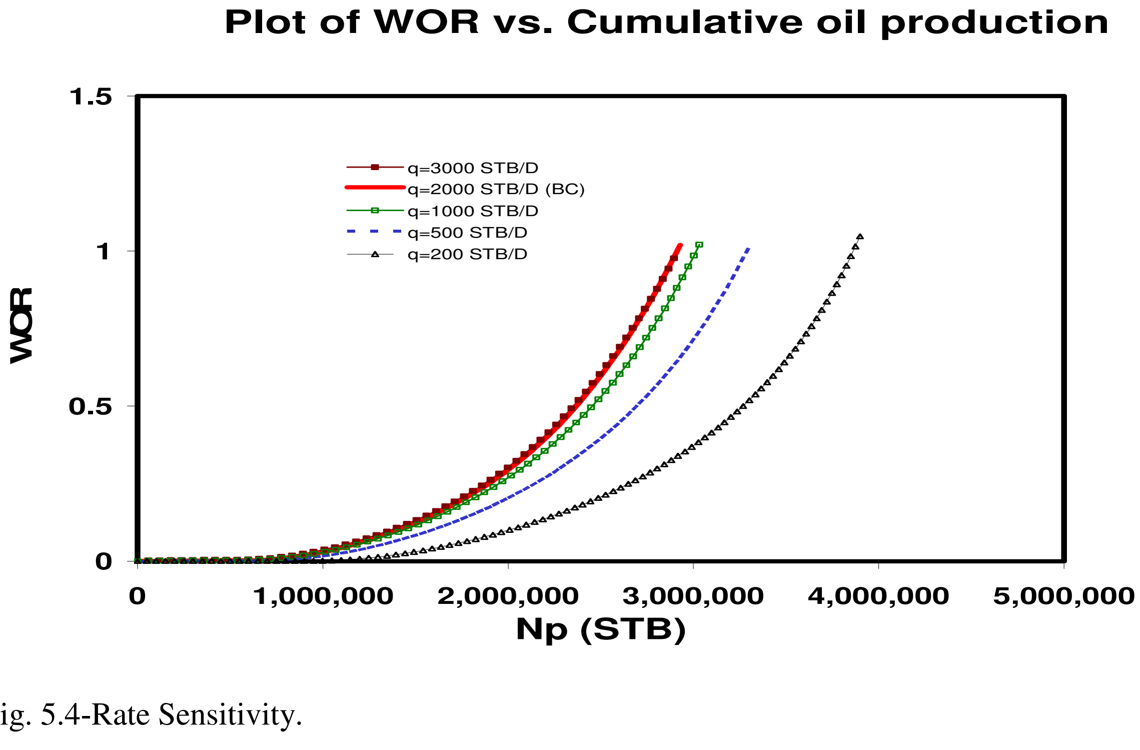

Fig. 5.4-Rate Sensitivity.

Effect of Endpoint Mobility Ratio - *M*

To investigate the effect of mobility ratio, the same relative permeability curve was used for consistency. The oil viscosity was modified to achieve the various mobility ratio values investigated. Fig. 5.5a shows the effect of mobility ratio on edgewater cusping and coning performance. From the above plot, we have water breakthrough earlier in the most unfavorable case. This is expected. It was also observed that at end point mobility ratio greater than 3.5, the method doesn't give accurate results. This is a limitation on the correlation. A favorable mobility ratio leads to a higher slope. Fig. 5.5b shows the effect of end point mobility ratio on recovery. Recovery is highest in the most favorable mobility ratio case.

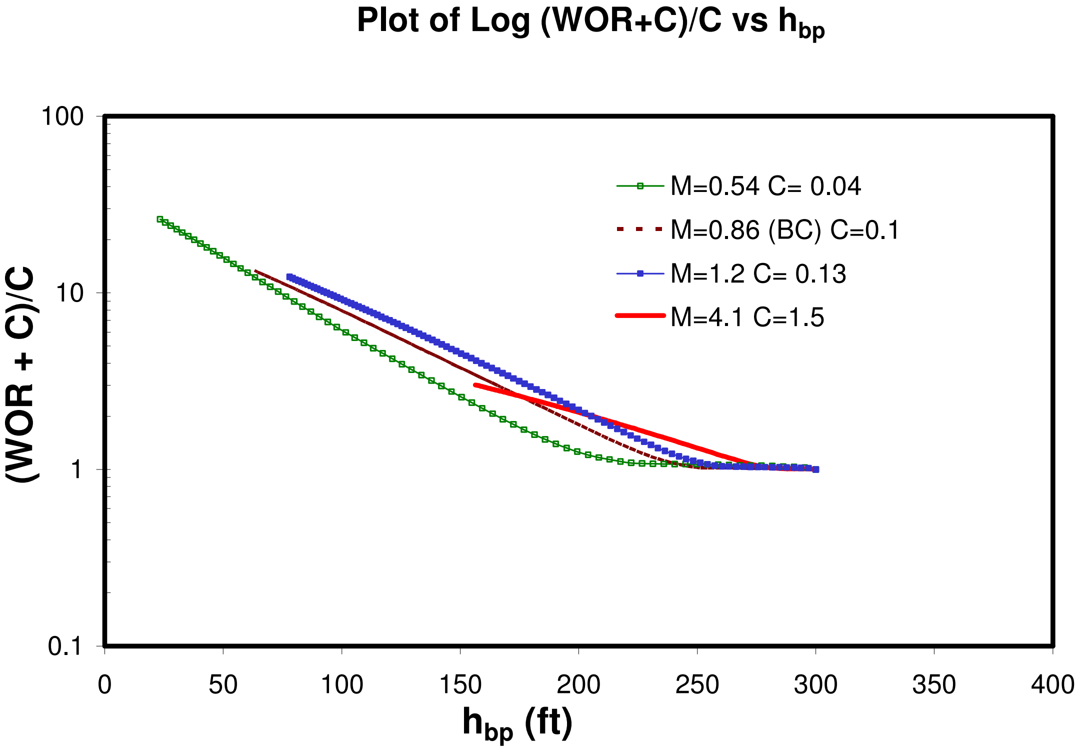

Fig. 5.5a-Effect of End Point Mobility Ratio - Log (WOR+C)/C vs. h_{bp}.

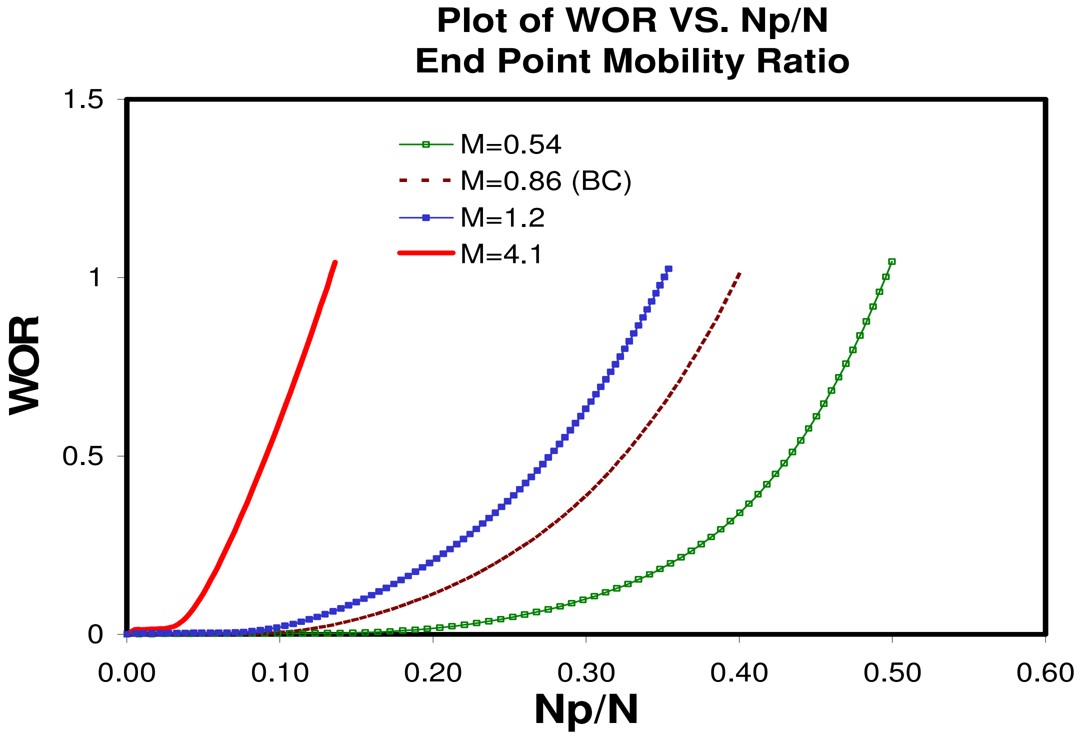

Fig. 5.5b-Effect of End Point Mobility Ratio - *WOR* vs. N_p/N.

Effect of Horizontal Permeability - k_h

The effect of horizontal permeability was investigated with a fixed k_v/k_h ratio of 0.1. Permeability ranges of 100 – 2000md was investigated. Fig. 5.6a illustrates the horizontal permeability effect on edgewater cusping and coning. As permeability decreases, the average oil column height below perforation increases with a decreasing slope. Fig. 5.6b shows the effect of horizontal permeability on recovery. We observe that there is a higher recovery in a high permeability reservoir.

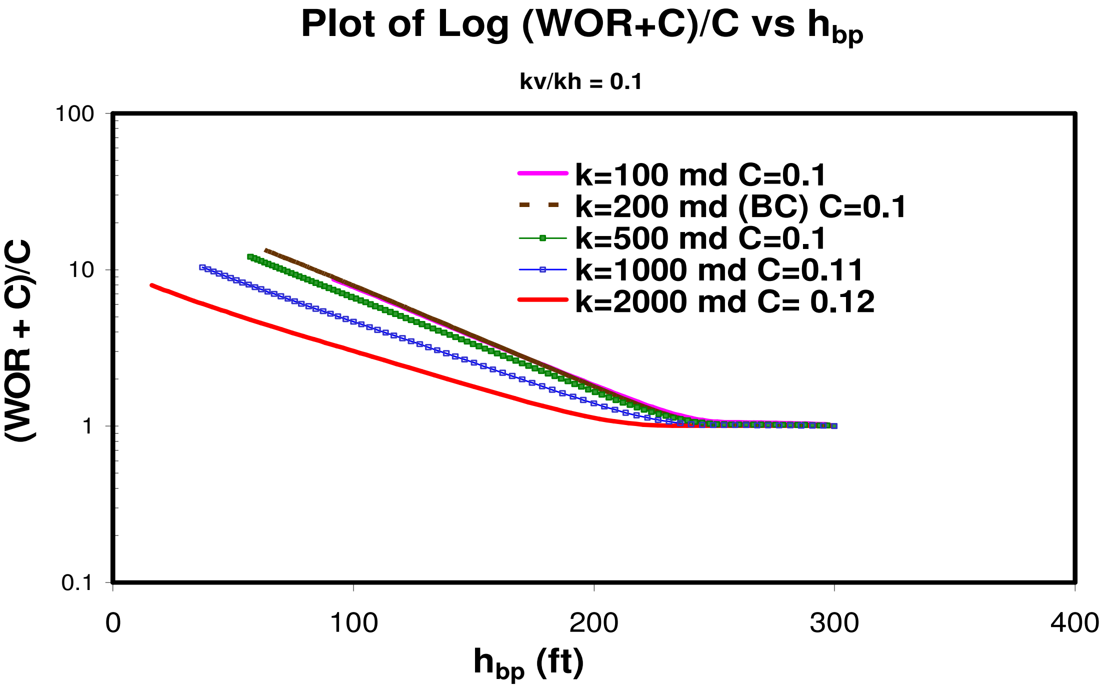

Fig. 5.6a-Effect of Horizontal Permeability - Log (WOR+C)/C vs. h_{bp}.

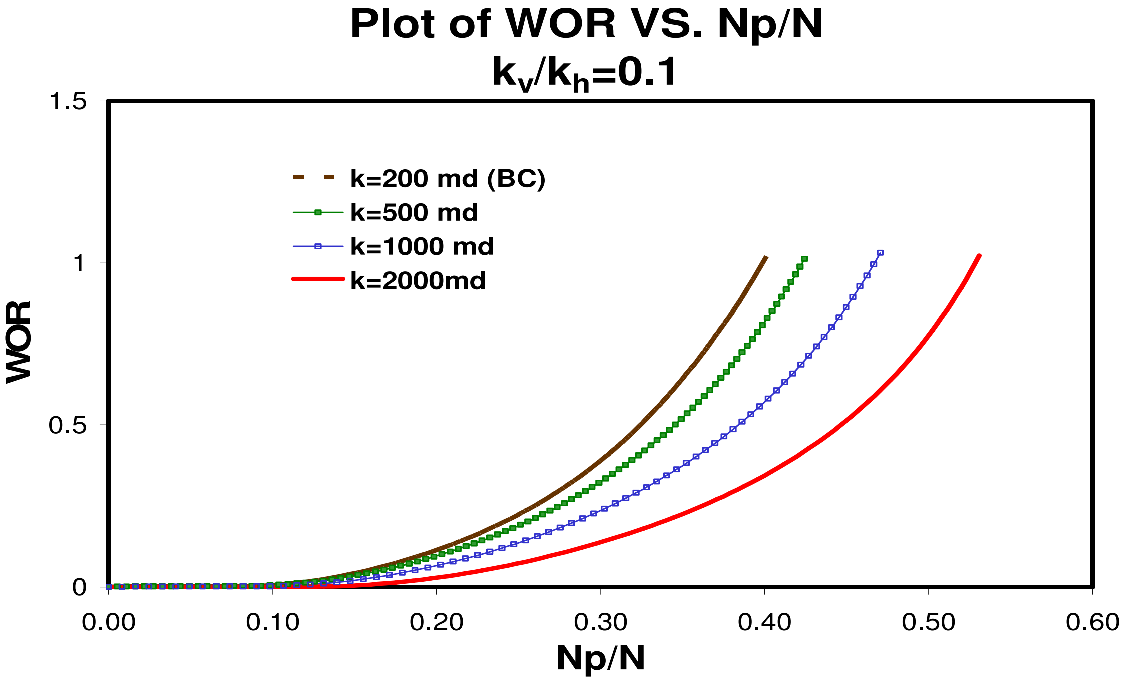

Fig. 5.6b-Effect of Horizontal Permeability - *WOR* vs. N_p/N.

Effect of Vertical Permeability – k_v/k_h

For a dipping reservoir, vertical permeability is defined as the direction across the depth of the reservoir and horizontal permeability refers to absolute permeability along the principal direction of flow. Fig. 5.7a shows the effect of vertical permeability on edgewater cusping and coning. The vertical permeability was modified with k_h held constant at the base case permeability of 200md for k_v/k_h range of 0.001 -1. Our results show that vertical permeability does not have a significant effect on edgewater cusping and coning. Fig. 5.7b shows the effect of permeability anisotropy on recovery. For a dipping reservoir, you can recover more when you have a high vertical permeability.

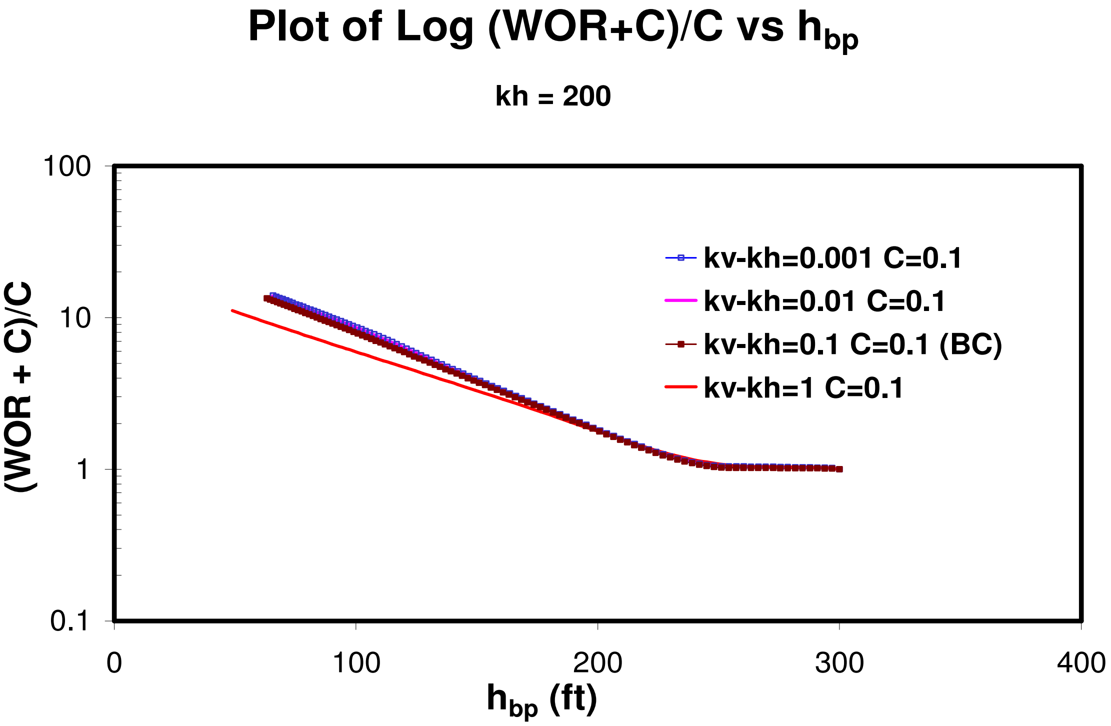

Fig. 5.7a-Effect of Vertical Permeability - Log (WOR+C)/C vs. h_{bp}.

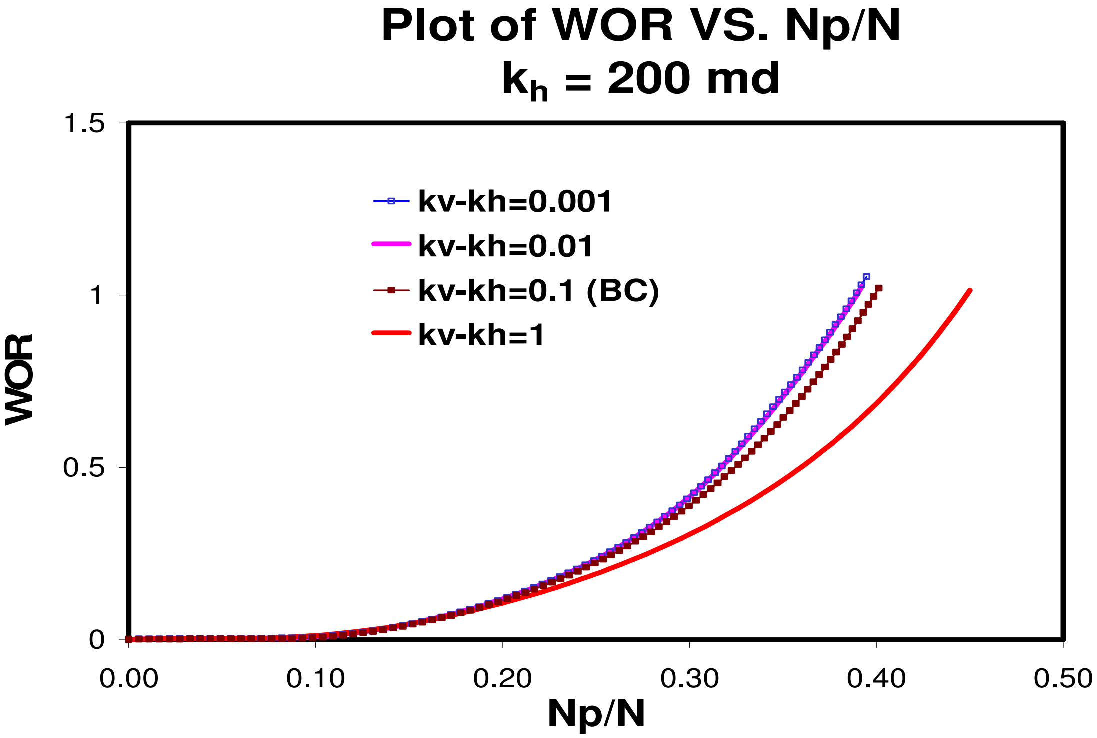

Fig. 5.7b-Effect of Vertical Permeability - *WOR* vs. N_p/N.

Effect of Perforation Thickness - h_p

Fig. 5.8a shows the effect of perforation thickness on edgewater cusping and coning. The effect of the perforated interval was investigated keeping the *OWC* constant i.e. all perforation starts from the *OWC*. The effect of completing 20% to 100% of the oil zone thickness was investigated. As perforation thickness increases, the average oil column height below perforation decreases at a fixed production rate. Fig. 5.8b shows the effect of perforation thickness on recovery. Recovery is higher when the entire zone is perforated i.e. total penetration yield the most recovery.

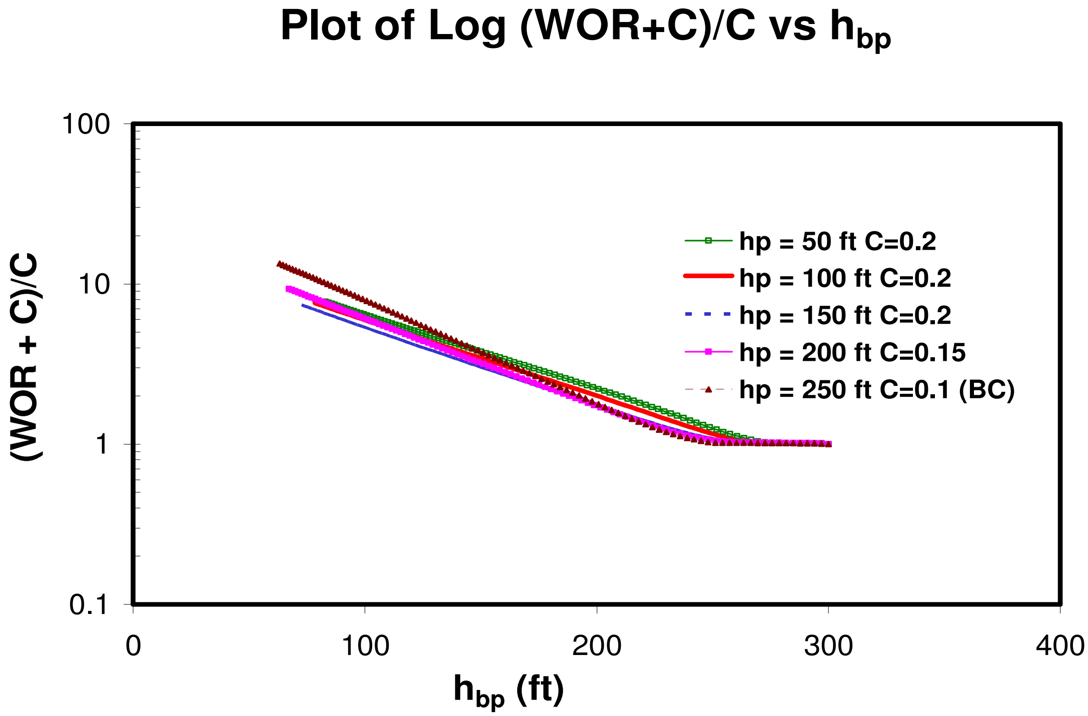

Fig. 5.8a-Effect of Perforation Thickness - Log (WOR+C)/C vs. h_{bp}.

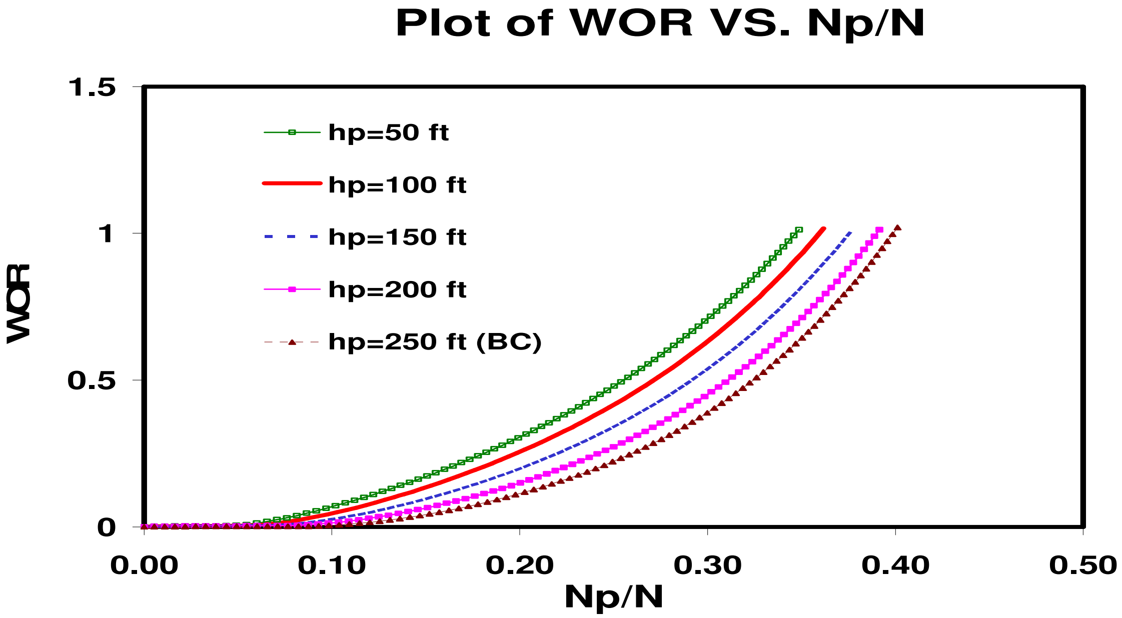

Fig. 5.8b-Effect of Perforation Thickness - *WOR* vs. N_p/N.

Effect of Water-Oil Gravity Gradient - $\Delta\gamma$

The effect of density difference on edgewater cusping and coning is shown in Fig. 5.9a. To obtain the various gravity gradient used in the sensitivity, the water gravity gradient is held constant with varying oil gravity gradient values. The 21° *API* oil gives a density difference of 0.095 psi/ft. The 60° *API* oil gives a density difference of 0.18 psi/ft for the case under investigation. It was observed that the denser fluid breakthrough first. Fig. 5.9b shows the effect of fluid density difference on recovery. Recovery is higher for high *API* oil.

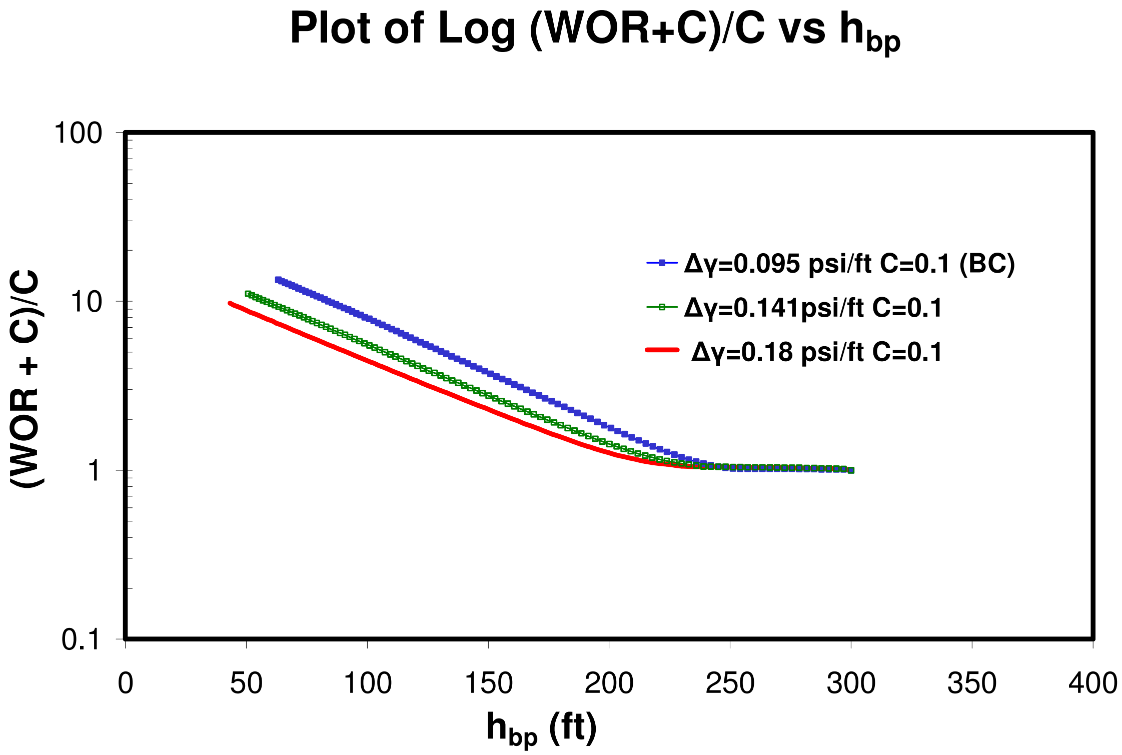

Fig. 5.9a-Effect of Water-Oil Gravity Gradient - Log (WOR+C)/C vs. h_{bp}.

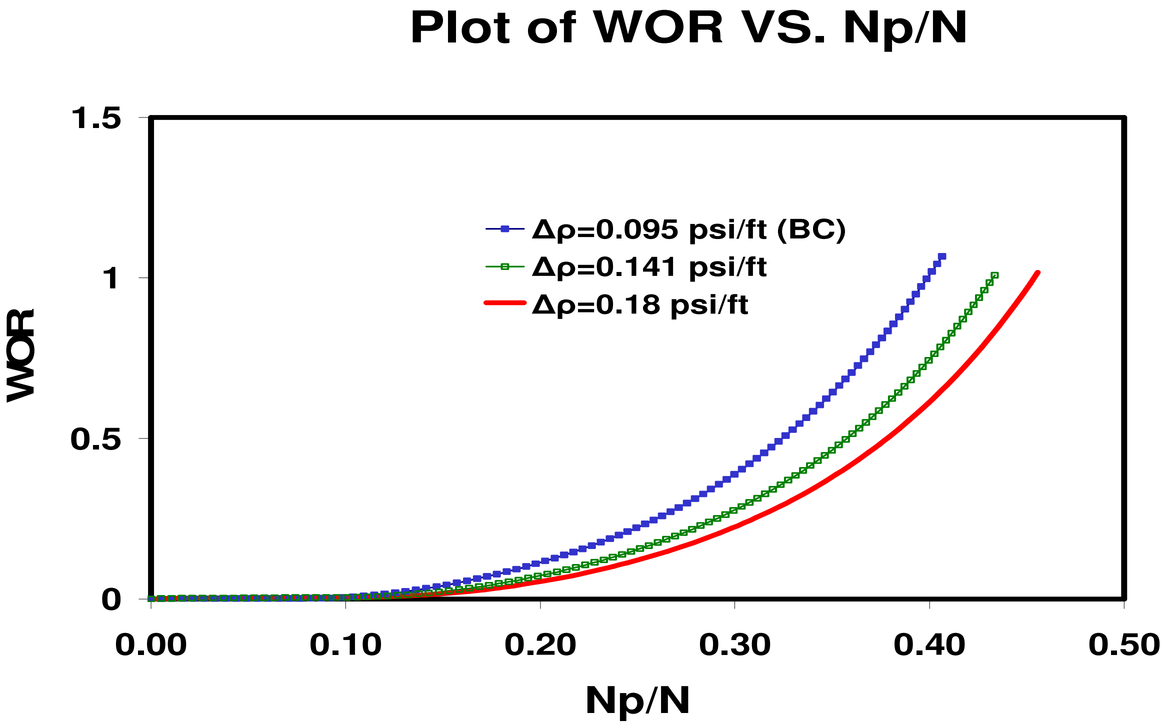

Fig. 5.9b-Effect of Water-Oil Gravity Gradient - *WOR* vs. N_p/N.

Effect of k_{ml}/k_{max} Ratio

Early water breakthrough and heterogeneity modeling as observed on the field was achieved with the use of Hearn type relative permeability. In other to quantify the relative permeability curves, the ratio of the most likely permeability, k_{ml} to the maximum permeability, k_{max} assuming k_{min} is equal to zero was used. Since permeability is log normally distributed, k_{ml}/k_{max} ratio of 0.1 - 0.5 is considered. This implies a skewness of 0.5 – 0. Fig. 5.10a shows the effect. Fig. 5.10b shows the effect of the relative permeability curve on recovery.

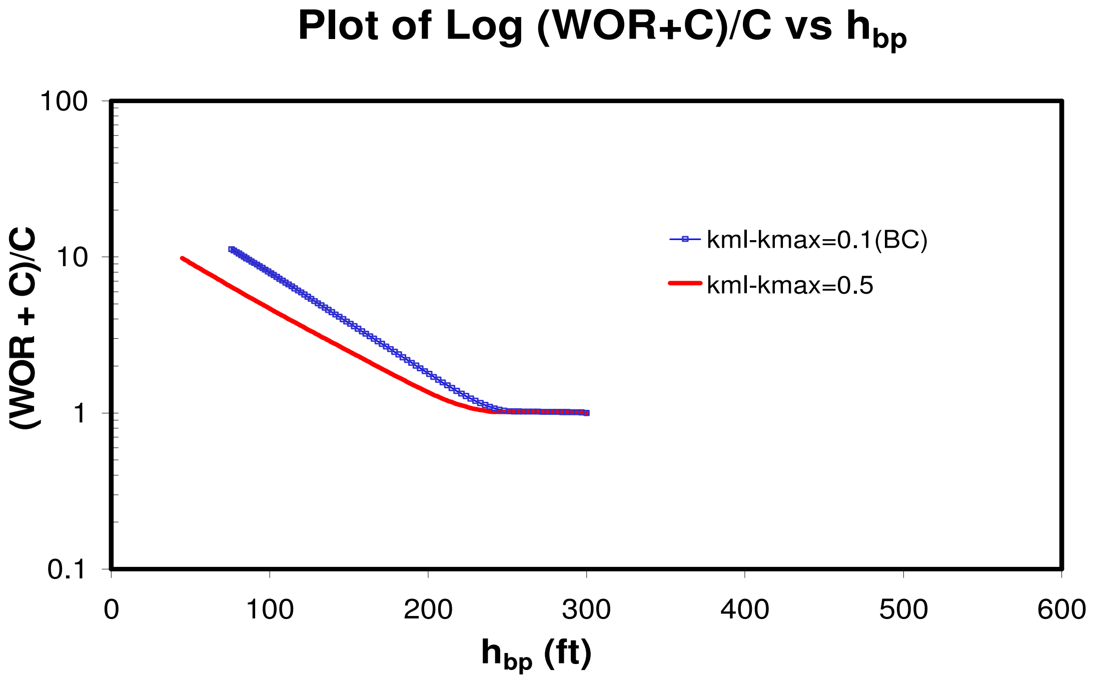

Fig. 5.10a-Effect of $k_{m}l/k_{max}$ Ratio - Log (WOR+C)/C vs. $h_{bp.}$

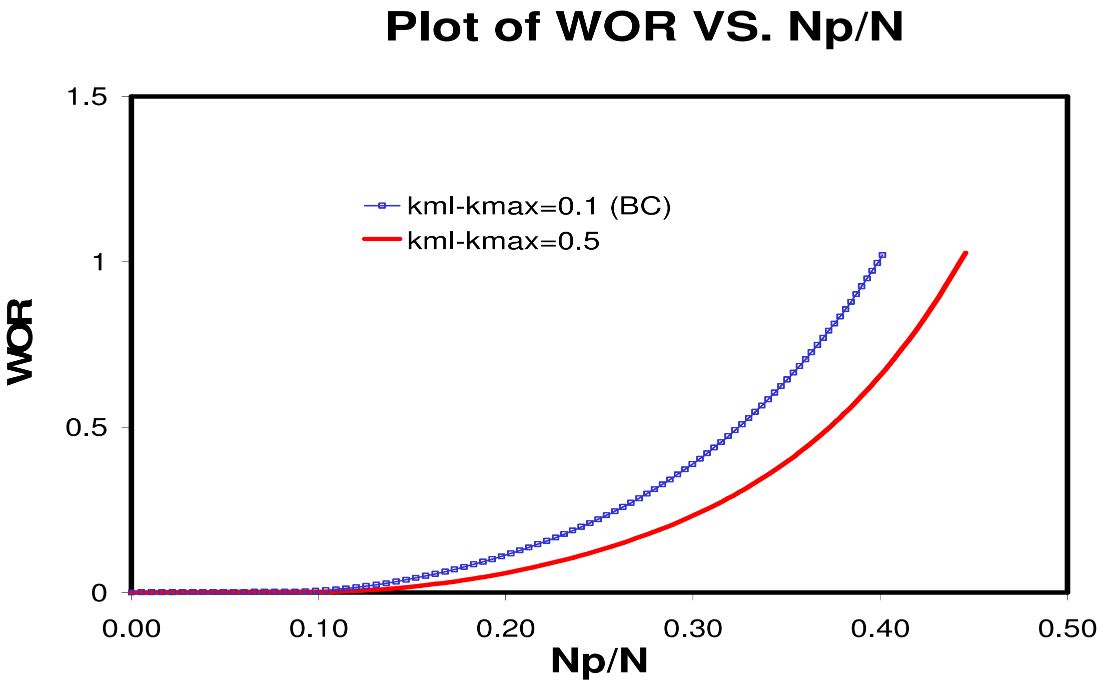

Fig. 5.10b-Effect of k_{ml}/k_{max} Ratio - *WOR* vs. N_p/N.

Effect of Reservoir Length - *L*

Model parameters reservoir length, formation thickness, dip angle and vertical distance are not mutually exclusive variables.

The effect of reservoir size on edgewater cusping and coning was quantified by considering the sensitivity of the length of the reservoir in x-direction. Fig. 5.11a Increasing the length increases the oil in place. It was observed that as the length increases, the average oil column height below perforation increases. Fig. 5.11b shows the effect of reservoir length on recovery.

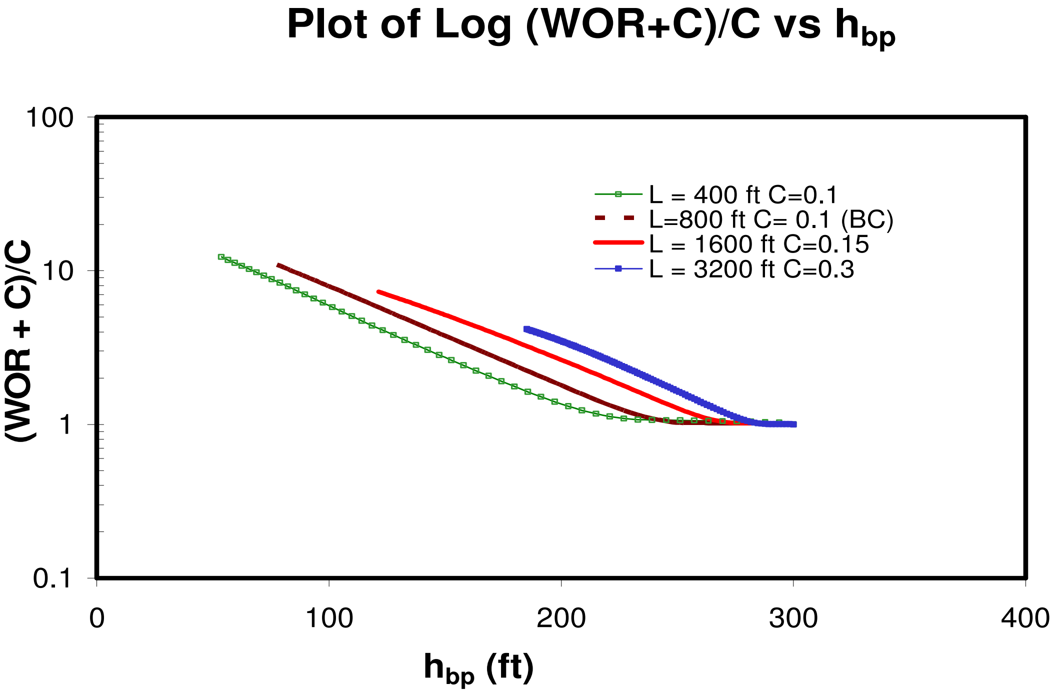

Fig. 5.11a-Effect of Reservoir Length - Log (WOR+C)/C vs. h_{bp}.

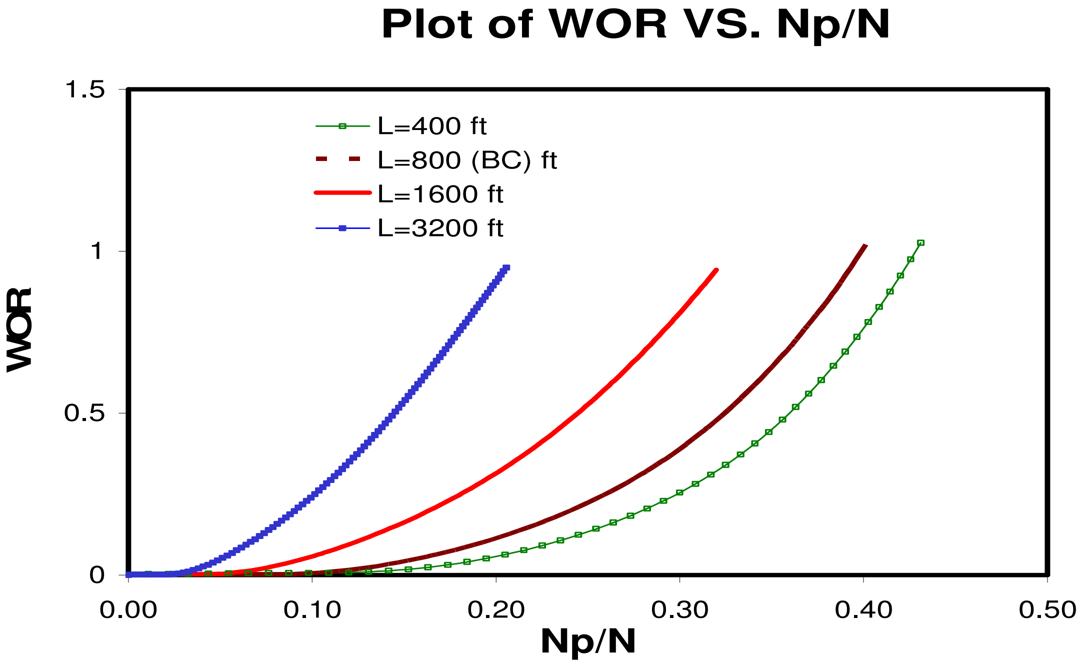

Fig. 5.11b-Effect of Reservoir Length - WOR vs. N_p/N.

Effect of Formation Thickness - *h*

To further quantify the effect of reservoir size on edgewater cusping and coning, the sensitivity of the formation thickness was considered. Although increasing the thickness obviously increases the oil in place, 120 ft of perforation was completed in all the four cases while the vertical distance was held constant at 300 ft for all the cases. Fig. 5.12a shows that as the formation thickness increases, the average oil column height below perforation increases. Fig. 5.12b shows the effect of formation thickness on recovery.

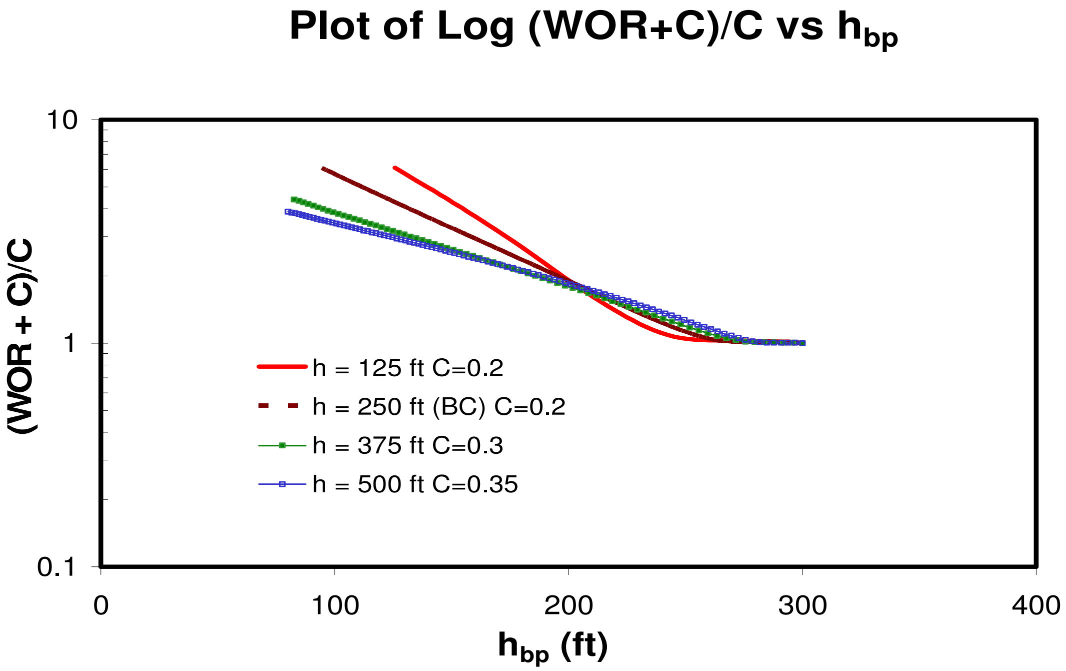

Fig. 5.12a-Effect of Formation Thickness - Log (WOR+C)/C vs. h_{bp}.

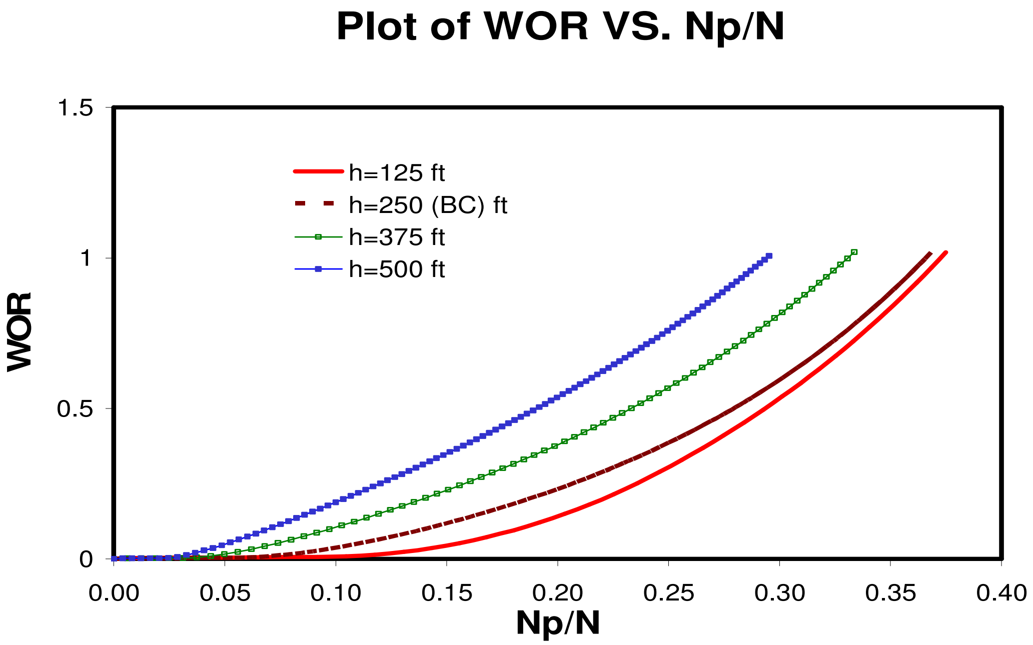

Fig. 5.12b-Effect of Formation Thickness - *WOR* vs. N_p/N.

Effect of Dip Angle - α

Fig. 5.13a shows the effect of dip angle. As dip angle increases, the average oil column height below perforation increases. It is important to note that changing the dip angle means changing the distance to the top of the formation which implies changing the vertical distance. Thus a lower dip angle has higher oil in place. The higher the dip angle, the higher the tendency to have earlier water breakthrough. Fig. 5.13b shows the effect of dip angle on recovery. It was observed that a cross-over exist on the recovery plot. A plot of WOR vs. Time was made to check the simulation results. There is no cross-over Fig. 5.13c. Gravity number was also calculated at breakthrough and found to be approximately the same – from 0.048 - 0.051.

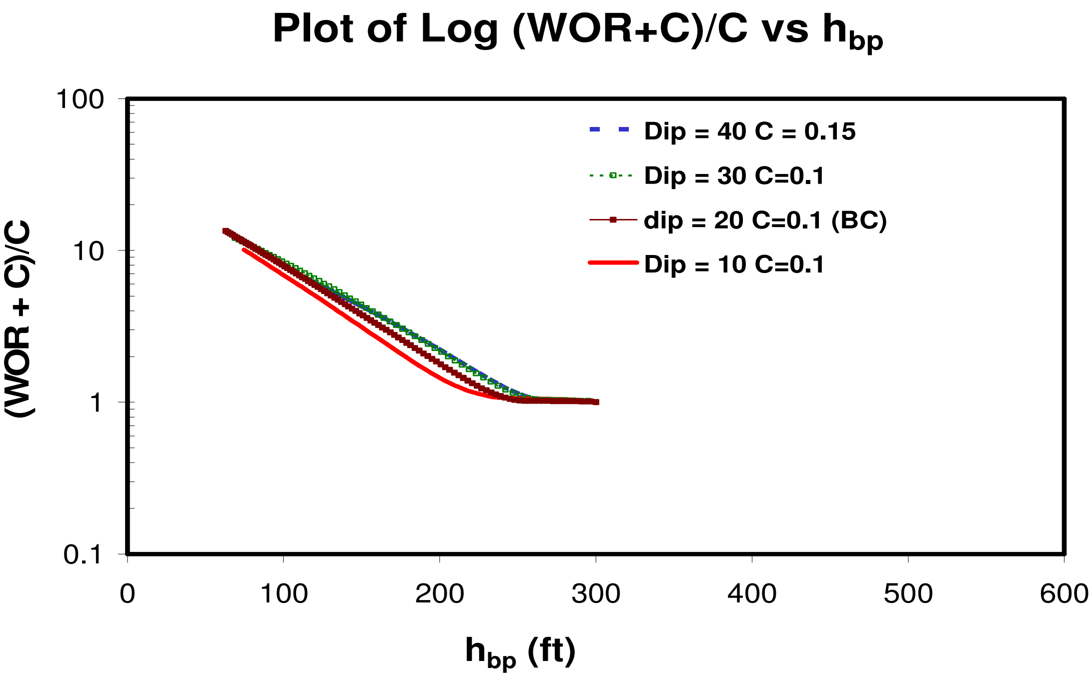

Fig. 5.13a-Effect of Dip Angle - Log (WOR+C)/C vs. h_{bp}.

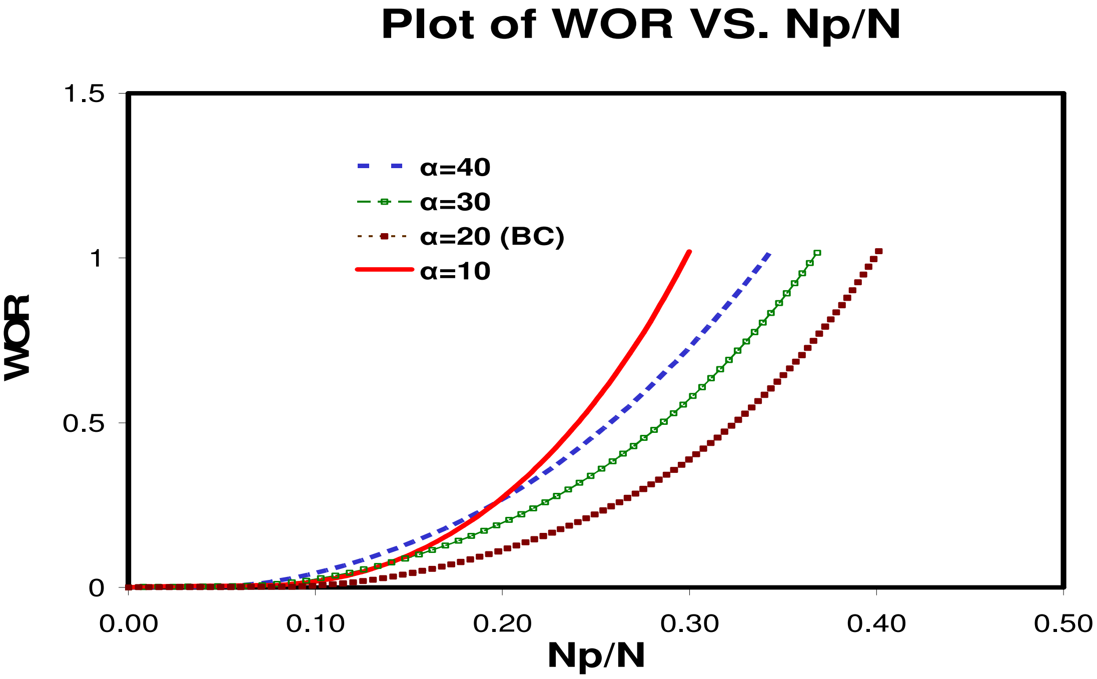

Fig. 5.13b-Effect of Dip Angle - *WOR* vs. N_p/N.

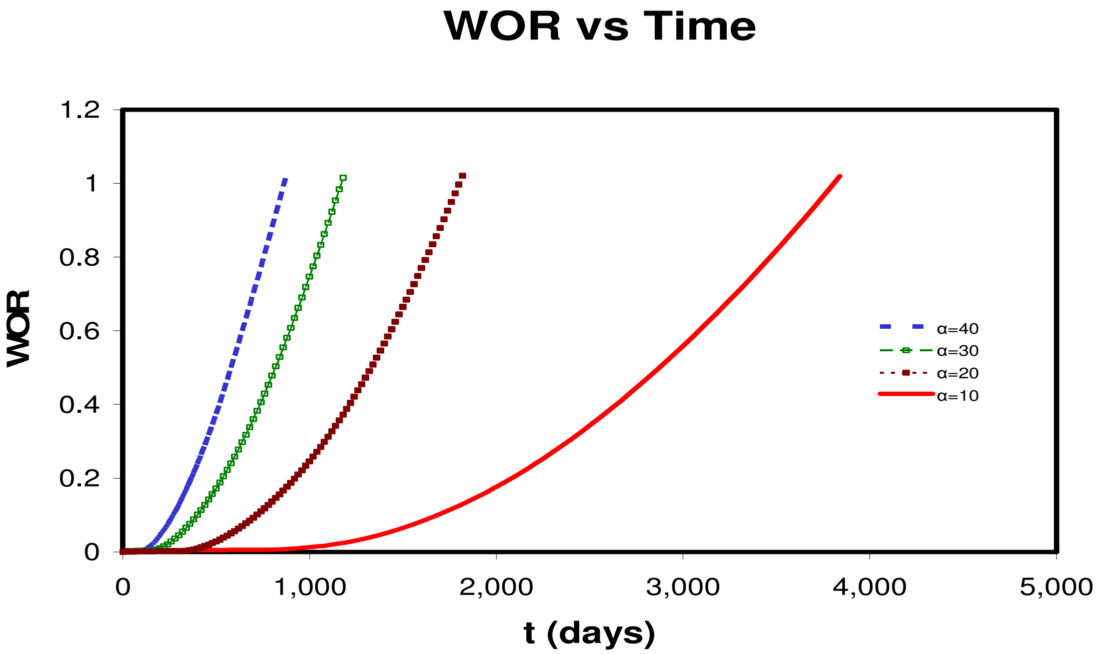

Fig. 5.13c-*WOR* vs. *Time* - Dip Angle.

Effect of Vertical Distance to Water-Oil Contact (WOC) - h_v

Fig. 5.14a shows the effect of vertical distance to *WOC* (initial stand off) for different distances observed. By moving the water-oil contact the target vertical distance is achieved. Increasing the vertical distance implies increasing the oil in place. As the vertical distance increases, the slope of the *WOR* plot decreases. Fig. 5.14b shows the effect of vertical distance on recovery. To investigate the presence of a cross-over in the recovery plot, a plot of WOR vs. Time was made to check the simulation results Fig. 5.14c. Gravity number obtained at breakthrough for distances 200 – 500 ft was 0.032 - 0.08 and monotonic.

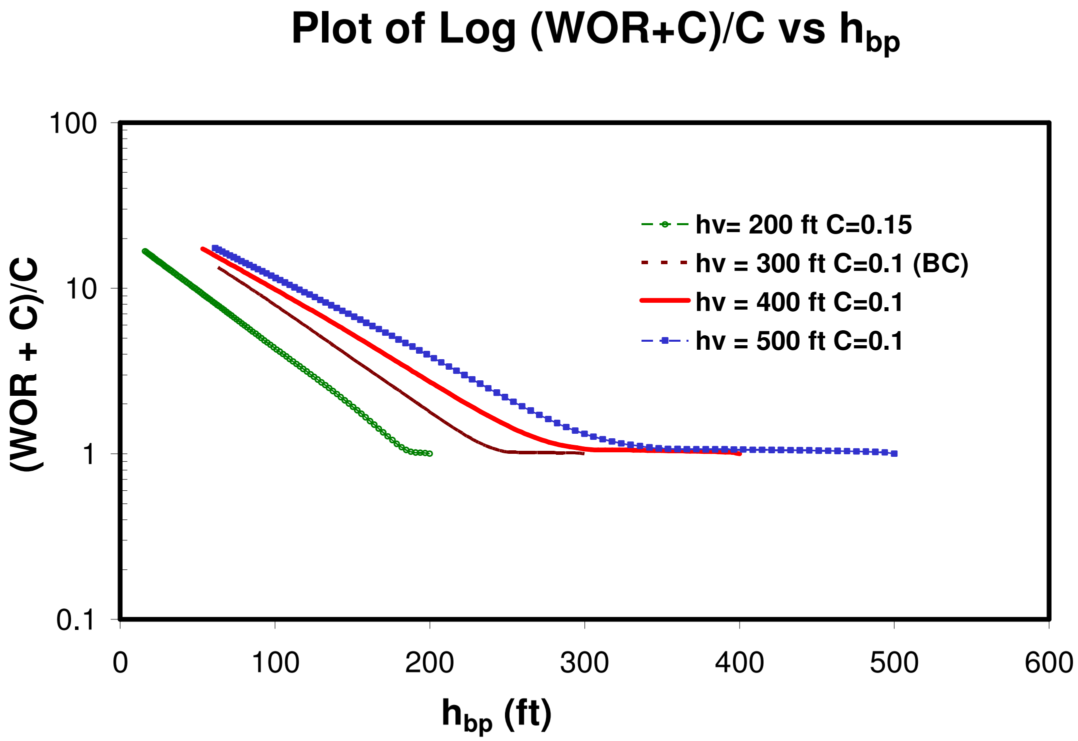

Fig. 5.14a-Effect of Vertical Distance - Log (WOR+C)/C vs. h_{bp}.

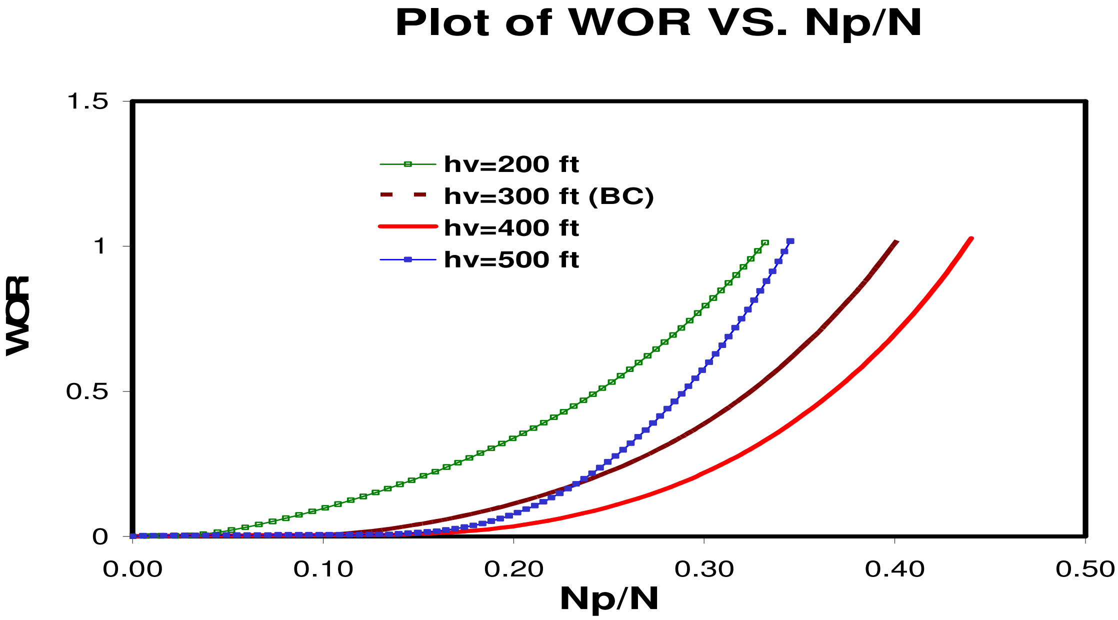

Fig. 5.14b-Effect of Vertical Distance - *WOR* vs. N_p/N.

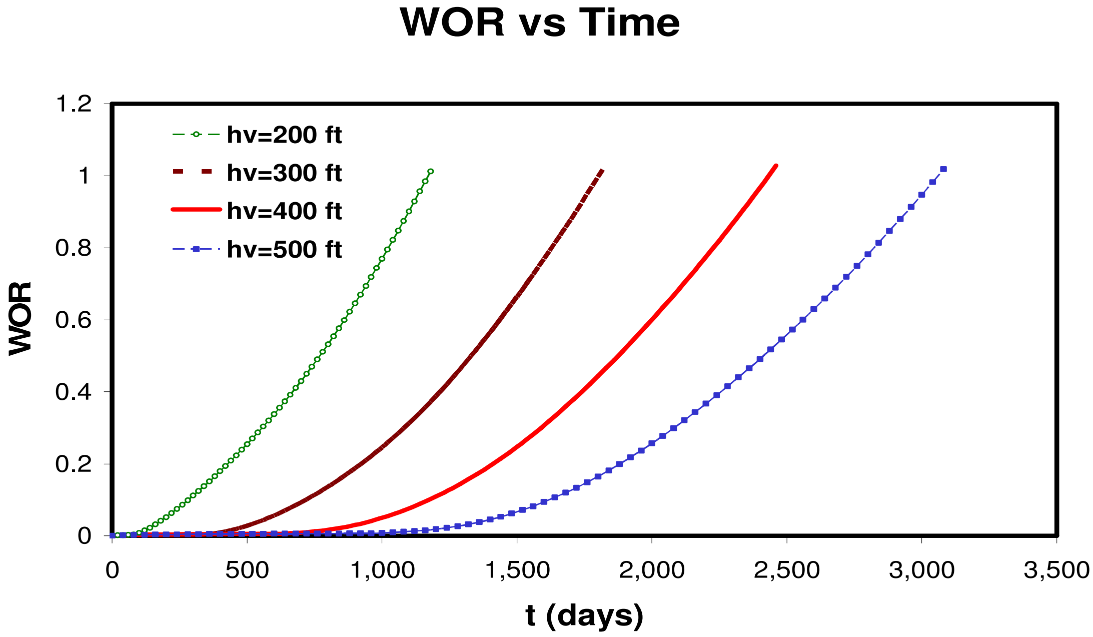

Fig. 5.14c-*WOR* vs. *Time* – Vertical Distance.

Generalized Correlations and Parameter Groups

Following the Addington approach and using the spider plot procedure as described in Appendix B, a correlation that relates the average oil column height at water breakthrough, h_{wb}, slope of the water-oil ratio plot, m and constant C to the various reservoir and fluid properties was developed based on the sensitivity analysis.

Three parameter groups were defined for h_{wb}, m and C. These are P_1, P_2 and P_3 respectively. The parameter group P_1 for the average oil column height at water breakthrough h_{wb}, is related to the model parameters by the equation below:

$$P_1 = \frac{q_t^{0.04} M^{0.13} h_v^{0.57} h^{0.11} L^{0.12} \tan\alpha^{0.1} \left(\frac{k_v}{k_h}\right)^{0.01}}{k_h^{0.1} hp^{0.1} \Delta\gamma^{0.2} {\frac{k_{ml}}{k_{\max}}}^{0.1}} \quad \text{……..……………………....……} \tag{5.1}$$

The parameter group P_2 for the slope of the water-oil ratio plot is related to the model parameters by the equation below:

$$P_2 = \frac{k_h^{0.1} h_p^{0.2} L^{0.03}}{q_t^{0.04} h_v^{0.4} \Delta\gamma^{0.16} M^{0.31} {\frac{k_v}{k_h}}^{0.03} \tan\alpha^{0.1} {\frac{k_{ml}}{k_{\max}}}^{0.1} h^{0.51}} \quad \text{……. ………………......} \tag{5.2}$$

The parameter group P_3 for the constant value used to obtain a straight line is related to the model parameters by the equation below:

$$P_3 = \frac{M^{1.8} L^{0.8} \tan\alpha^{0.6} h^{0.4} k_h^{0.1}}{h_v^{0.44} h_p^{0.43}} \quad \text{……………………………………………..} \tag{5.3}$$

The model parameters represented in the three parameter groups were varied independently and incorporated into the three parameter groups on the basis of their relationship as independent variables as discussed above. These parameter groups are not dimensionless. The effect on h_{wb}, m and C were also determined.

The effect of the parameter groups on h_{wb}, m and C was quantified by comparing the values obtained from the parameter groups to the observed values. To achieve a match the correlation was fitted to equations of the form:

$$h_{wb} = 2 * P_1 \quad \text{(5.4)}$$

$$m = 0.1 * P_2 \quad \text{(5.5)}$$

$$C = 0.016 * P_3 \quad \text{(5.6)}$$

Parameter Group Experimental Range

Fig. 5.15 – 5.17 shows the plot of the observed properties versus the parameter groups obtained from the correlation. The experimental range for parameter group 1, P_1 is 97-163, for parameter group 2, P_2 is 0.0377 – 0.0765 and parameter group 3, P_3 is 2.69 – 98.71.

Fig. 5.15 shows how equation 5.4 fits the experimental range. We can safely say equation 5.4 describes the plot well. Fig. 5.16 shows how equation 5.5 fits the experimental range. We observe a good fit. Equation 5.6 is the straight line plot in Fig. 5.17. One might suggest that a reason for not having a perfect fit is that C is visually determined which is really subjective.

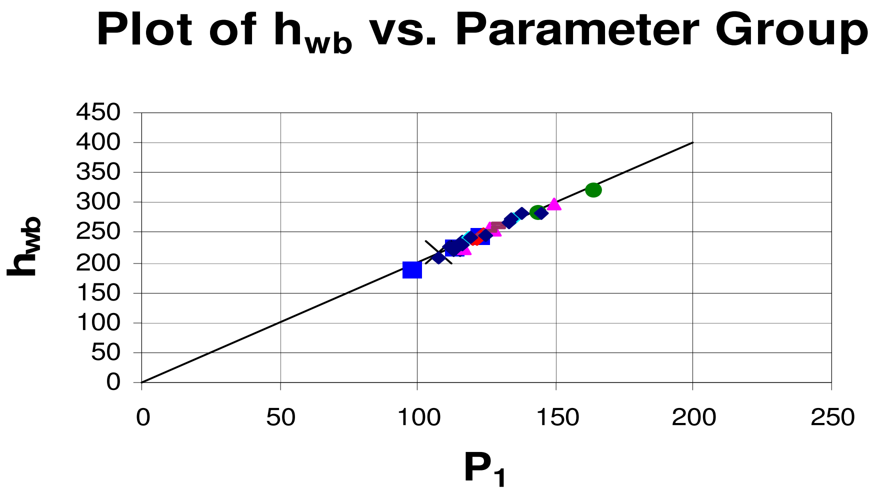

Fig. 5.15-Comparison of h_{wb} Observed and h_{wb} Obtained From Eq. 5.4 Within the Experimental Range.

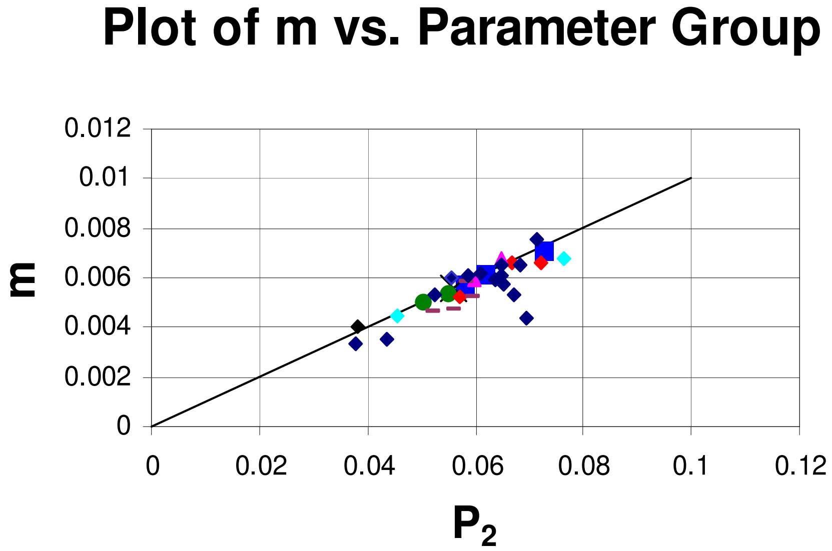

Fig. 5.16-Comparison of m Observed and m Obtained From Eq. 5.5 Within the Experimental Range.

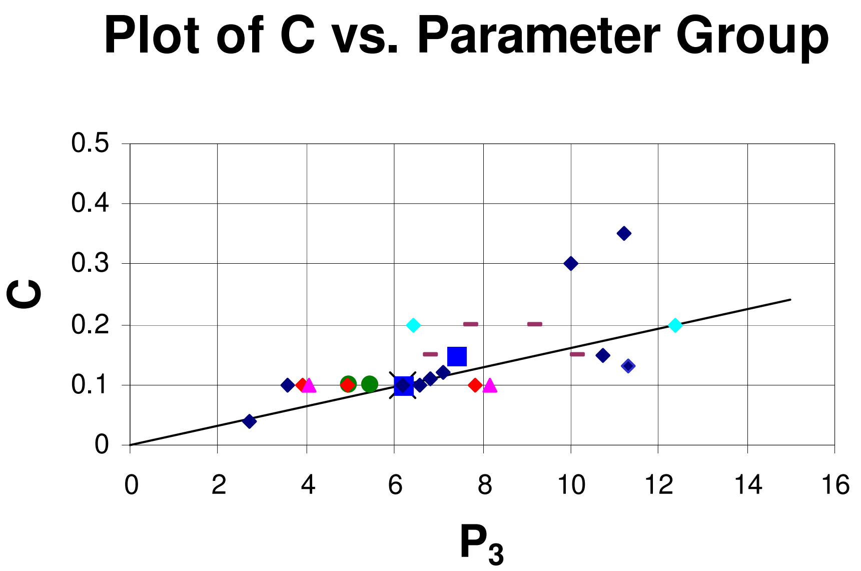

Fig. 5.17-Comparison of *C* Observed and *C* Obtained From Eq. 5.6 Within the Experimental Range.

Basic Equations

The research approach is based on the observation that a straight line results when the *(WOR +C)/C* is plotted against the average oil column height below perforations on a semi-log scale. The entire cusping and coning performance can be described by the equation below:

$$\log\left[\frac{WOR+C}{C}\right] = m(h_{wb} - h_{bp}) \text{ .... (5.7)}$$

The average oil column height below perforation for each time step can be calculated from equation 5.8. h_{wb} can be obtained from Eq. 5.4. Appendix A shows the derivation of the equation for calculating the height of the water invaded zone ΔH for each time step.

$$h_{bp} = H_t - \Delta H - h_{ap} - h_p \text{ .... (5.8)}$$

$$\Delta H = \frac{N_p B \tan\alpha}{hL\phi(1 - S_{wc} - S_{or})} \quad \text{...} \quad (5.9)$$

From equation 5.7, *WOR* can be calculated

$$WOR = C\left[10^{m(hwb-hbp)}\right] - C \quad \text{..} \quad (5.10)$$

If the average oil column height below perforation, h_{bp} is greater than the average oil column height at water breakthrough, $h_{wb,}$ then *WOR* = 0, else *WOR* can be obtained from Eq. 5.10.

For two phase flow,

$$q_o + q_w = q_t \quad \text{...} \quad (5.11)$$

$$\frac{q_w}{q_o} = WOR \quad \text{...} \quad (5.12)$$

From 5.11 and 5.12,

$$q_o = \frac{q_t}{1 + WOR} \quad \text{..} \quad (5.13)$$

$$q_w = q_o * WOR \quad \text{...} \quad (5.14)$$

We can obtain the equation for calculating the cumulative production at water breakthrough and subsequently breakthrough time by substituting Eq. 5.9 into Eq.5.8 at water breakthrough.

$$(N_p)_{bt} = \frac{hL\phi(1 - S_{wc} - S_{or})(H_t - h_{wb} - h_{ap} - h_p)}{5.615 B \tan\alpha} \quad \text{..............................} \quad (5.15)$$

$$t_{bt} = \frac{(N_p)_{bt}}{q_t} \quad \text{...} \quad (5.16)$$

Summary

A single well model was calibrated to reservoir simulation runs by carrying out an extensive parametric sensitivity analysis of the various reservoir and fluid properties. A tank or material balance model was used to establish the relationship between results from simulation runs and reservoir parameters to determine and quantify the movement of the water-oil interface for every time-step. A new plotting method was introduced for interpreting the sensitivity of each model parameters. The relationship between each model parameters and three graphical variables was used to develop the set of empirical correlations.

CHAPTER VI

COMPUTER PROGRAM AND APPLICATION

Overview

In the last two chapters, we introduced the procedure for the development of the simulation model and constitutive equations. In this chapter, we introduce the development of the computer program that incorporates the techniques presented in this dissertation and the application of the program.

The importance of a simple, predictive tool at the start of a field planning/simulation project cannot be over-emphasized. Accurate and valid information is the "life blood" of the petroleum industry. Making effective decisions require that data is processed and analyzed quickly. The above challenges impelled the development of the computer program. The developed correlations were incorporated into a computer program to estimate water breakthrough time and water-oil ratio performance after breakthrough. It can also be used to predict oil rate, water rate, water-cut and cumulative oil production.

The program can be used by reservoir engineers to hasten their decision-making processes. It allows the engineer to conduct series of "what-if" analysis and evaluate numerous prediction techniques. It allows the engineers to design and plan operations within the program and thus prepare for reality. The program was developed using the Excel Visual Basic Programming language (Excel VBA). One of the major reasons why Excel VBA was chosen is that it's available on most computers. The language also provides powerful features such as graphical user interfaces, event handling, objectoriented features, error handling, structured programming etc. These features afford the user the opportunity to continuously interact with the input data as well as a dynamic visual appreciation of the implication of such interactions with the interface. The various part of the program is briefly explained in the following sections. Fig. 6.1 shows the program front page.

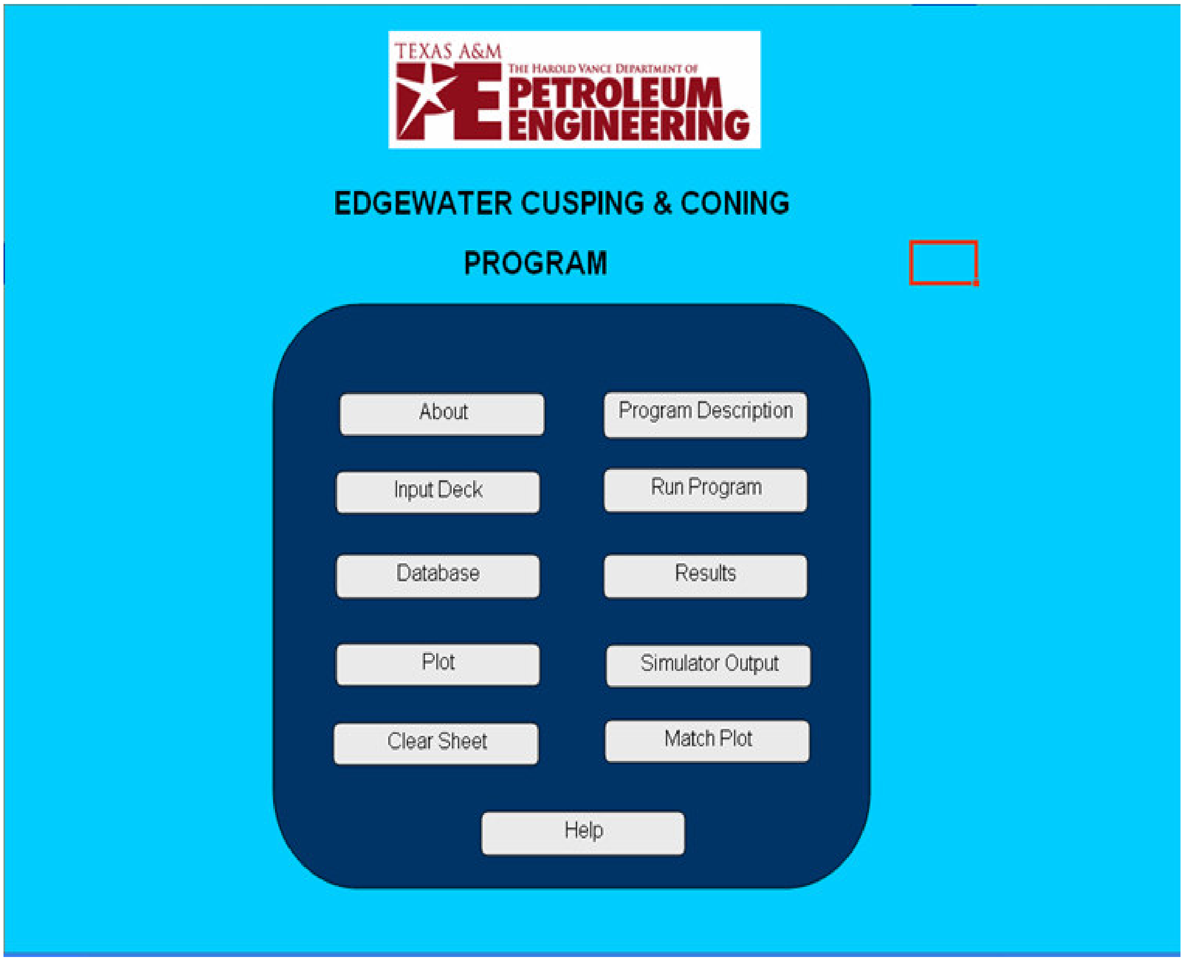
TEXAS A&M
THE HAROLD VANCE DEPARTMENT OF
PETROLEUM ENGINEERING
EDGEWATER CUSPING & CONING
PROGRAM
About
Program Description
Input Deck
Run Program
Database
Results
Plot
Simulator Output
Clear Sheet
Match Plot
Help

Fig. 6.1-Edgewater Program Front Page.

Program Layout

The program is made up of several worksheets which include the Program description, Input deck, Run program, Database, Results, Plot and Simulator output worksheets. Fig. 6.2 is a flow chart of the program.

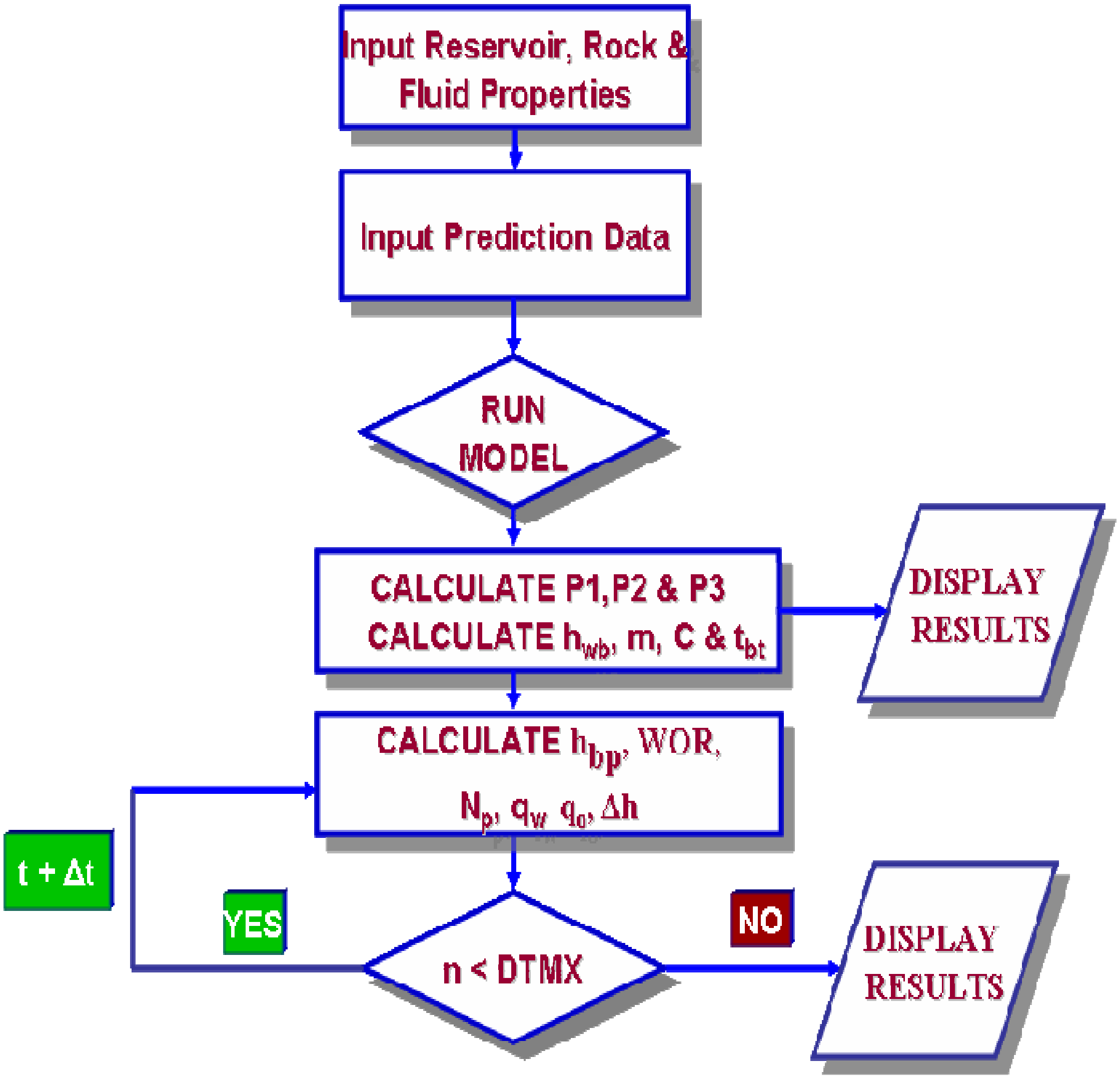
Input Reservoir, Rock & Fluid Properties
Input Prediction Data
RUN MODEL
CALCULATE P1,P2 & P3
CALCULATE h_{wb}, m, C & t_{bt}
DISPLAY RESULTS
CALCULATE h_{bp}, WOR, N_p, q_w q_o, Δh
t + Δt
YES
n < DTMX
NO
DISPLAY RESULTS

Fig. 6.2-Edgewater Program Flow Chart.

Program Description

This worksheet familiarizes the program user with the various terms and symbol used. This includes the meaning and representation of what the terms means.

Data Input

The edgewater cusping and coning program is made up of an input data form called Reservoir information. Reservoir properties, rock properties, fluid properties and prediction information can be inputted.

- Reservoir properties

  Information on reservoir dimensions, total vertical thickness, vertical formation thickness, vertical distance, perforation thickness, height above and below perforation and dip angle can be inputted in this sub menu. The program provides the capability to use different set of units in computation. Input parameters can be specified in meters or feet.

- Rock properties

  Permeability, porosity, anisotropy, connate water saturation, residual water saturation and end-point mobility ratio are some of the information that can be inputted in this submenu.

- Fluid properties

  Densities of oil and water, oil formation volume factors are input for the module.

- Prediction data

Since the simulation is carried out under total rate condition, the Total liquid flow rate is specified. The time- step is also specified in days. This is for the output format as computation and result-output is based on the number specified. The critical rate calculation is based on a specified height. Therefore, this information is inputted to obtain oil critical rate at a specific height. The initial average oil column height below perforation is inputted.

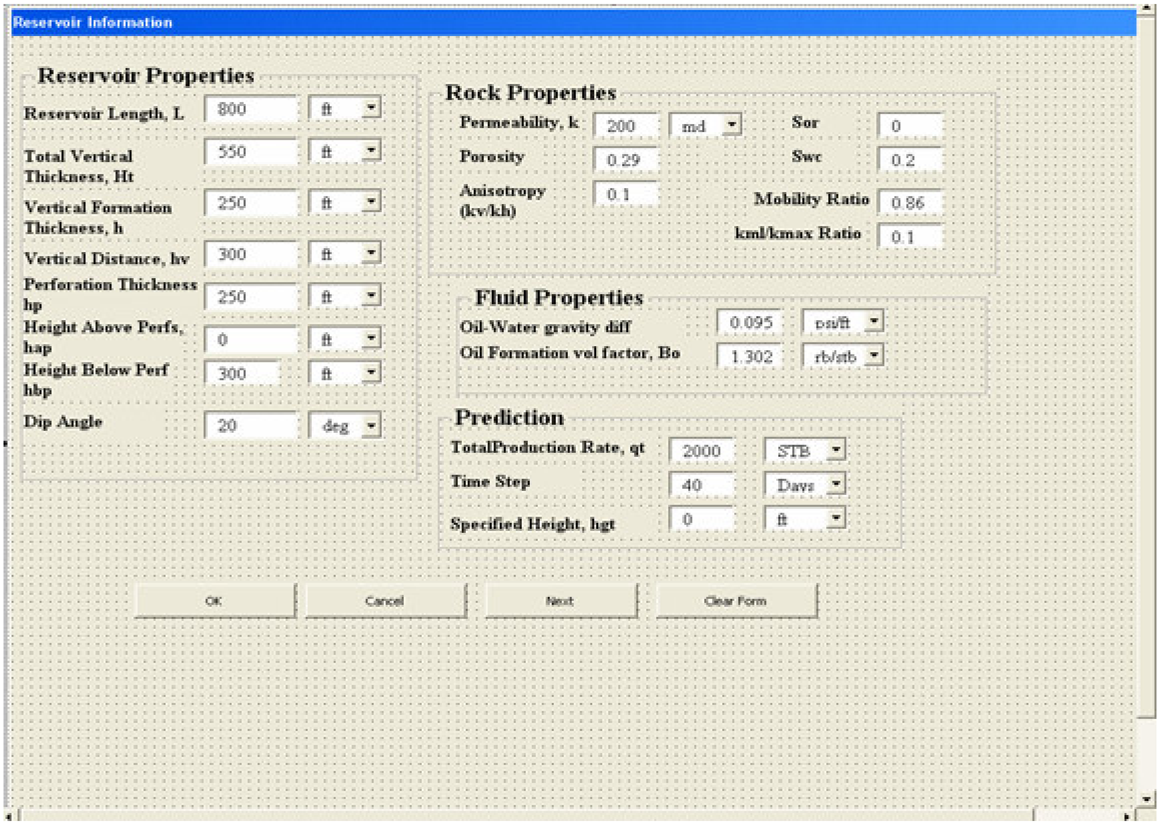

Reservoir Properties

Reservoir Length, L	800	ft
Total Vertical Thickness, Ht	550	ft
Vertical Formation Thickness, h	250	ft
Vertical Distance, hv	300	ft
Perforation Thickness hp	250	ft
Height Above Perfs, hap	0	ft
Height Below Perf hbp	300	ft
Dip Angle	20	deg

Rock Properties

Permeability, k	200	md
Porosity	0.29	
Anisotropy (kv/kh)	0.1	
Sor	0	
Swc	0.2	
Mobility Ratio	0.86	
kml/kmax Ratio	0.1	

Fluid Properties

Oil-Water gravity diff	0.095	psi/ft
Oil Formation vol factor, Bo	1.302	rb/stb

Prediction

TotalProduction Rate, qt	2000	STB
Time Step	40	Days
Specified Height, hgt	0	ft

Fig. 6.3-Input Form.

Run Program

The program can be run from the input deck or by clicking the run program button on the front page.

Simulator Output Worksheet

The program has the capability to read any simulator output file e.g. Eclipse. The sheet displays the various properties written to results file of the simulator. This is compared to the result obtained from the correlation.

Database Worksheet

The worksheet handles the various data processing/manipulation within the program.

Plot Worksheet

Plot displays the comparison of simulator output with correlation prediction.

Program Calculation Procedure

The VBA program follows the steps listed below.

1. Read in reservoir, rock, fluid and time-step information.
2. Read Simulator result file if needed for comparison purposes only.
3. Calculate the three parameter groups.
4. From the parameters groups, calculate h_{wb}, m, and C.

5. Calculate N_{pbt} and t_{bt}.
6. At time step n, calculate h_{bp}, ΔH, N_p, q_o
7. At time step $n+1$, if $h_{bp} > h_{wb}$ then $WOR = 0$, else calculate WOR, h_{bp}, ΔH, N_p, q_w,q_o

Model Validation

The model was validated by reproducing all the plots obtained from simulation using the empirical correlations. The results are shown in the following plot of Log ((WOR+C)/C) vs. h_{bp} for all the model parameters.

Total Liquid Flow Rate

Fig. 6.4 shows the comparison between simulation and correlation results for liquid rates 500 – 3000 STB/D.

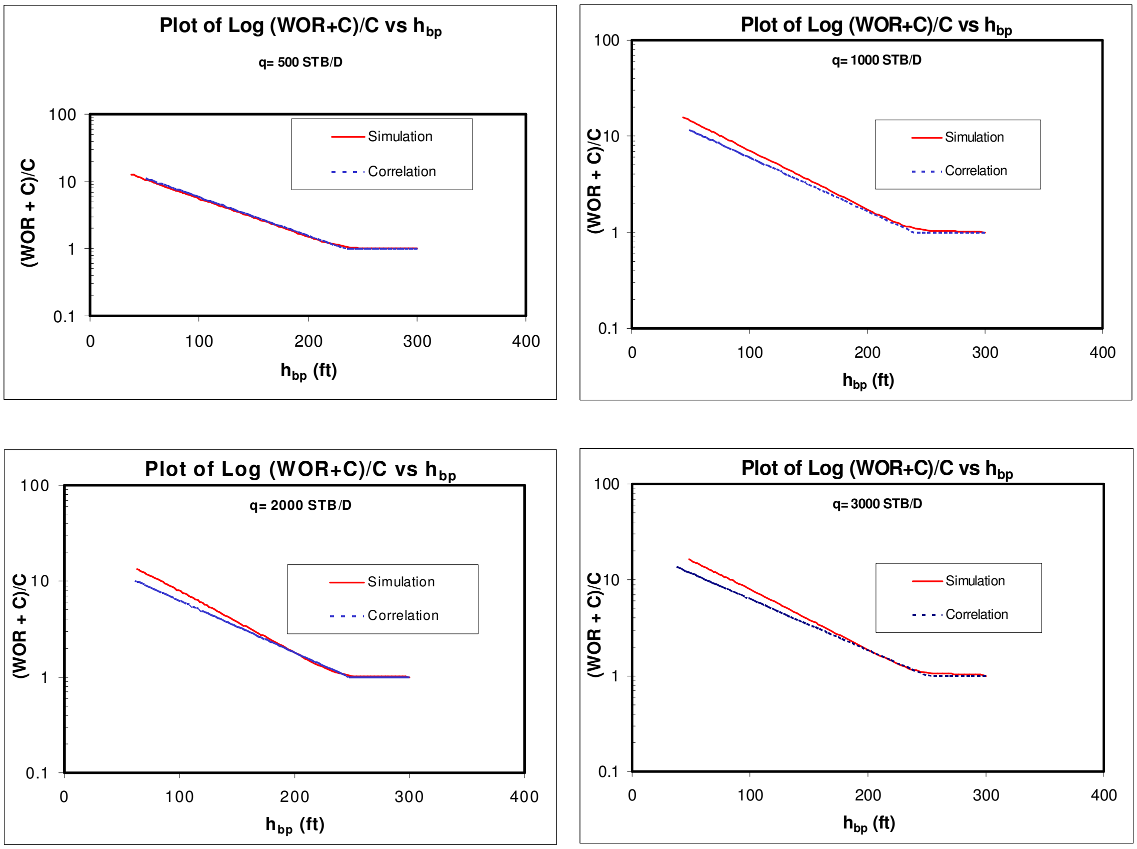

Fig. 6.4-Total Liquid Flow Rate Match.

Endpoint Mobility Ratio

Fig. 6.5 shows the comparison between simulation and correlation results for the various end-point mobility ratios considered.

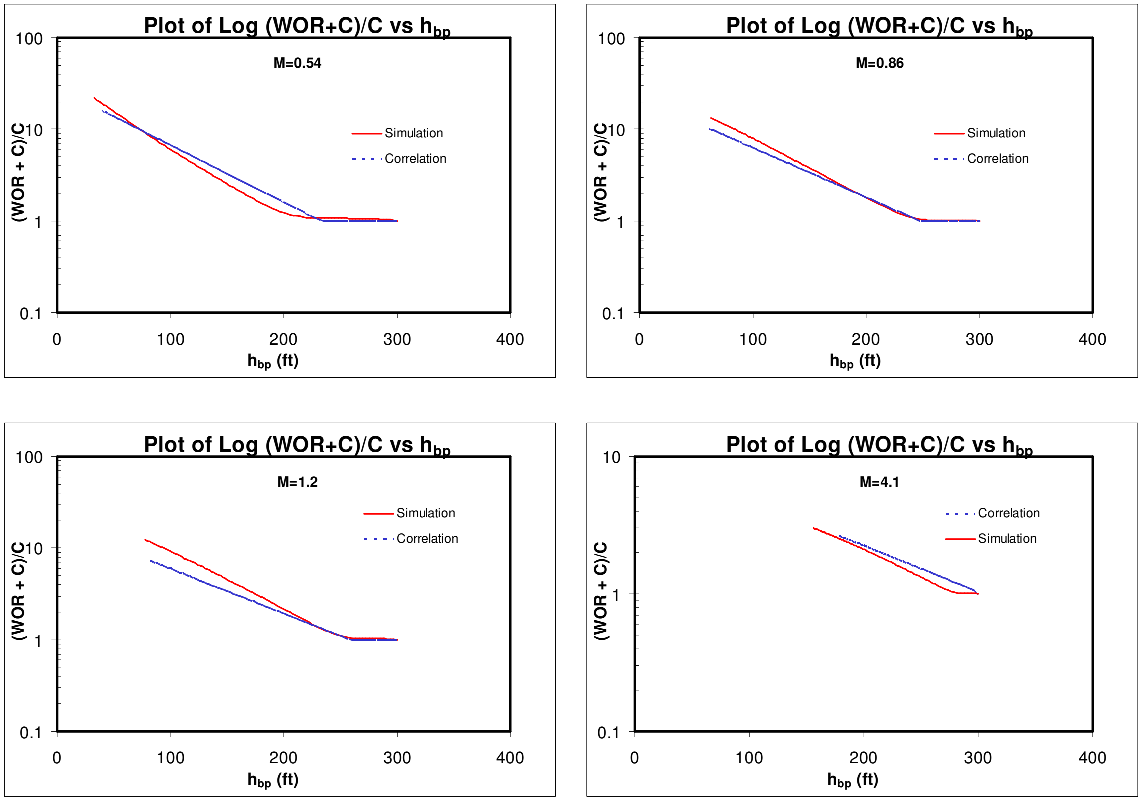

Fig. 6.5-End Point Mobility Ratio Match.

Effect of Horizontal Permeability

Fig. 6.6 shows the comparison between simulation and correlation results for horizontal permeability ranging from 100 – 2000 md.

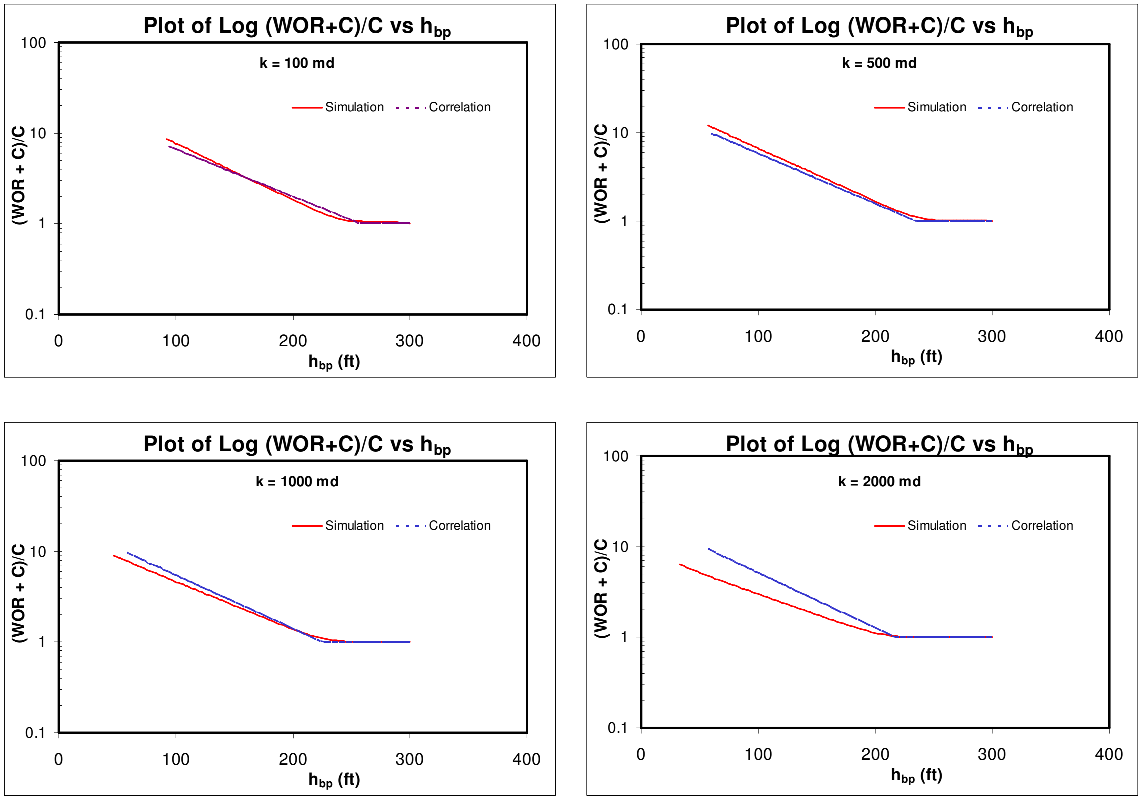

Fig. 6.6-Horizontal Permeability Match.

Effect of Vertical Permeability

Fig. 6.7 shows the comparison between simulation and correlation results for k_v/k_h ranging from 0.001 – 1.

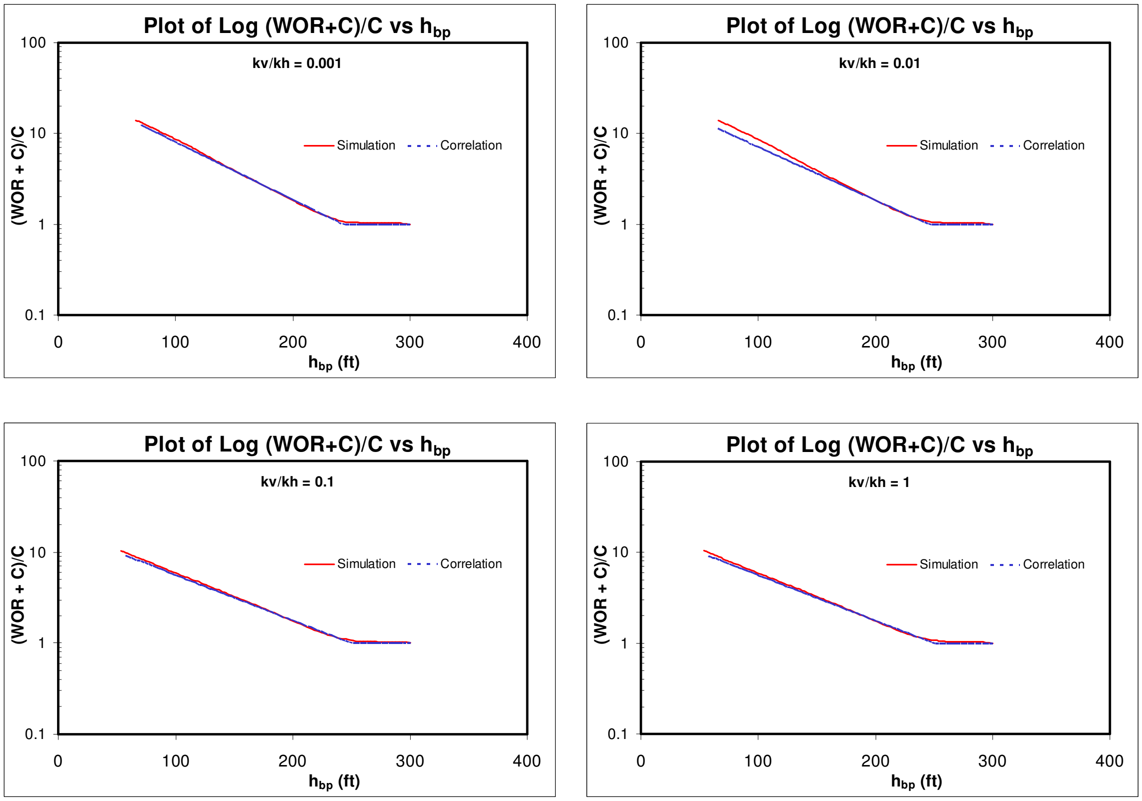

Fig. 6.7-Vertical Permeability Match.

Effect of Perforation Thickness

Fig. 6.8 shows the comparison between simulation and correlation results for various percentage of the oil formation thickness completed.

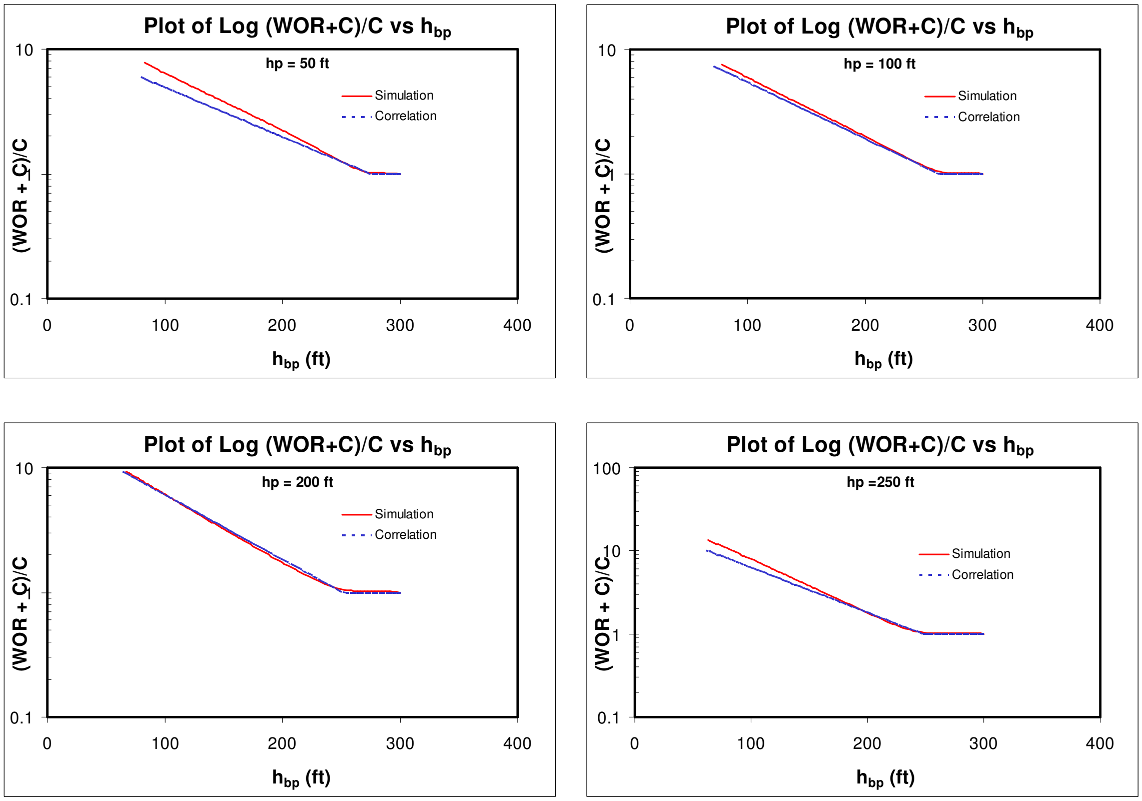

Fig. 6.8-Perforation Thickness Match.

Effect of Water-Oil Gravity Gradient

Fig. 6.9 shows the comparison between simulation and correlation results for gravity gradient ranging from 0.1 – 0.18 psi/ft.

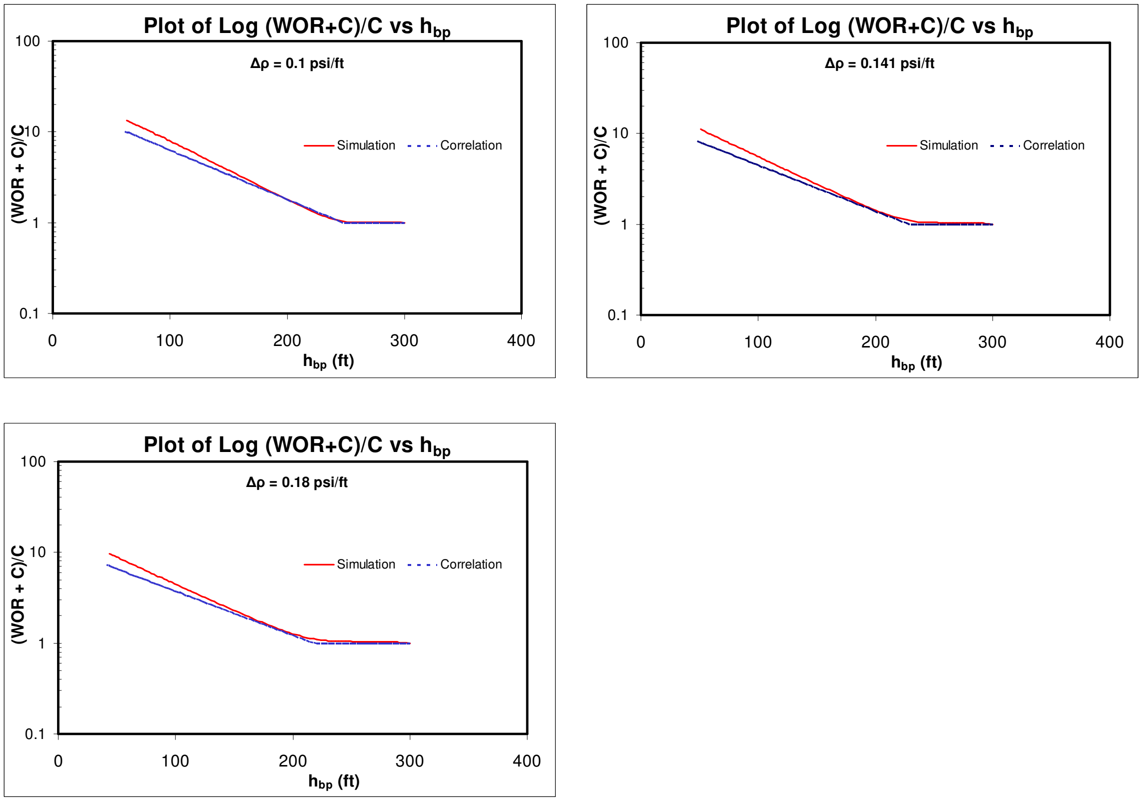

Fig. 6.9-Water-Oil Gravity Gradient Match.

k_{ml}/k_{max} Ratio

Fig. 6.10 shows the comparison between simulation and correlation results for the relative permeability curves.

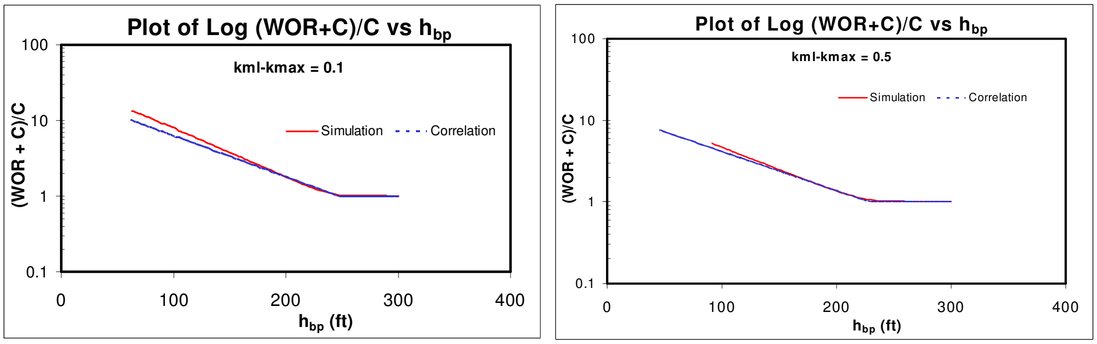

Fig. 6.10- k_{ml}/k_{max} Match.

Reservoir Length

Fig. 6.11 shows the comparison between simulation and correlation results for different reservoir length.

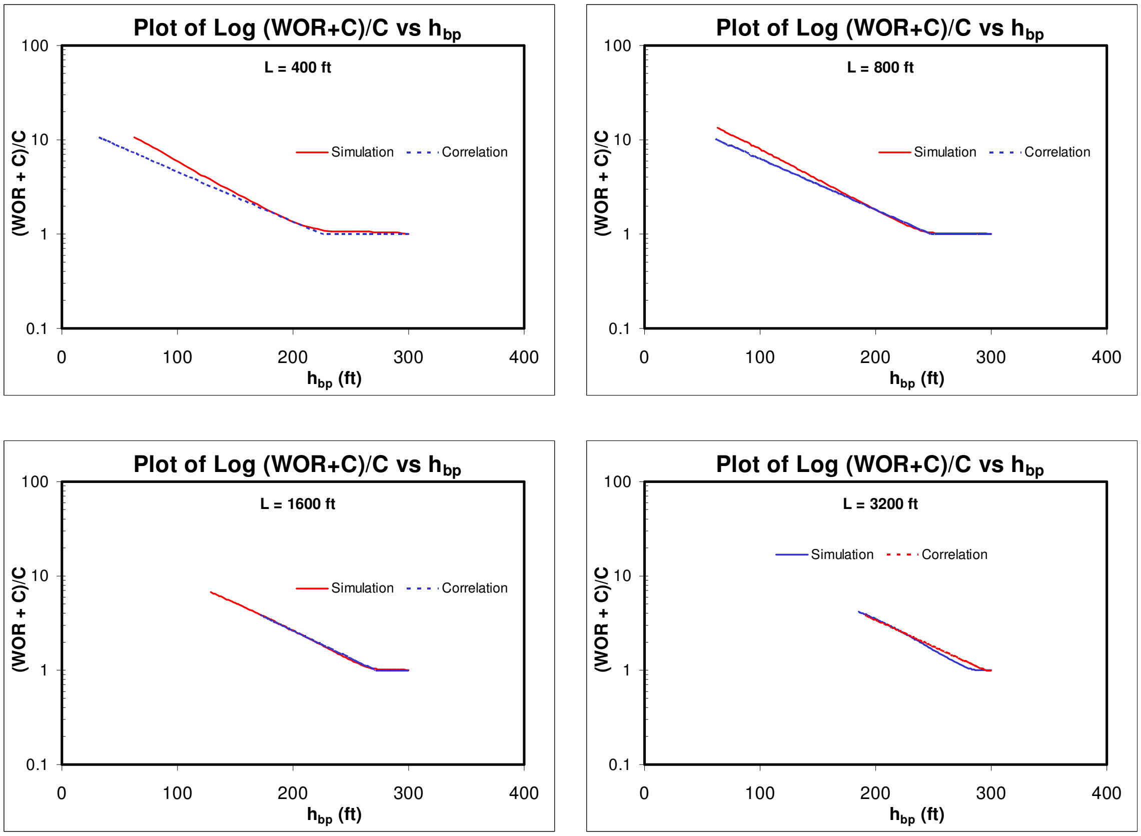

Fig. 6.11-Reservoir Length Match.

Formation Thickness

Fig. 6.12 shows the comparison between simulation and correlation results for formation thickness ranging from 125ft – 500ft.

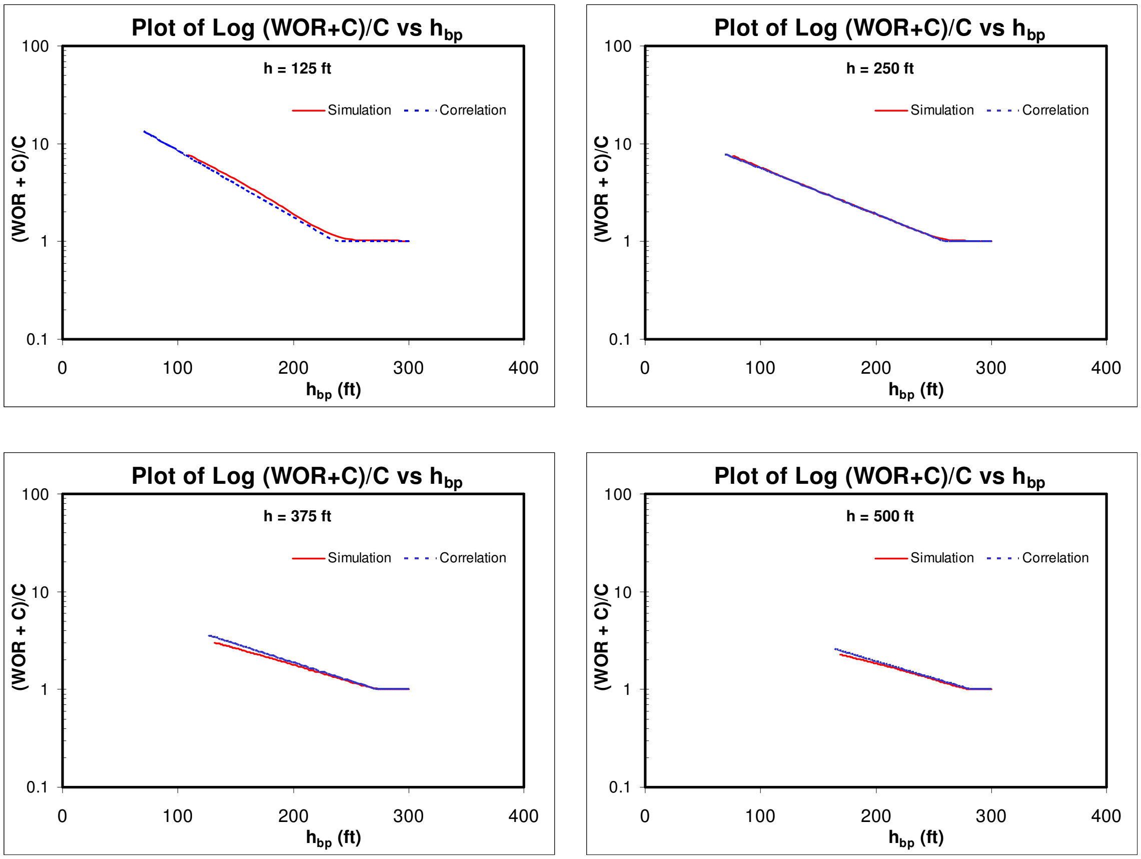

Fig. 6.12-Formation Thickness Match.

Dip Angle

Fig. 6.13 shows the comparison between simulation and correlation results for the dip angles ranging from 10 – 40^{o}.

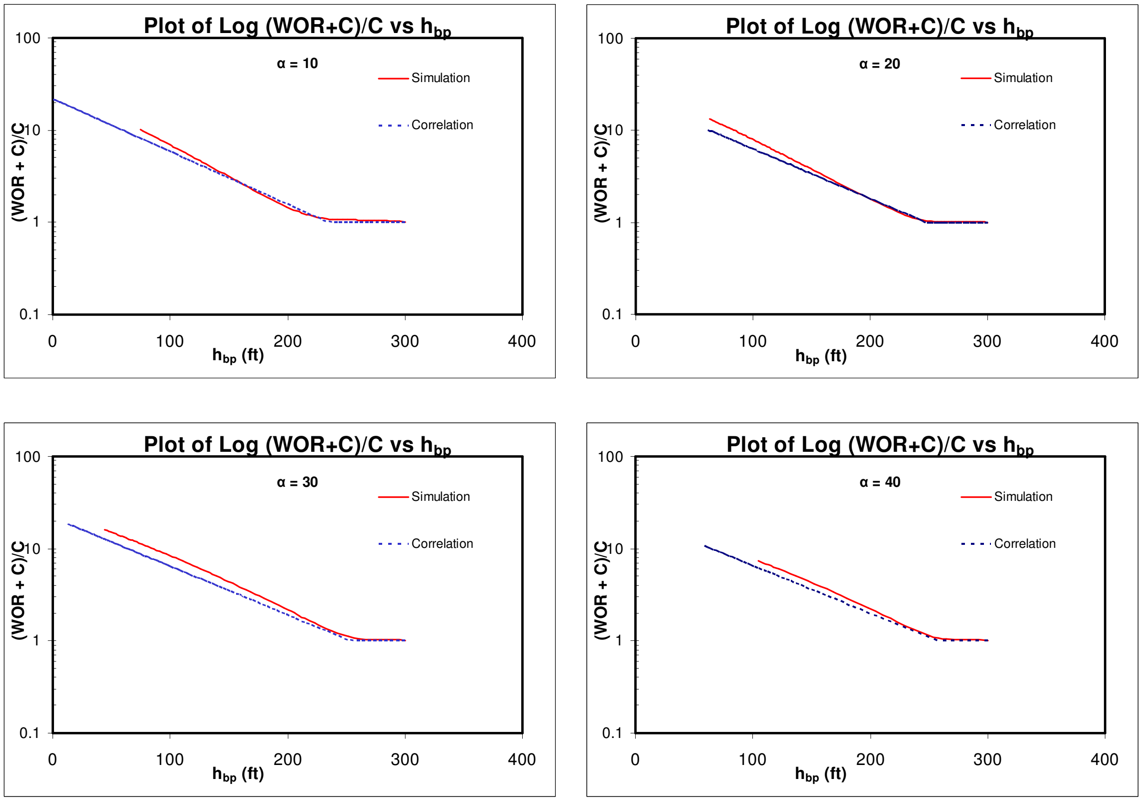
Plot of Log (WOR+C)/C vs h_{bp}

Fig. 6.13-Dip Angle Match.

Vertical Distance

Fig. 6.14 shows the comparison between simulation and correlation results for the vertical distance ranging from 200 – 500ft.

Summary

The developed correlations were used to replicate simulation results for validation purpose and the performance compared. The results showed a good accuracy for breakthrough time and performance after breakthrough.

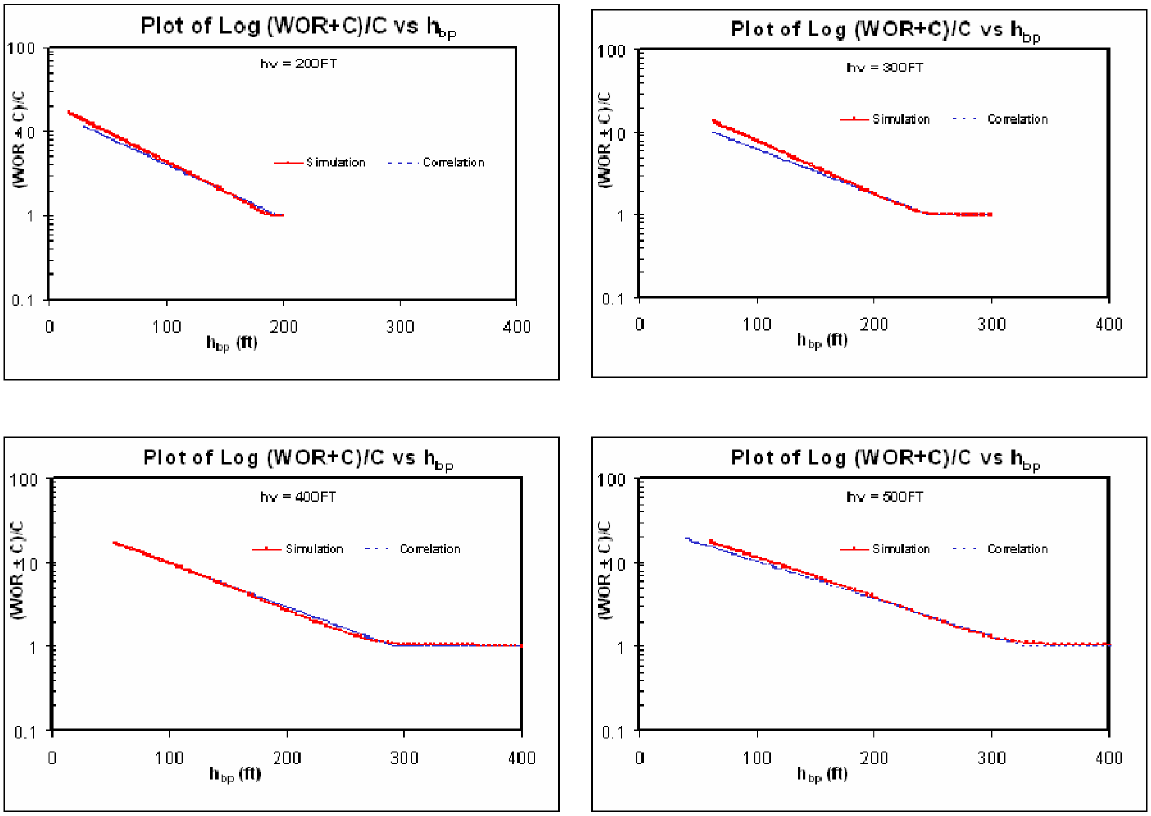

Fig. 6.14-Vertical Distance Match.

Application and Prediction – Synthetic Case

Reservoir properties, rock properties, fluid properties (Table 6.1) are inputted into Eclipse and also into the program and the performance of the developed correlation and program compared. The program was used to match and predict oil rate, water rate, cumulative production, WOR and water cut. Fig.6.15 – 6.19 shows the result. The program was used to match the simulator output after 2000 days of production and to forecast additional 1000 days into the future.

Table 6.1 Synthetic Case Model Parameters			
Model Parameters	**Symbol**	**Value**	**Units**
Total Liquid Flow Rate	q_t	2000	STB/D
End Point Mobility Ratio	M	0.86	
Vertical Distance	h_v	300	ft
Vertical Formation Thickness	h	250	ft
Reservoir Length (in x-dir)	L	800	ft
Permeability	k	200	md
Anisotropy Ratio	k_v/k_h	0.1	
Perforation Thickness	h_p	250	ft
Dip Angle	α	20	deg
Water-oil gravity gradient	$\Delta\gamma$	0.095	psi/ft
Ratio of k_{ml}/k_{max}	k_{ml}/k_{max}	0.1	
Oil formation volume factor	B_o	1.302	RB/STB
Porosity	ϕ	0.29	
Connate Water Sat.	S_{wc}	0.2	
Residual Oil Sat.	S_{or}	0.2	
Height above Perfs	h_{ap}	0	ft
Total Vertical Thickness	H_t	550	ft
Specified height	H_{gt}	0	ft
Time -step	Δt	20	days
Height below perforation	h_{bp}	300	ft

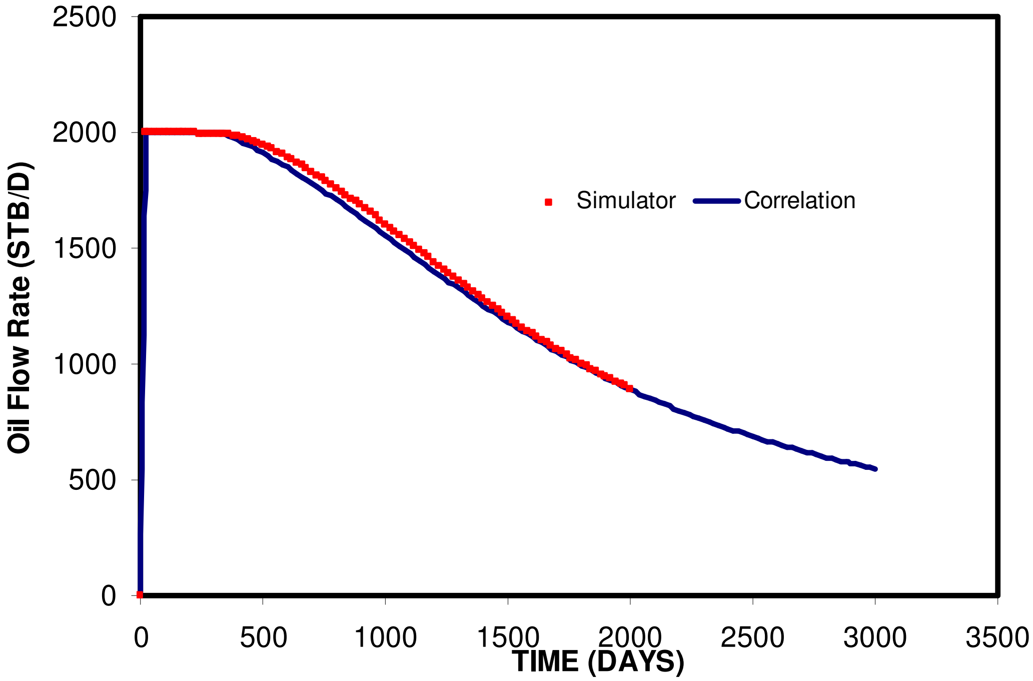

Fig. 6.15-Oil Rate Match and Prediction-Simulation and Correlation Comparison.

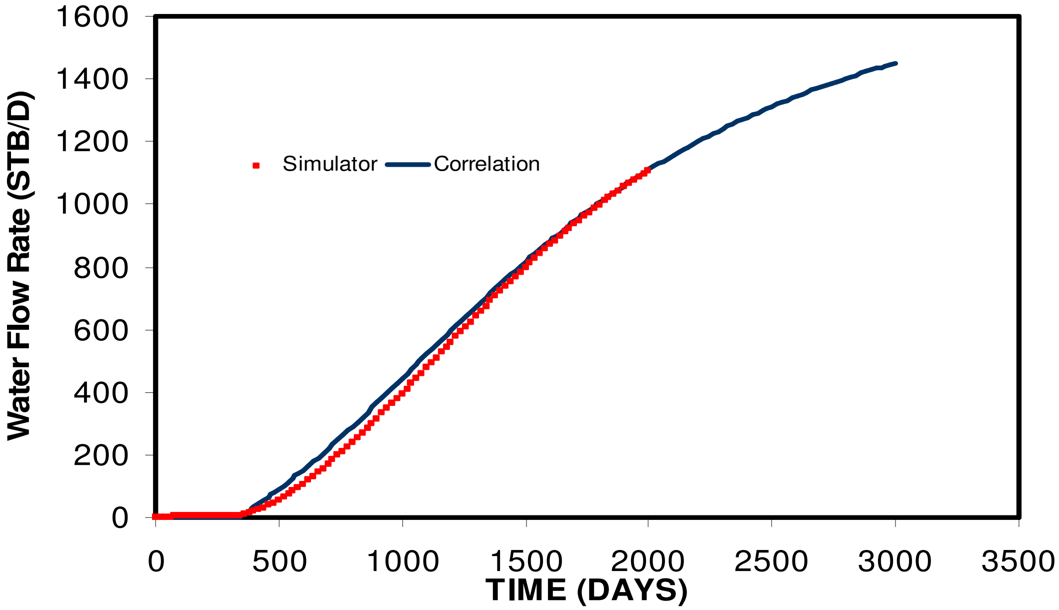

Fig. 6.16-Water Rate Match and Prediction-Simulation and Correlation Comparison.

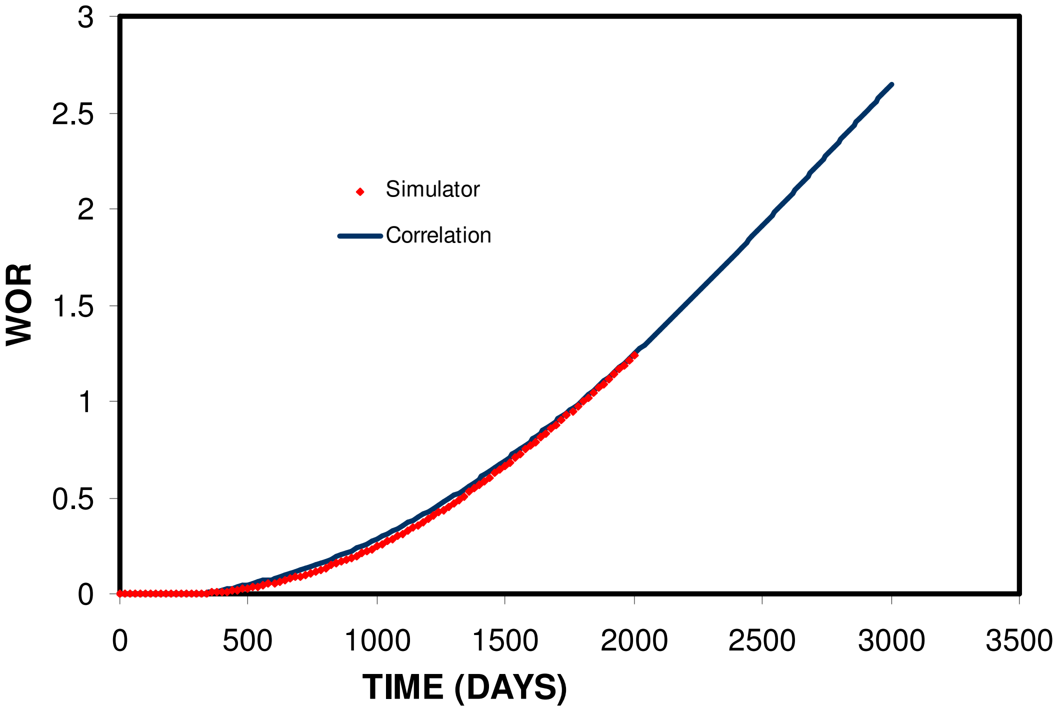

Fig. 6.17-WOR Match and Prediction-Simulation and Correlation Comparison.

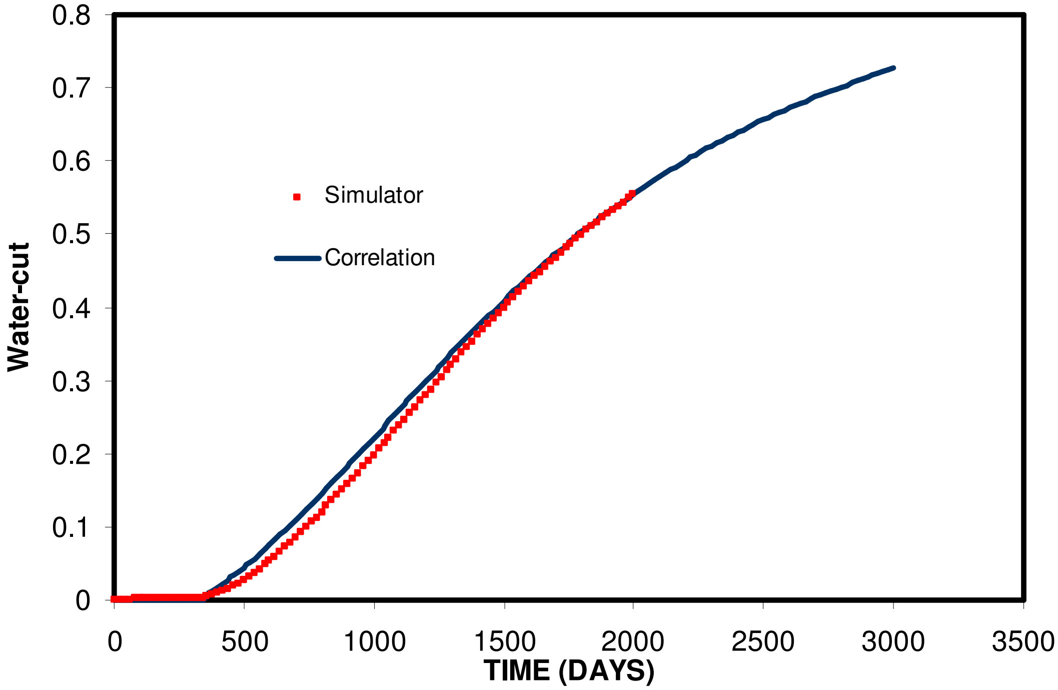

Fig. 6.18-Water-Cut Match and Prediction-Simulation and Correlation Comparison.

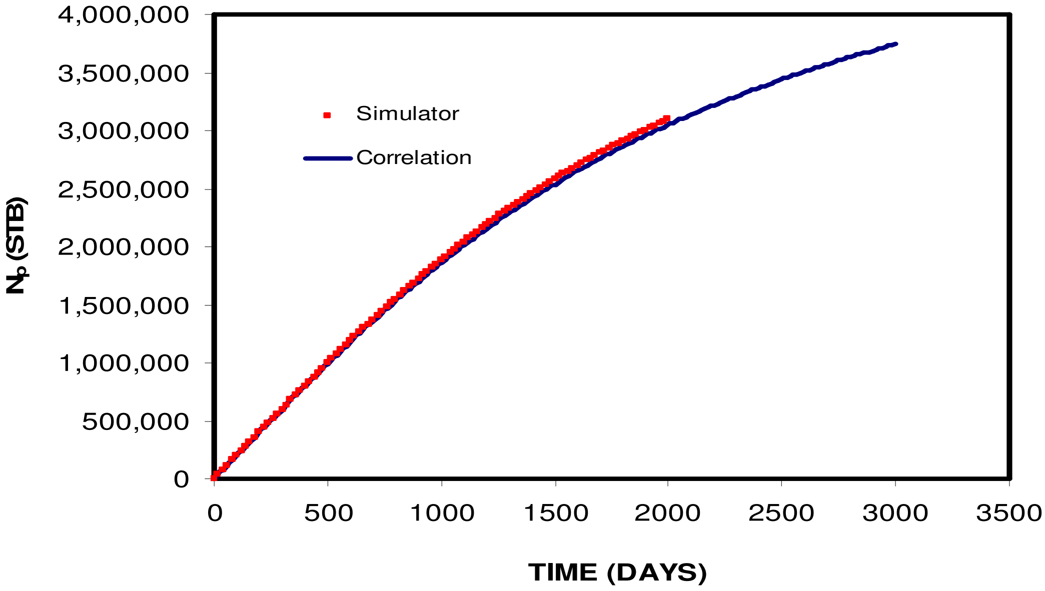

Fig. 6.19-Cumulative Oil Production Match and Prediction- Simulation and Correlation Comparison.

Variable Rate Case Prediction

The developed correlation was tested for variable rate cases. Two cases were considered:

- Rate change before water breakthrough
- Rate change after water breakthrough

Rate Change before Water Breakthrough

Prediction was based on the assumption that WOR has no hysteresis i.e. WOR is only a function of current height below perforation and current production rate. Previous production history has no influence on the current WOR.

In this case, the well was flowed for 200 days at the rate of 2000 STB/D. The rate was dropped to 500 STB/D and flowed for one thousand eight hundred days. Water didn't breakthrough until after 1000 days. The rate was later increased to 1000 STB/D and flowed for another 3000 days. Fig.6.18 shows the comparison between the correlation and simulation results.

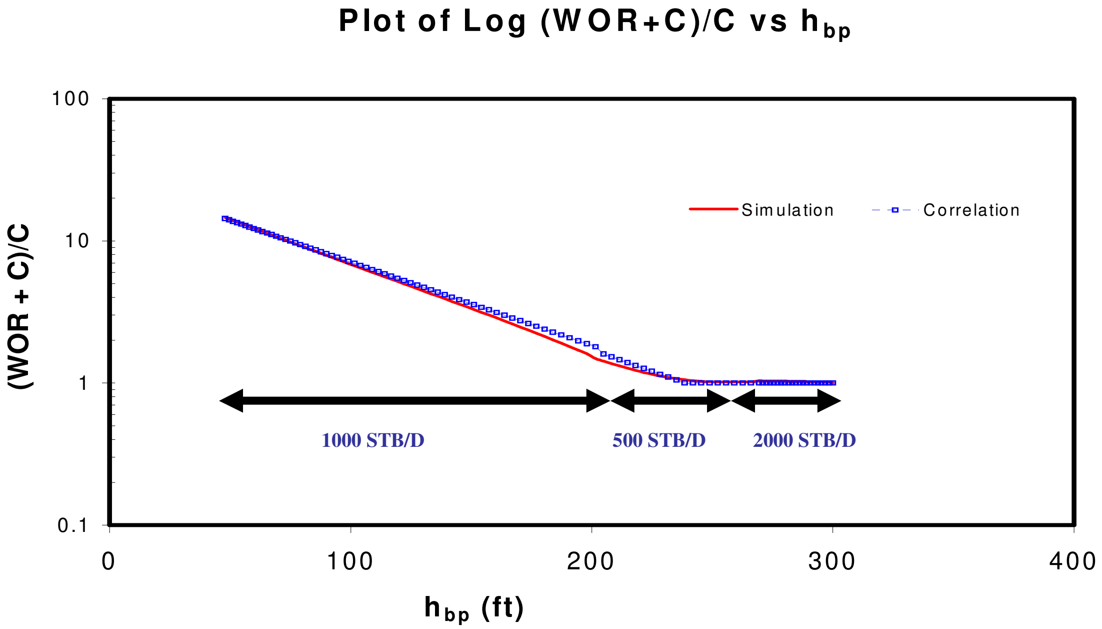

Fig. 6.20-Rate Change before Water Breakthrough.

Rate Change after Water Breakthrough

Here, the well was flowed for 800 days at 2000 STB/D with water breakthrough after 280 days. The rate was later dropped to 500 STB/D and flowed for 2000 days. The production rate was later increased to 1000 STB/D for another 2200 days. This is shown in Fig. 6.19. We show that the correlation captures the effect of rate changes. This confirms the earlier assumption to be correct unlike Yang's observation.

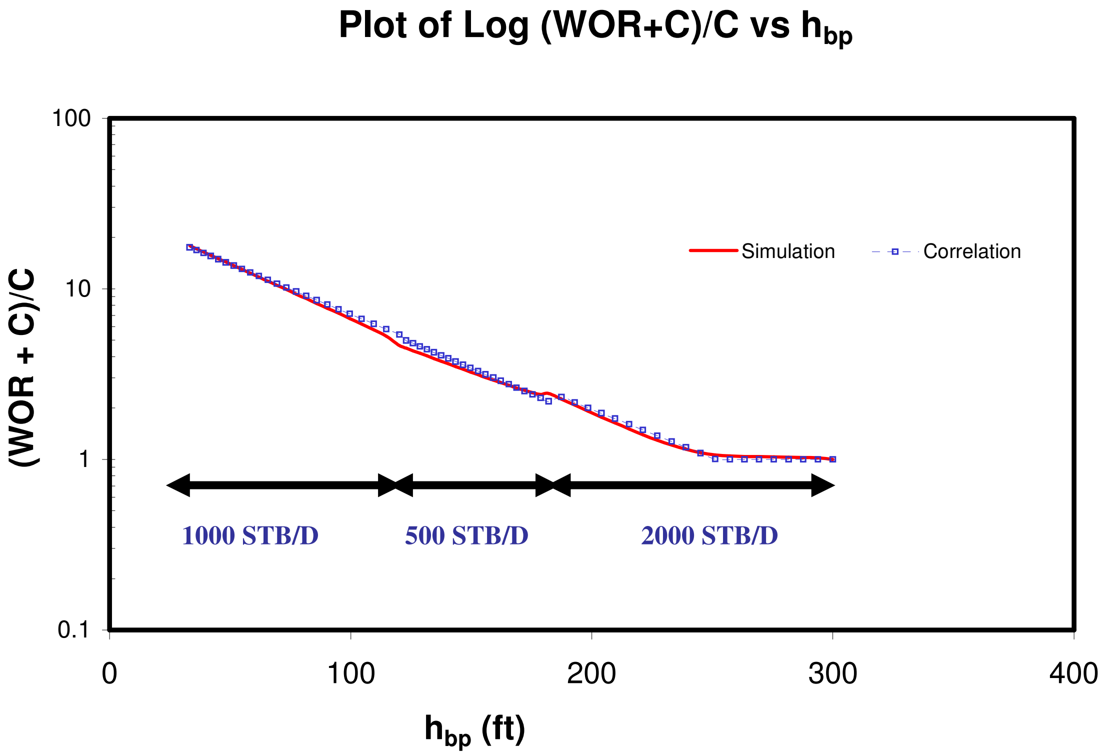

Fig. 6.21-Rate Change after Water Breakthrough.

Field Case Application

The performance of the developed program was compared to field data. The results show good agreement with the real field example. Table 6.2 is the field data inputted into the program. Fig. 6.22 shows the result.

Table 6.2 Field Data Model Parameters

Model Parameters	**Symbol**	**Value**	**Units**
Total Liquid Flow Rate	q_t	25,000	STB/D
End Point Mobility Ratio	M	0.86	
Vertical Distance	h_v	313	ft
Vertical Formation Thickness	h	1000	ft
Reservoir Length (in x-dir)	L	893	ft
Permeability	k	200	md
Anisotropy Ratio	k_v/k_h	0.1	
Perforation Thickness	h_p	1000	ft
Dip Angle	α	20	degrees
Water-oil gravity gradient	$\Delta\gamma$	0.095	psi/ft
Ratio of k_{ml}/k_{max}	k_{ml}/k_{max}	0.1	
Oil formation volume factor	B_o	1.302	RB/STB
Porosity	ϕ	0.29	
Connate Water Sat.	S_{wc}	0.2	
Residual Oil Sat.	S_{or}	0.2	
Height above Perfs	h_{ap}	0	
Total Vertical Thickness	H_t	1313	
Specified height	H_{gt}	0	ft
Time -step	Δt	90	days
Height below perforation	h_{bp}	313	ft

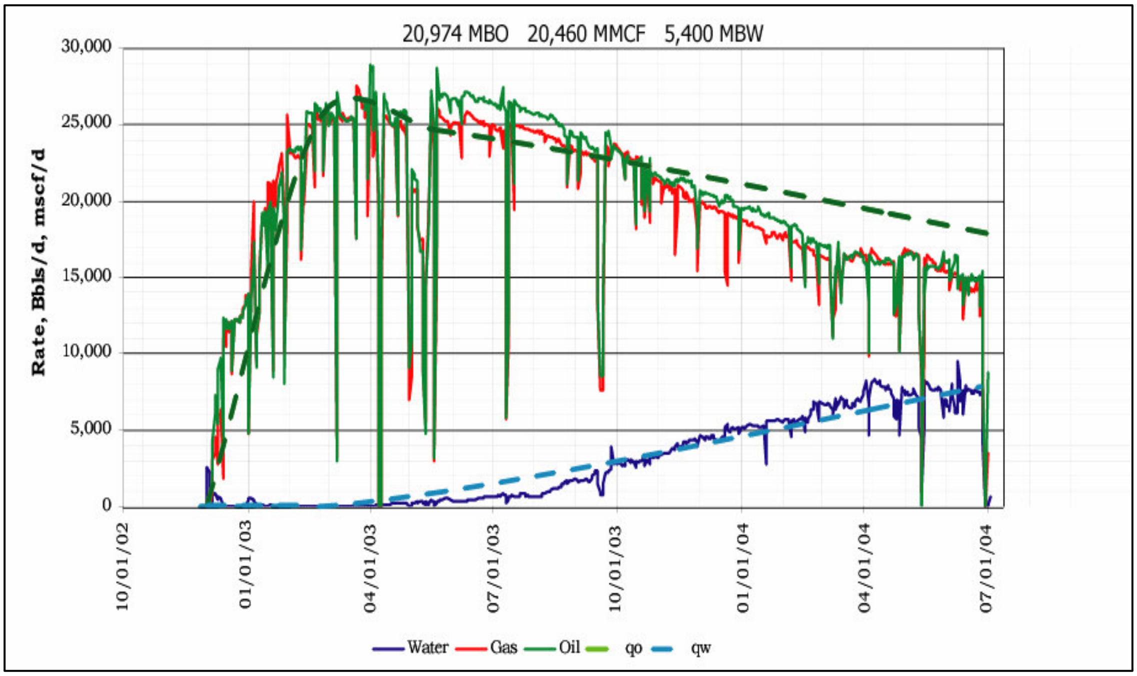

Fig. 6.22-Field Plot Match.

Chapter Summary

This chapter reviews the different part of the program. The program was validated by using the developed correlation to replicate simulation results. Furthermore, the program was applied to both synthetic and field data. Overall, the results obtained showed good agreement.

CHAPTER VII

CONCLUSIONS AND RECOMMENDATIONS

Conclusions

This work presents the results of a systematic study of edgewater cusping and coning in a monocline reservoir. Studying the displacement of oil by water before and after breakthrough with an edgewater drive was the scope of this work. Consequently, if the advancement of the water-oil interface is well established, it can be used to evaluate the oil recovery efficiency at any stage in the depletion process. The procedure, correlation and computer program developed in this work gives a good understanding of the dynamics of edgewater cusping and coning. The result provides a good starting block before embarking on a full simulation study or field development. The emphasis of the project is to produce an easy to use program for making quick and informed decisions at the beginning of a project where the value of accurate information is at the highest.

The major conclusions of this work can be summarized as follows:

1. A new approach to cusping and coning problems was developed.
2. The theory assumes $\frac{WOR + C}{C}$ varies linearly with h_{bp} after water breakthrough on a semi-log plot.
3. The entire cusping and coning performance can be described when m, C and h_{wb} are known.

4. A new set of correlations for estimation of critical flow rate, breakthrough time and WOR after breakthrough was developed. These correlations take into account the main reservoir parameters that affect flow.
5. WOR can be predicted for both constant and variable rate cases i.e. when rate changes. Although the correlation is based on the assumption of hysteresis, the developed correlation gave excellent match.
6. WOR is not rate sensitive at high flow rates in the region of the experimental range of investigation. The insensitivity at higher rates is the result of low gravity numbers.
7. The ability to obtain a straight line slope after water breakthrough is important to be able to estimate WOR performance after breakthrough. The flexibility of using different constant enables us to achieve this.
8. A computer program that incorporates the developed equations and correlations was developed. The program is easy to use and fast. It allows the simulation of various scenarios and allows comparison with field and simulation data.
9. The experimental range of investigation and parameter group range are stated in the previous chapters. Results obtained within the range of investigation are encouraging. The accuracy may be less for values outside these ranges.

Recommendations for Future Work

Based on the results of this research, the following recommendation and direction for future work are made to improve critical flow rate estimation, breakthrough time prediction and performance after water breakthrough estimation.

1. The developed methodology can be applied to other systems Gas-Oil systems and 3-phase flow e.g. Gas-Oil-Water.
2. Determination of constant C is subjective and based on visual best fit. A more scientific way could be investigated.
3. Further research may address situations where high end point mobility ratio is encountered.

NOMENCLATURE

A_c = cross sectional area

B_o = oil formation volume factor, RB/STB

C = constant used to obtain a straight line

d_c = distance from production well to the position of the original OWC or the GWC

g = gravitational acceleration, ft/s^2

G = dimensionless gravity number

h = vertical formation thickness, ft

h_{ap} = average oil column height above perforation, ft

h_{bp} = average oil column height below perforation, ft

h_{gb} = average oil column height at gas breakthrough, ft

h_p = perforation thickness, ft

h_v = vertical distance or initial standoff, ft

h_w = height of water column

h_{wb} = average oil column height at water breakthrough, ft

H_t = total vertical thickness, ft

$\tilde{k}$ = pseudo relative permeability

k_{ij} = intrinsic permeability tensor of the porous medium

k_{or} = relative permeability to oil at connate water saturation

$\tilde{k}_{rw}$ = water pseudo relative permeability

$\tilde{k}_{ro}$ = oil pseudo relative permeability

k_r = relative permeability

$k_{h\,=}$ horizontal permeability, md

k_v/k_h = anisotropy – ratio of vertical to horizontal permeability

k_{rw} = relative permeability to water at residual oil saturation

$k_{v\,=}$ vertical permeability, md

L = reservoir length in x-direction, ft

m = slope of the log (WOR+C)/C vs. h_{bp} plot

M = end point mobility ratio

n = layers for which water breakthrough has occurred

N = total layers in the system

N_{Grav} = Gravity Number

N_p = cumulative oil production, STB

$N_{pbt\,=}$ cumulative oil production at breakthrough, STB

p = phase pressure

P_{cp} = pseudo capillary pressure

q = source/sink term (flow rate per unit volume)

$q_{o\,=}$ oil flow rate, STB/D

$q_{w\,=}$ water flow rate, STB/D

$q_{t\,=}$ total liquid flow rate, STB/D

Rnd = Random Number

S = phase saturation

S_{wc} = connate water saturation

S_{or} = residual oil saturation

$\tilde{S}_w$ = average water saturation

w = width of the drainage area of one production well (= well spacing)

WOR = producing water oil ratio

WOC = water oil contact

z = vertical spatial coordinate

Greek Symbols

α = dip angle, degrees

β = the angle between the fluids interface

$\Delta\gamma$ = Water-oil gravity gradient, psi/ft

ΔH = average vertical height of the water invaded zone, ft

ϕ = porosity, %

ρ = density, lbm/ft^3

μ = viscosity, cp

REFERENCES

1. Addington, D.V.: “An Approach to Gas-Coning Correlations for a Large Grid Cell Reservoir Simulator,” *JPT* (Nov. 1981) 2267-74.
2. Yang, W. and Wattenbarger, R.A.: “Water Coning Calculations for Vertical and Horizontal Wells,” paper SPE 22931 presented at the 1991 SPE Annual Technical Conference, Dallas, TX, 6-9 October.
3. Ahmed, T.: *Reservoir Engineering Handbook*, Gulf Publishing, Houston, TX, (2000)
4. “Production Handbook,” Shell International Petroleum Maatschappij B.V., The Netherlands (1991) 4.
5. Yang, W.: “Water Coning Calculations for Vertical and Horizontal Well,” MS Thesis, Texas A&M University, College Station (1990)
6. Luiz Serra de Souza, A.: “Correlations for Cresting Behavior in Horizontal Wells,” PhD Dissertation, Stanford University, Stanford, CA (1997)
7. Muskat, H. I. and Wyckoff, R.D.: “An Approximate Theory of Water Coning in Oil Production,” *Trans.*, AIME (1935) **114**, 144-161.
8. Meyer, M. and Garder, A.O.: “Mechanics of Two Immiscible Fluids in Porous Media,” *J. Appl. Physics*, (1954) **25**, No.11, 1400-06.
9. Chaney, P.E., Noble, M.D., Henson, W.L. and Rice, T.D.: “How To Perforate your Well to Prevent Water and Gas Coning,” *OGJ.* (May 1956) 108.
10. Chierici, G.L., Ciucci, G.M., and Pizzi, G.: “A Systematic Study of Gas and Water Coning by Potentiometric Models,” *JPT.* (Aug 1964) 923-29.

11. Schols, R.S.: "An Empirical Formula for the Critical Oil Production Rate," *Erdoel Erdgas*, (Jan 1972) **88**, No.1, 6-11.
12. Wheatley, M.J.: "An Approximate Theory of Oil/Water Coning," paper SPE 14210, presented at the 1985 SPE Annual Technical Conference, Las Vegas, 22 – 25 September.
13. Arbabi, S., and Fayers, F.J.: "Comparative Aspects of Coning Behavior in Horizontal and Vertical Wells," *Proc*, Eighth European Symposium on Improved Oil Recovery, Vienna, Austria, May 15-17, 1995.
14. Hoyland, L.A., Papatzacos, P., and Skjaeveland, S.M.: "Critical Rate for Water Coning: Correlation and Analytical Solution," *SPERE*, (Nov. 1989) 495-502.
15. Giger, F.M.: "Analytic Two-Dimensional Models of Water Cresting before Breakthrough for Horizontal Wells," *SPERE*, Nov. 1989 409-416.
16. Menouar, H.K. and Hakim, A.A.: "Water Coning and Critical Rates in Vertical and Horizontal Wells," paper SPE 29877 presented at the 1995 SPE Middle East Oil Show, Bahrain, 11-14 March.
17. Kidder, R.E.: "Flow of Immiscible Fluids in Porous Media: Exact Solution of a Free Boundary Problem," *Journal of Applied Physics*, **27**, 8, (Aug. 1956) 867-869.
18. Sobocinski, D. P., and Cornelius, A. J.: "A Correlation for Predicting Water Coning Time," paper SPE 894, presented at the 1965 SPE Annual Fall Meeting, Houston, TX, 11 – 14 October.

19. Bournazel, C., and Jeanson, B.: "Fast Water-Coning Evaluation Method," paper SPE 3628, presented at the 1971 SPE Annual Fall Meeting, New Orleans, LA, 3 – 6 October.
20. Ozkan, E., and Raghavan, R.: "A Breakthrough Time Correlation for Coning toward Horizontal Wells," paper SPE 20964, presented at Europec 90, Hague, The Netherlands, October 22-24, 1990.
21. Papatzacos, P. et al: "Cone Breakthrough Time for Horizontal Wells," *SPERE*, (Aug. 1991) 311-318.
22. Zamonsky, G., Lacentre, P.E., and Larreteguy, A.E.: "Towards Better Correlations for Water Production Prediction Using Sensitivity Analysis and Numerical Simulation Models," paper SPE 94457, presented at the 2005 SPE Europe/EAGE Annual Conference, Madrid, Spain, 13-16 June.
23. Chappelear, J.E., and Hirasaki, G.J.: "A Model of Oil-Water Coning for Two-Dimensional, Areal Reservoir Simulation," paper SPE 4980, presented at the 1974 SPE-AMIE Annual Fall meeting, Houston, TX, 6-9 October.
24. Kuo, M.C.T., and DesBrisay, C.L.: "A Simplified Method for Water Coning Predictions," paper SPE 12067, presented at the 1983 SPE Annual Technical Conference, Dallas, TX, 5-8 September.
25. Lee, S.H. and Tung, W.B.: "General Coning Correlations Based on Mechanistic Studies," paper SPE 20742 presented at the 1990 SPE Annual Technical Conference, New Orleans, LA, 23-26 September.

26. De Souza, A.L.S., Arbabi, S., and Aziz, K.: "Practical Procedure to Predict Cresting Behavior of Horizontal Wells," *SPEJ*, (Dec. 1998) 382-392.
27. Johns, T.R., Lake, L.W., and Delliste, A.M.: "Prediction of Capillary Fluid Interfaces during Gas or Water Coning in Vertical Wells," paper SPE 77772, presented at the 2002 SPE Annual Technical Conference and Exhibition, San-Antonio, TX, September 29-October 2.
28. Ezuka, I.O., Egbele, E.E., and Onyekonwu, M.O.: "Productivity Enhancement through Single well Numerical Modeling," paper SPE 88966, presented at the 2004 Annual SPE International Technical Conference and Exhibition, Abuja, Nigeria, 2-4 August.
29. Osisanya, S.O., Recham, R. And Touami, M.: "Effects of Water Coning on the Performance of Vertical and Horizontal wells – A Reservoir Simulation Study of Hassi R'Mel Field, Algeria," paper 2000-39 prepared for presentation at the 2000 Canadian International Petroleum Conference, Calgary, Canada, 4-8 June.
30. Singhal, A.K.: "Water and Gas Coning/Cresting: A Technology Overview," *JCPT* (1996) **35**, 4, 56-62.
31. Hernandez, J.C., and Wojtanowicz, A.K.: "Assessment of Un-Recovered Oil in Dipping Reservoirs from Analysis of Water Cut Development," paper 2006-200 prepared for presentation at the 2006 Canadian International Petroleum Conference, Calgary, Canada, 13-15 June.

32. Chan, K.S.: “Water Control Diagnostic Plots,” paper SPE 30775 presented at the 1995 SPE Annual Technical Conference and Exhibition, Dallas, TX, 22- 25 October.
33. Seright, R.S., Lane, R.H., and Sydansk, R.D.: “A Strategy for Attacking Excess Water Production,” paper SPE 70067, presented at the 2001 SPE Permian Basin Oil and Gas Recovery Conference, Midland, TX, 15- 16 May.
34. Ehlig-Economides, C.A., Chan, K.S., and Spath, J.B.: “Production Enhancement Strategies for Strong Bottom Water Drive Reservoirs,” paper SPE 36613, presented at the 1996 SPE Annual Technical Conference and Exhibition, Denver, CO, 6- 9 October.
35. Amenta, N., and Wojtanowicz, A.: “Severity of Water Coning in Gas Wells,” paper SPE 75720, presented at the 2002 SPE Gas Technology Symposium, Calgary, Alberta, April 30-May 2.
36. Beraldo, V.T., Pedrosa, O.A., and Remacre, A.Z.: “Simulation of Water Coning Behavior Using Geostatistic Techniques to Represent Reservoir Heterogeneities,” paper SPE 27020, presented at the 1994 Latin American/Caribbean Conference, Buenos Aires, Argentina, 27-29 April.
37. Knopp, C. R.: “Bottom-Water and Edge-Water Effects on Low Gravity Oil Production,” *JPT*, (Feb. 1960) 45-51.
38. Azar-Nejad, F., Tortike, W.S., and Farouq Ali, S.M.: “Water and Gas Coning in the Oil Reservoirs with Steady State and Transient Flow (Part 1: Vertical

Wells)," paper SPE 35219, presented at the 1996 SPE Permian Basin Oil and Gas Recovery Conference, Midland, TX, 27- 29 March.

39. Richardson, J.G., Sangree, J.B., and Snelder, R.M.: "Coning," *JPT*, (Aug. 1987) 805-813.
40. Cao, H., and Aziz, K.: "About Kinds of Breakthrough and Maximum Recovery Factor in Dual Coning," paper SPE 37049, presented at the 1996 2nd SPE International Conference on Horizontal Well Technology, Calgary, Canada, 18-20 November.
41. Mjaavatten, A., *et al*: "A Model for Gas Coning and Rate-Dependent Gas/Oil Ratio in an Oil-Rim Reservoir," paper SPE 102390, presented at the 2006 SPE Russian Oil and Gas Technical Conference and Exhibition, Moscow, Russia, 3- 6 October.
42. Blades, D.N., and Stright, D.H.: "Predicting High Volume Lift Performance in Wells Coning Water," *J. Cdn. Pet. Tech.*, (Oct. - Dec. 1975) 62-70.
43. Manik, J., and Ertekin, T.: "Development and Application of Dynamic and Static Local Grid Refinement Algorithms for Water Coning Studies," paper SPE 39228, presented at the 1997 SPE Regional Meeting, Lexington, KY, 22- 24 October.
44. Kabir, C.S., Ma, E.D.C., Dashti, Q., and Al-Shammari, O.: "Understanding Coning Performance in a High Anisotropy Reservoir: The Burgan Reservoir Case Study," paper SPE 62993, presented at the 2000 SPE Annual Technical Conference, Dallas, TX, 1-4 October.

45. Dietz, D.N.: “A Theoretical Approach to the Problem of Encroaching and By-Passing Edge-water,” *Proc*, Series B, Koninklijke Nederlandse Akademie Van Wetenschappen, Amsterdam, The Netherlands, 1953.
46. Sheldon, J.W., and Fayers, F.J.: “The Motion of an Interface between Two Fluids in a Slightly Dipping Porous Medium,” *SPEJ*, (Sep. 1962) 275-282.
47. Fayers, F.J., and Muggeridge, A.H.: “Extensions to Dietz Theory and Behavior of Gravity Tongues in Slightly Tilted Reservoirs,” *SPERE*, (Nov. 1990) 487-493.
48. Hernandez, J.C., Wojtanowicz, A.K. and White, C.D.: “Effects of Anisotropy on Water Invasion in Edge-Water Drive Reservoirs,” paper 2006-199 prepared for presentation at the 2006 Canadian International Petroleum Conference, Calgary, Canada, 13-15 June.
49. Hernandez, J.C., and Wojtanowicz, A.K.: “Prediction of By-passed Oil with Correlations in Side-Water Drive Reservoirs,” paper 2005-196 prepared for presentation at the 2005 Canadian International Petroleum Conference, Calgary, Canada, 7-9 June.
50. Hernandez, J.C., and Wojtanowicz, A.K.: “Qualification of Un-recovered Reserves Due to Production Process Dynamics in Water-Drive Reservoirs,” paper 2005-237 prepared for presentation at the 2005 Canadian International Petroleum Conference, Calgary, Canada, 7-9 June.
51. Dake, L.P.: *Fundamentals of Reservoir Engineering*, Elsevier, Scientific Publishing Company, New York City (1978).

52. Zhou, D., Fayers, F.J., and Orr, F.M.: "Scaling of Multiphase Flow in Simple Heterogeneous Porous Media," paper SPE 27833 presented at the 1993 ASME Winter meeting, New Orleans, LA, November 28 – December 3.
53. Shook, M., Dachang, L., and Lake, L.W.: "Scaling Immiscible Flow Through Permeable Media by Inspectional Analysis," *INSITU*, 16(4), 311-349 (1192).
54. White, C.D., and Royer, S.A.: "Experimental Design as a Framework for Reservoir Studies," paper SPE 79676, presented at the 2003 SPE Reservoir Simulation Symposium, Houston, TX, 3- 5 February.
55. Wood, D.J., Lake, L.W., Johns, R.T., and Nunez, V.: "A Screening Model for CO_2 Flooding and Storage in Gulf Coast Reservoirs Based on Dimensionless Groups," paper SPE 100021, presented at the 2006 SPE/DOE Symposium on Improved Oil recovery, Tulsa, OK, 22- 26 April.
56. Christie, M.A.: "High-Resolution Simulation of Unstable Flows in Porous Media," *SPERE*, (Aug. 1989) 297-303.
57. Eclipse Technical Description Manual, Vers. 2005A, Schlumberger, Houston (2005).
58. Mattax, C.C. and Dalton, R.L.: *Reservoir Simulation*, Monograph Series, SPE, Richardson, Texas (1990), **13**.
59. Aziz, K. and Settari, A.: *Petroleum Reservoir Simulation*, Elsevier, Scientific Publishing Company, New York City (1986).
60. Carlson, M.R.: *Practical Reservoir Simulation*, PennWell, Tulsa, Oklahoma (2003).

61. Nabor, G.W., and Barham, R.H.: "Linear Aquifer Behavior," *JPT*, (Dec. 1963) 561-563.
62. Coats, K.H., Dempsey, J.R., and Henderson, J.H.: "The Use of Vertical Equilibrium in Two-Dimensional Simulation of Three-Dimensional Reservoir Performance," *SPEJ*, (March. 1971) 63-71.
63. Coats, K.H., Nielsen, R.L., Terhune, M.H., and Weber, A.G.: "Simulation of Three-Dimensional, Two-Phase Flow in Oil and Gas Reservoirs," *SPEJ*, (Dec. 1967) 377-388.
64. Woods, E.G., and Khurana, A.K.: "Pseudofunctions for Water Coning in a Three-Dimensional Reservoir Simulator," paper SPE 5525 presented at the 1975 SPE-AIME Annual Technical Conference and Exhibition, Dallas, TX, September 28-October 1.
65. Hearn, C.L.: "Simulation of Stratified Waterflooding by Pseudo Relative Permeability Curves," *SPEJ*, (July. 1971) 805-813.
66. Jacks, H.H., Smith, O.J.E., and Mattax, C.C.: "The Modeling of a Three-Dimensional Reservoir with a Two-Dimensional Reservoir Simulator – The Use of Dynamic Pseudo Functions," paper SPE 4071, presented at the 1972 SPE-AIME Annual Fall Meeting, San-Antonio, TX, 8-11 October.
67. Dake, L.P.: *The Practice of Reservoir Engineering*, Elsevier, Scientific Publishing Company, (1994).
68. Emanuel, A.S., and Cook, G.W.: "Pseudo Relative Permeability for Well Modeling," *SPEJ*, (Feb. 1974) 7-9.

69. Azoug, Y., and Tiab, D.: "The Performance of Pseudofunctions in the Upscaling Process," paper SPE 80910, presented at the 2003 SPE Production and Gas Operations Symposium, Oklahoma City, OK, 22- 25 March.
70. Cao, H., and Aziz, K.: "Evaluation of Pseudo Functions," paper SPE 54589, presented at the 1999 SPE Western Regional Meeting , Anchorage, AK, 26- 28 May.
71. Corey, A.T.: "The Interrelation Between Gas and Oil Relative Permeabilities," *Producers Monthly*, (Nov. 1954) 38-41.
72. Bailey, B., Elphick, J., Kuchuk, F., Romano, C. and Roodhart, L.: "Water Control," Schlumberger Oilfield Review **12** (Spring 2000) 30-51.

APPENDIX A

DERIVATION OF THE EQUATION FOR CALCULATING THE HEIGHT OF THE WATER INVADED ZONE FOR EACH TIME STEP

One of the assumptions of the tank model is that water displaces oil in a piston-like fashion and also the OWC is fairly straight. For every time step, we can calculate the vertical height of the water invaded zone, ΔH by treating the reservoir as a tank model. Fig. A.1 shows a sketch of the reservoir.

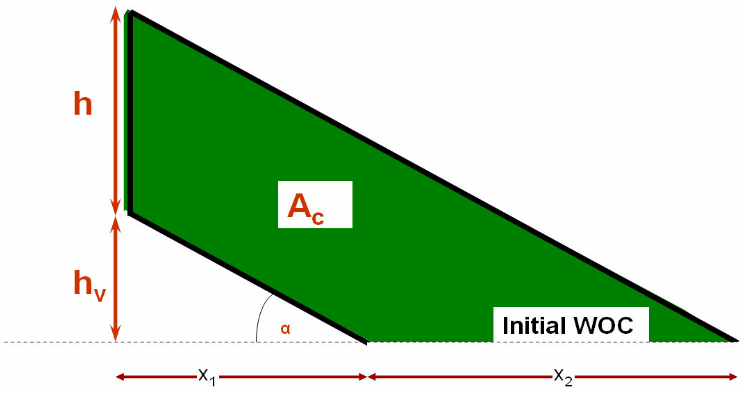

Fig. A.1 Sketch of the material balance model at initial conditions.

From Fig. A.1,

$$\tan\alpha = \frac{h_v}{x_1} = \frac{h+h_v}{x_1+x_2} = \frac{h}{x_2} \quad \ldots\ldots\ldots \text{(A.1)}$$

The cross-sectional area A_c of the reservoir is given by

$$A_c = \frac{1}{2}(h+h_v)(x_1+x_2) - \frac{1}{2}h_v x_1 \tag{A.2}$$

Hydrocarbon pore volume V_p is given by

$$V_p = A_c L\phi \tag{A.3}$$

The original oil in place OIP is given by

$$OOIP = V_p(1-S_{wc})/B_o \tag{A.4}$$

The Moveable OIP is

$$= V_p(1-S_{wc}-S_{or})/B_o \tag{A.5}$$

$$OOIP = A_c L\phi(1-S_{wc})/B_o = \left[\frac{1}{2}(h+h_v)(x_1+x_2) - \frac{1}{2}h_v x_1\right]\frac{L\phi(1-S_{wc})}{B_o} \tag{A.6}$$

$$OOIP = \left[\frac{1}{2}(h+h_v)\frac{h+h_v}{\tan\alpha} - \frac{1}{2}h_v\frac{h_v}{\tan\alpha}\right]\frac{L\phi(1-S_{wc})}{B_o} \tag{A.7}$$

$$OOIP = \frac{1}{2\tan\alpha}\left[(h+h_v)^2 - h_v^{\,2}\right]\frac{L\phi(1-S_{wc})}{B_o} \tag{A.8}$$

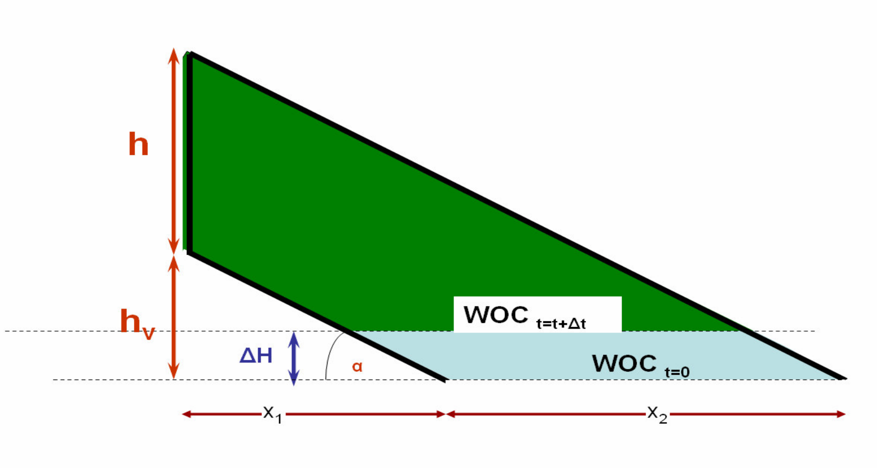

Fig. A.2 Sketch of the material balance model at a later time with water invasion.

If we look at the sketch at a later time, we will have an invaded zone (assuming horizontal interfaces and piston-like displacement) that represents the displaced reservoir oil. This will be equal to the cumulative reservoir oil produced, which can be expressed as:

$$OIP_{t=0} - OIP_t = N_p = \Delta H \frac{h}{\tan\alpha} \frac{L\phi(1 - S_{wc} - S_{or})}{B_o} \quad \text{...} \quad (A.9)$$

This equation is used to calculate ΔH for the material balance model, given the actual N_p from the simulation at any given time-step. The corresponding *WOR* from that time-step is then used in plotting *WOR* and ΔH. The expression is

$$\Delta H = \frac{N_p B_o \tan\alpha}{hL\phi(1 - S_{wc} - S_{or})} \quad \text{...} \quad (A.10)$$

So the values of *WOR* and ΔH are calculated for each time-step of the simulations and used to construct the various plots used for the correlation.

APPENDIX B

SPIDER PLOT PROCEDURE

The spider plot approach is a technique for discovering unique features contained in the data. It gives a visual comparison of several variables.

The correlation developed is a function of eleven variables that affect the performance of edgewater cusping and coning. The variables include Total liquid flow rate, formation thickness, reservoir length, vertical distance (initial standoff), perforation thickness, dip angle, end point mobility ratio, density difference, vertical permeability, horizontal permeability, ratio of most likely permeability to maximum permeability for Hearn relative permeability curves. The relationship between the height at water breakthrough h_{wb}, slope of the water-oil ratio curve m and constant C versus the eleven variables was determined using the spider plot approach.

The procedure used in developing the correlation is outlined in the following steps:

- The log-log plot of h_{wb}, m and C versus each of the parameters is made.
- The slope for each parameter is determined from $\frac{\log(y_2 / y_1)}{\log(x_2 / x_1)}$
- The obtained slope is the exponent of the parameter. This was put together as the developed correlation.

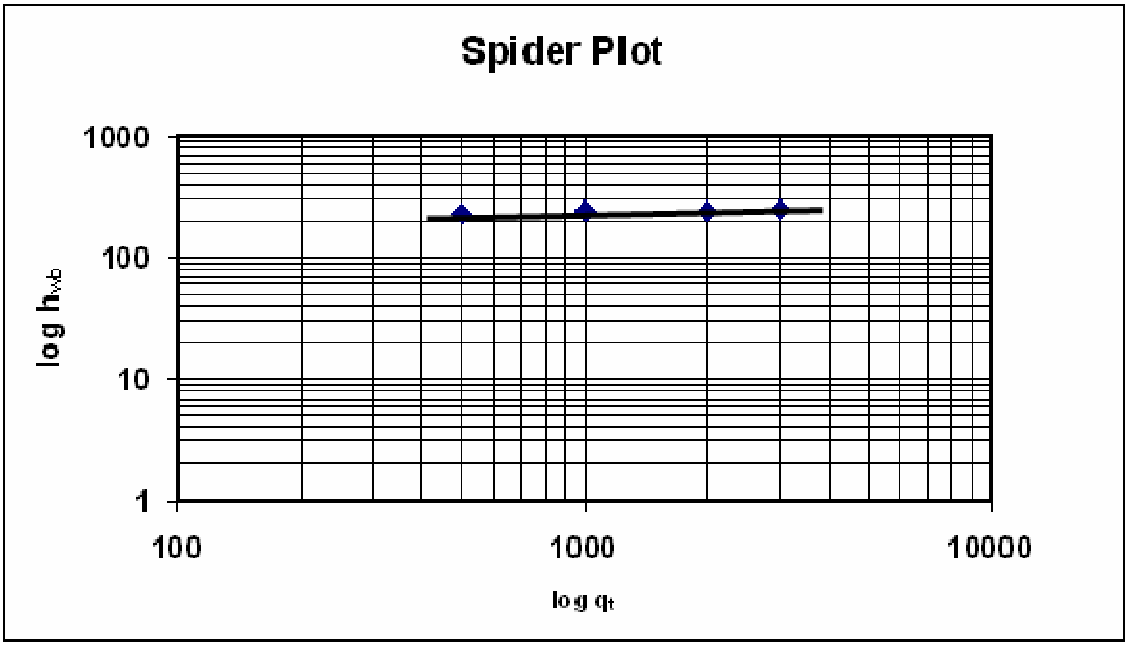

Fig. B.1 Spider plot of log h_{wb} vs. q_t. slope = 0.04

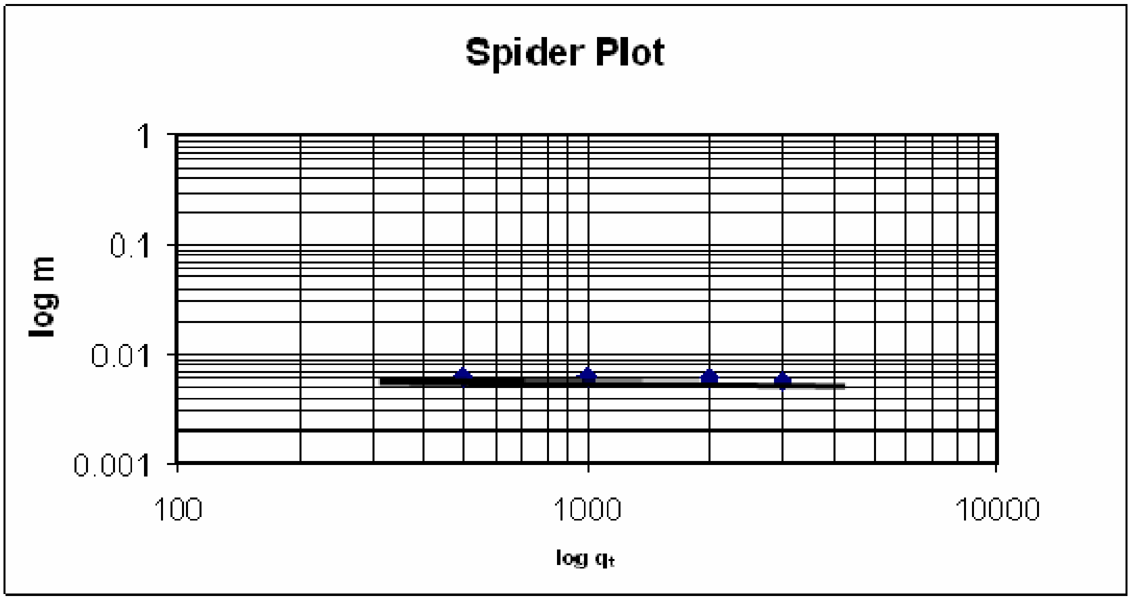

Fig. B.1 Spider plot of log m vs. q_t. slope = -0.04

APPENDIX C

DETERMINATION OF THE HEIGHT AT WATER BREAKTHROUGH AND SLOPE OF THE WATER-OIL RATIO PLOT FROM SIMULATOR OUTPUT

The entire coning performance can be described with three key variables: the height at water breakthrough, h_{wb}, slope of the water-oil ratio curve, m and constant C which is added to obtain the straight line.

Since the constant C is visually determined, a systematic procedure was devised in Excel to obtain h_{wb} and m after the value of C is obtained. From the cumulative oil production data, oil flow rate and water flow rate information and using the equations derived in Appendix A, the (WOR+C)/C versus the average oil column height below perforation is made on a semi-log plot. Using the semi-log plot of Log (WOR+C)/C versus h_{bp}, the equations for calculating the height at water breakthrough, h_{wb} and the slope of the water-oil ratio curve, m can be derived by analyzing the figure below.

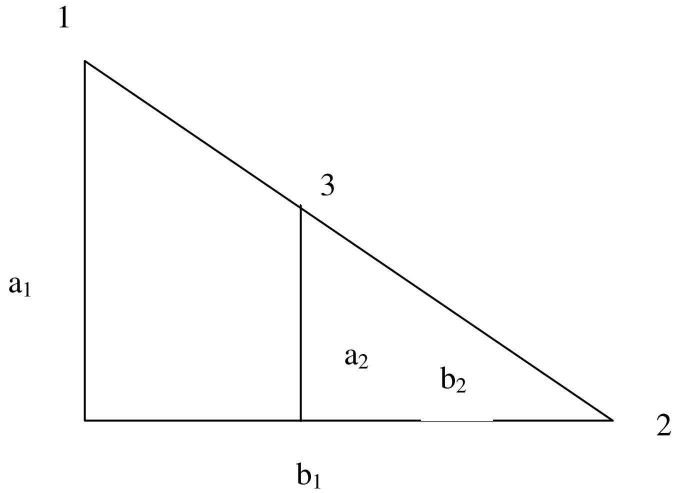

From a semi-log plot,

$$\log(y) = a + bx \qquad \text{(C.1)}$$

Where b is slope and a is the intercept. Using our notation,

$$\log(\frac{WOR + C)}{C} = a + mh_{bp} \qquad \text{(C.2)}$$

From the figure above,

$$\frac{a_1}{b_1} = \frac{a_2}{b_2} \qquad \text{(C.3)}$$

$$\frac{\log y_1 - \log y_2}{x_1 - x_2} = \frac{\log y_3 - \log y_2}{x_3 - x_2} \qquad \text{(C.4)}$$

$$x_3 - x_2 = (x_1 - x_2)\frac{\log(C/(C * y_2))}{\log(y_1/y_2)} \qquad \text{(C.5)}$$

$$slope = m = \frac{\log(y_1/y_2)}{x_1 - x_2} \qquad \text{(C.6)}$$

$$x_3 = x_2 + \frac{1}{slope}\log(C/(C * y_2)) \qquad \text{(C.7)}$$

The above expression is used to calculate ($h_{bp} = X_3$)

APPENDIX D

EXAMPLE CALCULATION PROCEDURE

This section discusses the steps for analyzing a run from Eclipse. From the simulation data file, the oil in place in STB, cumulative production in STB, water and oil flow rate and water cut for a specific time step are outputted to the result summary file. The WOR, (WOR+C)/C, height of the water invaded zone and average oil column height below perforation are computed using the equations described earlier. Table D.1 shows a sample run. Fig. D.1 shows the semi log plot of Log (WOR+C)/C vs. $h_{bp.}$ C in this example is 0.1. This is the constant added to obtain a straight line. The sensitivity is carried out for a certain range of values. For each run, the average column height at water breakthrough h_{wb}, slope of the plot m and the constant C are read. The spider plot procedure as described in Appendix B is used to obtain the exponent of the parameter.

Table D.1

TIME	FOIP	FOPR	FOPT	FWPR	FWCT	WOR	(WOR+C)/(	ΔH	h_{bp}
(DAYS)	(STB)	(STB/DAY	(STB)	(STB/DAY)				ft	ft
0	7298639.5	0	0	0	0	0	1	0	300
20	7258675	1998.183	39966.37	1.8172171	0.000909	0.000909	1.009094	3.055921	296.9441
40	7218718	1997.856	79923.5	2.1435025	0.001072	0.001073	1.010729	6.111135	293.8889
60	7178766.5	1997.58	119875.1	2.4196424	0.00121	0.001211	1.012113	9.165927	290.8341
80	7138819.5	1997.339	159821.9	2.661129	0.001331	0.001332	1.013323	12.22035	287.7797
100	7098877	1997.123	199764.3	2.8773642	0.001439	0.001441	1.014408	15.27444	284.7256
120	7058938.5	1996.926	239702.8	3.074362	0.001537	0.00154	1.015395	18.32823	281.6718
140	7019004	1996.744	279637.7	3.2559922	0.001628	0.001631	1.016307	21.38174	278.6183
160	6979072.5	1996.575	319569.2	3.4250464	0.001713	0.001715	1.017155	24.435	275.565
180	6939144	1996.417	359497.6	3.5834928	0.001792	0.001795	1.01795	27.48801	272.512
200	6899218.5	1996.267	399422.9	3.7328584	0.001866	0.00187	1.018699	30.5408	269.4592
220	6859296	1996.126	439345.4	3.8742616	0.001937	0.001941	1.019409	33.59336	266.4066
240	6819376.5	1995.991	479265.3	4.0087371	0.002004	0.002008	1.020084	36.64572	263.3543
260	6779459	1995.863	519182.5	4.1370921	0.002069	0.002073	1.020728	39.69789	260.3021
280	6739544.5	1995.739	559097.3	4.2609615	0.00213	0.002135	1.02135	42.74987	257.2501
300	6699632	1995.607	599009.4	4.3931327	0.002197	0.002201	1.022014	45.80164	254.1984
320	6659726.5	1995.288	638915.2	4.7123165	0.002356	0.002362	1.023617	48.85293	251.1471
340	6619858.5	1993.402	678783.2	6.5977163	0.003299	0.00331	1.033098	51.90133	248.0987
360	6580062	1989.82	718579.6	10.179708	0.00509	0.005116	1.051159	54.94425	245.0557
380	6540344.5	1985.872	758297.1	14.127966	0.007064	0.007114	1.071142	57.98114	242.0189
400	6500721.5	1981.154	797920.1	18.84609	0.009423	0.009513	1.095127	61.01081	238.9892
420	6461211.5	1975.497	837430.1	24.502777	0.012251	0.012403	1.124033	64.03183	235.9682
440	6421827.5	1969.195	876814	30.805496	0.015403	0.015644	1.156437	67.04322	232.9568
460	6382591	1961.821	916050.4	38.178864	0.019089	0.019461	1.194609	70.04332	229.9567
480	6343510	1954.045	955131.3	45.954723	0.022977	0.023518	1.235177	73.03154	226.9685
500	6304608.5	1945.088	994033.1	54.912453	0.027456	0.028231	1.282314	76.00606	223.9939
520	6265890	1935.922	1032752	64.078522	0.032039	0.0331	1.330998	78.96656	221.0334
540	6227373	1925.862	1071269	74.137672	0.037069	0.038496	1.384958	81.91168	218.0883
560	6189066.5	1915.323	1109575	84.676956	0.042338	0.04421	1.442103	84.84068	215.1593
580	6150979.5	1904.339	1147662	95.660789	0.04783	0.050233	1.502331	87.75288	212.2471
600	6113121	1892.932	1185521	107.068	0.053534	0.056562	1.56562	90.64763	209.3524
620	6075501.5	1880.97	1223140	119.0304	0.059515	0.063281	1.632814	93.5241	206.4759
640	6038125.5	1868.801	1260516	131.19891	0.065599	0.070205	1.702049	96.38196	203.618
660	6001001.5	1856.2	1297640	143.79951	0.0719	0.07747	1.774698	99.22054	200.7795
680	5964140	1843.07	1334502	156.92964	0.078465	0.085146	1.851458	102.0391	197.9609
700	5927540.5	1829.981	1371101	170.01875	0.085009	0.092907	1.929074	104.8375	195.1625
720	5891216	1816.235	1407426	183.76518	0.091883	0.101179	2.011792	107.615	192.385
740	5855165.5	1802.503	1443476	197.49696	0.098748	0.109568	2.095682	110.3715	189.6285
760	5819399	1788.33	1479242	211.67006	0.105835	0.118362	2.183619	113.1063	186.8937
780	5783919	1774.001	1514723	225.99872	0.112999	0.127395	2.273949	115.8192	184.1808
800	5748727	1759.61	1549915	240.38976	0.120195	0.136615	2.366153	118.51	181.49
820	5713834	1744.639	1584808	255.36096	0.12768	0.146369	2.463689	121.178	178.822
840	5679236	1729.914	1619406	270.086	0.135043	0.156127	2.561268	123.8235	176.1765
860	5644939.5	1714.827	1653702	285.1731	0.142587	0.166298	2.662985	126.4459	173.5541
880	5610950.5	1699.433	1687691	300.56757	0.150284	0.176863	2.768635	129.0447	170.9553
900	5577267.5	1684.146	1721374	315.85422	0.157927	0.187546	2.875457	131.6202	168.3798
920	5543900	1668.398	1754742	331.60211	0.165801	0.198755	2.987548	134.1716	165.8284
940	5510841.5	1652.921	1787800	347.07944	0.17354	0.20998	3.099795	136.6993	163.3007
960	5478098.5	1637.153	1820543	362.84711	0.181424	0.221633	3.21633	139.2029	160.7971
980	5445679	1620.962	1852963	379.03809	0.189519	0.233835	3.338353	141.6818	158.3182
1000	5413577	1605.1	1885065	394.9003	0.19745	0.246029	3.460285	144.1364	155.8636
1020	5381799.5	1588.872	1916842	411.12836	0.205564	0.258755	3.587549	146.5661	153.4339
1040	5350347.5	1572.61	1948294	427.39047	0.213695	0.271772	3.717715	148.9711	151.0289
1060	5319219.5	1556.399	1979422	443.60141	0.221801	0.285018	3.850179	151.3512	148.6488
1080	5288423.5	1539.809	2010218	460.1915	0.230096	0.298863	3.988628	153.7059	146.2941
1100	5257953.5	1523.486	2040688	476.51413	0.238257	0.312779	4.127788	156.0357	143.9643
1120	5227813.5	1507.012	2070828	492.98801	0.246494	0.327129	4.271295	158.3403	141.6597
1140	5198007	1490.321	2100635	509.6792	0.25484	0.341993	4.419929	160.6193	139.3807
1160	5168529	1473.884	2130112	526.1156	0.263058	0.356959	4.569585	162.8733	137.1267
1180	5139385.5	1457.175	2159256	542.82538	0.271413	0.372519	4.725191	165.1017	134.8983
1200	5110575	1440.549	2188067	559.45068	0.279725	0.388359	4.883593	167.3046	132.6954
1220	5082092	1424.144	2216550	575.85614	0.287928	0.404353	5.043525	169.4825	130.5175
1240	5053944.5	1407.369	2244697	592.63141	0.296316	0.421092	5.210918	171.6347	128.3653
1260	5026128.5	1390.798	2272513	609.20184	0.304601	0.438023	5.380232	173.7616	126.2384
1280	4998638	1374.515	2300003	625.48523	0.312743	0.455059	5.550589	175.8635	124.1365
1300	4971480	1357.923	2327162	642.07745	0.321039	0.472838	5.728381	177.9401	122.0599
1320	4944647.5	1341.613	2353994	658.38727	0.329194	0.490743	5.907432	179.9918	120.0082
1340	4918134.5	1325.65	2380507	674.34991	0.337175	0.508694	6.086938	182.019	117.981
1360	4891946	1309.425	2406696	690.57513	0.345288	0.527388	6.273882	184.0215	115.9785
1380	4866080.5	1293.267	2432561	706.7334	0.353367	0.546472	6.464715	185.9992	114.0008
1400	4840527.5	1277.662	2458114	722.33789	0.361169	0.565359	6.653591	187.9531	112.0469
1420	4815280.5	1262.346	2483361	737.65405	0.368827	0.584352	6.843518	189.8835	110.1165
1440	4790345	1246.769	2508297	753.23065	0.376615	0.604146	7.041459	191.7901	108.2099
1460	4765719.5	1231.283	2532922	768.71741	0.384359	0.624322	7.243225	193.673	106.327
1480	4741395.5	1216.192	2557246	783.80804	0.391904	0.644477	7.444773	195.5329	104.4671
1500	4717367.5	1201.411	2581274	798.58936	0.399295	0.66471	7.647098	197.3702	102.6298
1520	4693625	1187.135	2605017	812.86536	0.406433	0.684729	7.847289	199.1856	100.8144
1540	4670169	1172.784	2628473	827.21619	0.413608	0.705344	8.053441	200.9791	99.02094
1560	4647006	1158.165	2651636	841.83502	0.420918	0.72687	8.268697	202.7502	97.24982
1580	4624129	1143.834	2674513	856.16583	0.428083	0.748505	8.485053	204.4994	95.50062
1600	4601531.5	1129.868	2697110	870.13208	0.435066	0.770118	8.701184	206.2272	93.77278
1620	4579207.5	1116.216	2719434	883.78455	0.441892	0.791769	8.917687	207.9342	92.06582
1640	4557146	1103.065	2741496	896.93463	0.448467	0.813129	9.131292	209.6211	90.37894
1660	4535344	1090.102	2763298	909.89795	0.454949	0.834691	9.346906	211.2881	88.71191
1680	4513800	1077.206	2784842	922.79443	0.461397	0.856656	9.566558	212.9354	87.06461
1700	4492512.5	1064.374	2806129	935.6264	0.467813	0.87904	9.790395	214.5631	85.43692
1720	4471484.5	1051.389	2827157	948.61139	0.474306	0.902246	10.02246	216.1709	83.82908
1740	4450715.5	1038.464	2847926	961.53644	0.480768	0.925922	10.25922	217.759	82.24102
1760	4430198	1025.866	2868444	974.13379	0.487067	0.949572	10.49572	219.3278	80.67221
1780	4409926	1013.609	2888716	986.39136	0.493196	0.973148	10.73148	220.8778	79.12216
1800	4389893.5	1001.623	2908748	998.37665	0.499188	0.996759	10.96759	222.4096	77.59043
1820	4370094	989.9782	2928548	1010.0219	0.505011	1.020247	11.20247	223.9235	76.07652
1840	4350521	978.6416	2948121	1021.3584	0.510679	1.043649	11.43649	225.4201	74.57992
1860	4331173	967.4019	2967469	1032.5981	0.516299	1.067393	11.67393	226.8995	73.10053
1880	4312045.5	956.373	2986596	1043.627	0.521814	1.091234	11.91234	228.362	71.63799
1900	4293134.5	945.5543	3005507	1054.4457	0.527223	1.115161	12.15161	229.808	70.19202
1920	4274437.5	934.851	3024204	1065.149	0.532575	1.139378	12.39378	231.2376	68.7624
1940	4255952.5	924.2601	3042689	1075.7399	0.53787	1.163893	12.63893	232.651	67.34897
1960	4237677.5	913.7517	3060964	1086.2483	0.543124	1.188778	12.88778	234.0484	65.95162
1980	4219613.5	903.1984	3079028	1096.8016	0.548401	1.214353	13.14353	235.4296	64.57041
2000	4201763.5	892.4995	3096878	1107.5005	0.55375	1.240898	13.40898	236.7944	63.20556

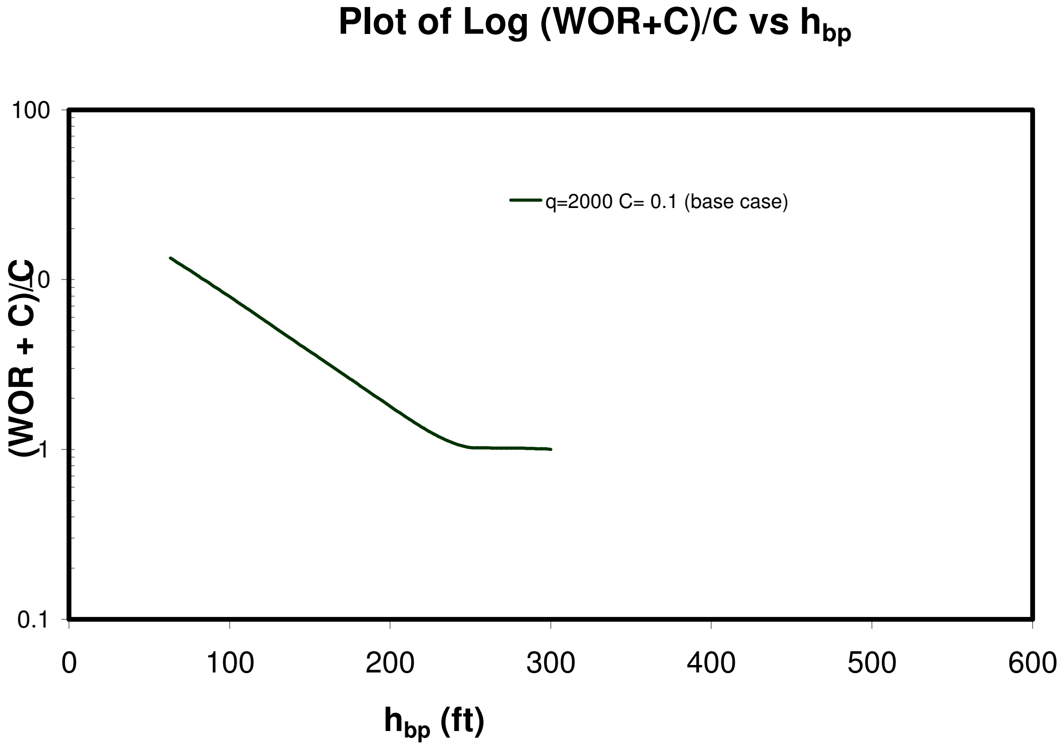

Fig. D.1 Semi-log plot

APPENDIX E

ADDINGTON METHOD

This section gives a detailed description of the Addington approach to gas coning. The Addington method is the basis of this research.

Addington[3] developed a generalized gas correlation for 3-D, 5 layer large grid cell model of the Prudhoe Bay field. The developed correlation can be used to predict critical coning rate and Gas-Oil ratio (GOR) of a well after coning. The gas-coning correlations were developed by simulating numerous one-well models at a constant total fluid production rate for a variety of well parameters. The one well model was run on an implicit radial simulator and contained grid blocks in the radial direction while the number of grid blocks in the vertical varied from 11 – 20 depending on the well parameters.

He observed that before gas breakthrough, the well produces at a GOR given by the dissolved gas. After gas breakthrough, a linear relationship existed when the plot of GOR versus the average oil column height above the perforations on a semi-log paper is made. The height at which gas breakthrough is referred to as average oil column height above perforation at gas breakthrough h_{gb}. The linear relationship is the basis for the generalized correlations. Fig. E.1 shows this relationship.

From the simulation runs and plot, it was observed that the gas coning behavior of any well could be predicted if the GOR slope, m and the oil column height above the perforation at gas breakthrough, h_{gb} are known. As a result, two generalized correlations were developed. These correlations are a function of production rate, horizontal permeability, vertical permeability, perforation thickness, well spacing, oil viscosity, water saturation and residual oil saturation. The variables represented in the parameter groups were varied independently and the effect on the oil column height above the perforation at gas breakthrough and GOR slope accounted for.

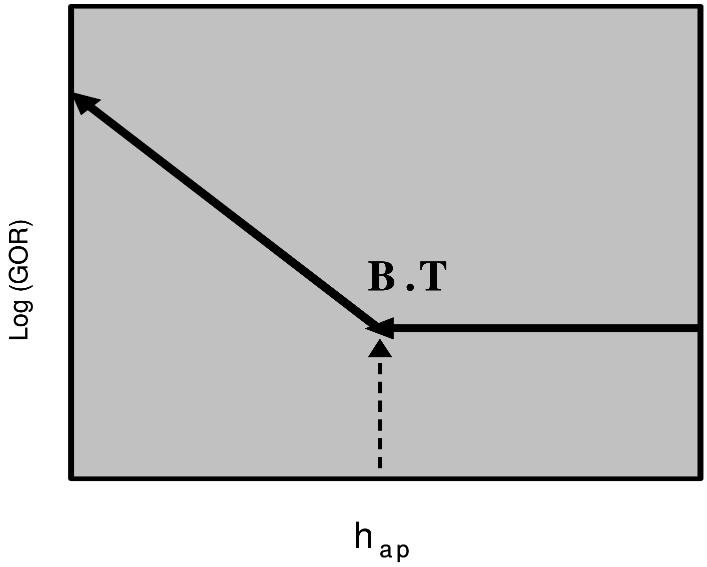

Fig. E.1 Log (GOR) vs. h_{ap} relationship

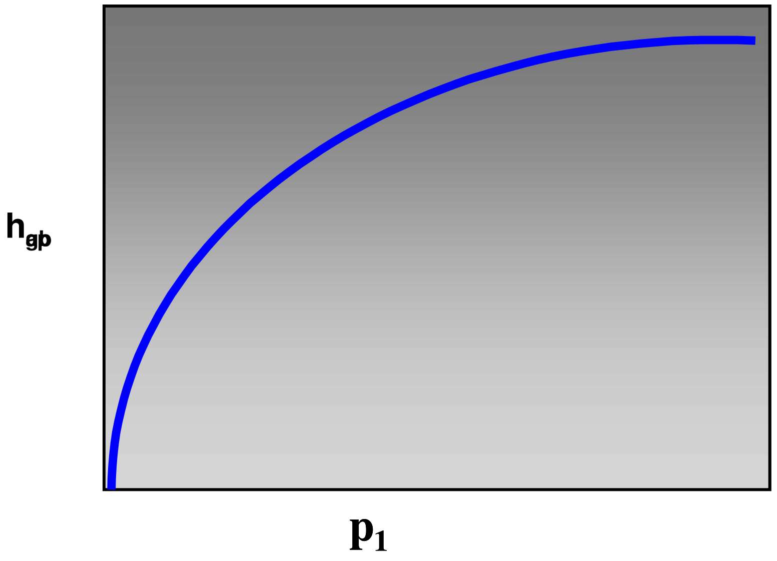

Fig. E.2 h_{gb} vs. P_1 Plot

The first correlation established the relationship between the oil column height above the perforation at gas breakthrough, the well parameters and production rate. Fig. E.2 shows the plot that describes the correlation followed by the equations that describes the correlation.

$$h_{gb} = 137.9\sqrt{P_1} \quad \text{(E.1)}$$

$$P_1 = \frac{q * \left(\frac{k_v}{k_h}\right)^{0.1} * \mu_o * F_1 * F_2}{k_h * \sqrt{h_p}} \quad \text{(E.2)}$$

Where:

F_1 = geometric factor = $\frac{h_p + h_{ap}}{h}$

F_2 = well spacing factor

q = Production rate

$\left(\frac{K_v}{K_h}\right)^{0.1}$ = vertical to horizontal permeability ratio

h = total oil column height

h_{ap} = average oil column height above the perforation

h_p = perforation thickness

uo = average oil viscosity around the well bore.

The correlation from the plot can be used to calculate critical rate.

The slope of the GOR is the second correlation. Fig. E.3 shows the plot.

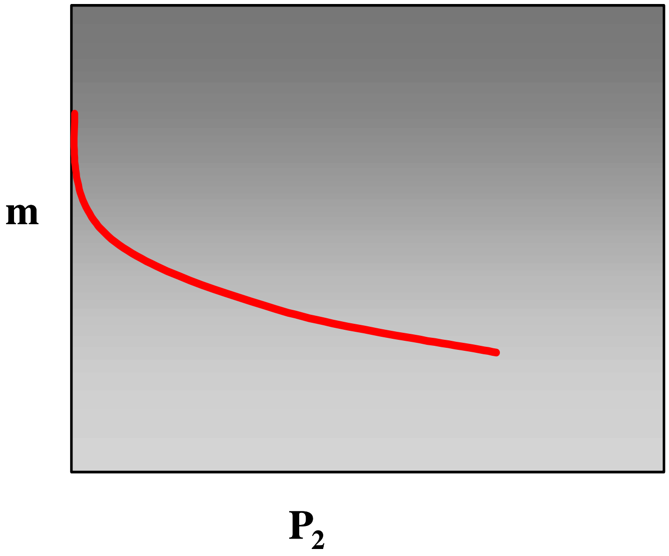

Fig. E.3 Slope correlation

This correlation can be used to establish GOR by applying the equations below:

$$\log\frac{GOR}{GOR_{BT}} = m\left[h_{gb} - h_{ap}\right] \quad \ldots\ldots\ldots\ldots\ldots\ldots\ldots\ldots \text{(E.3)}$$

$$P_2 = \frac{q * \left(\frac{k_v}{k_h}\right)^{0.5} * \mu_o * F_1 * F_3}{k_h * \sqrt{h_p}} \quad \ldots\ldots\ldots\ldots\ldots\ldots\ldots\ldots \text{(E.4)}$$

m = slope of GOR curve

F_3 = well spacing factor

APPENDIX F

ECLIPSE DATA FILE

```
-- EXAMPLE

-- Area of the pattern is
-- Grid dimensions are 800 ft by 700 ft by 250 ft in the oil reservoir
-- Grid dimensions are 800 ft by 29,365 ft by 250 ft in the entire
reservoir to account for infinite acting aquifer
-- Grid represents a 21x80x25 Cartesian model
-- production well is at the edge of the Grid
-- ouiesc + pseudo pc + hearn rel perm curve

RUNSPEC

-- Specifies the dimensions of the grid: 21x80x25
DIMENS
 21   80   25  /

-- Specifies phases present: oil, water
OIL

WATER

-- Field units to be used
FIELD

-- Specifies dimensions of saturation and PVT tables
TABDIMS
1    1   30    30    1   30 /

-- Specifies maximum number of well and groups of wells
WELLDIMS
1    30    1    1 /

-- PRESSURE modification to achieve initial quiescence (produce a true
steady state solution)
EQLOPTS
'QUIESC'                          'MOBILE'   /

-- Specifies start of simulation
START
1 'MAY' 2003   /

-- Specifies the size of the stack for Newton iterations
NSTACK
39 /

GRID
==============================================================
EQUALS

  'DX'      10    1     1     1     80    1     25    /
  'DX'      10    2     2     1     80    1     25    /
  'DX'      10    3     3     1     80    1     25    /
  'DX'      12    4     4     1     80    1     25    /
  'DX'      12    5     5     1     80    1     25    /
  'DX'      14    6     6     1     80    1     25    /
  'DX'      16    7     7     1     80    1     25    /
  'DX'      20    8     8     1     80    1     25    /
  'DX'      22    9     9     1     80    1     25    /
  'DX'      26    10    10    1     80    1     25    /
  'DX'      28    11    11    1     80    1     25    /
  'DX'      32    12    12    1     80    1     25    /
  'DX'      38    13    13    1     80    1     25    /
  'DX'      42    14    14    1     80    1     25    /
  'DX'      48    15    15    1     80    1     25    /
  'DX'      54    16    16    1     80    1     25    /
  'DX'      62    17    17    1     80    1     25    /
  'DX'      72    18    18    1     80    1     25    /
  'DX'      84    19    19    1     80    1     25    /
  'DX'      92    20    20    1     80    1     25    /
  'DX'      96    21    21    1     80    1     25    /
  'DY'      20    1     21    1     50    1     25    /
  'DY'      24    1     21    51    51    1     25    /
  'DY'      29    1     21    52    52    1     25    /
  'DY'      35    1     21    53    53    1     25    /
  'DY'      41    1     21    54    54    1     25    /
  'DY'      50    1     21    55    55    1     25    /
  'DY'      60    1     21    56    56    1     25    /
  'DY'      72    1     21    57    57    1     25    /
  'DY'      86    1     21    58    58    1     25    /
  'DY'      103   1     21    59    59    1     25    /
  'DY'      124   1     21    60    60    1     25    /
  'DY'      149   1     21    61    61    1     25    /
  'DY'      178   1     21    62    62    1     25    /
  'DY'      214   1     21    63    63    1     25    /
  'DY'      257   1     21    64    64    1     25    /
  'DY'      308   1     21    65    65    1     25    /
  'DY'      370   1     21    66    66    1     25    /
  'DY'      444   1     21    67    67    1     25    /
  'DY'      532   1     21    68    68    1     25    /
  'DY'      639   1     21    69    69    1     25    /
  'DY'      767   1     21    70    70    1     25    /
  'DY'      920   1     21    71    71    1     25    /
  'DY'      1104  1     21    72    72    1     25    /
  'DY'      1325  1     21    73    73    1     25    /
  'DY'      1590  1     21    74    74    1     25    /
  'DY'      1908  1     21    75    75    1     25    /
  'DY'      2290  1     21    76    76    1     25    /
  'DY'      2747  1     21    77    77    1     25    /
  'DY'      3297  1     21    78    78    1     25    /
  'DY'      3956  1     21    79    79    1     25    /
```

```
'DY'      4748  1     21    80    80    1     25    /
'DZ'      10    1     21    1     80    1     25    /

'PERMX'   200   1     21    1     80    1     25    /
'PERMY'   100   1     1     1     80    1     25    /
'PERMY'   200   2     21    1     80    1     25    /
'PERMZ'   10    1     1     1     80    1     25    /
'PERMZ'   20    2     21    1     80    1     25    /
'PORO'    0.145 1     1     1     80    1     25    /
'PORO'    0.29  2     21    1     80    1     25    /

'TOPS'    10000 1     21    1     1     1     1     /
'TOPS'    10007 1     21    2     2     1     1     /
'TOPS'    10014 1     21    3     3     1     1     /
'TOPS'    10021 1     21    4     4     1     1     /
'TOPS'    10027 1     21    5     5     1     1     /
'TOPS'    10034 1     21    6     6     1     1     /
'TOPS'    10041 1     21    7     7     1     1     /
'TOPS'    10048 1     21    8     8     1     1     /
'TOPS'    10055 1     21    9     9     1     1     /
'TOPS'    10062 1     21    10    10    1     1     /
'TOPS'    10068 1     21    11    11    1     1     /
'TOPS'    10075 1     21    12    12    1     1     /
'TOPS'    10082 1     21    13    13    1     1     /
'TOPS'    10089 1     21    14    14    1     1     /
'TOPS'    10096 1     21    15    15    1     1     /
'TOPS'    10103 1     21    16    16    1     1     /
'TOPS'    10109 1     21    17    17    1     1     /
'TOPS'    10116 1     21    18    18    1     1     /
'TOPS'    10123 1     21    19    19    1     1     /
'TOPS'    10130 1     21    20    20    1     1     /
'TOPS'    10137 1     21    21    21    1     1     /
'TOPS'    10144 1     21    22    22    1     1     /
'TOPS'    10150 1     21    23    23    1     1     /
'TOPS'    10157 1     21    24    24    1     1     /
'TOPS'    10164 1     21    25    25    1     1     /
'TOPS'    10171 1     21    26    26    1     1     /
'TOPS'    10178 1     21    27    27    1     1     /
'TOPS'    10185 1     21    28    28    1     1     /
'TOPS'    10192 1     21    29    29    1     1     /
'TOPS'    10198 1     21    30    30    1     1     /
'TOPS'    10205 1     21    31    31    1     1     /
'TOPS'    10212 1     21    32    32    1     1     /
'TOPS'    10219 1     21    33    33    1     1     /
'TOPS'    10226 1     21    34    34    1     1     /
'TOPS'    10233 1     21    35    35    1     1     /
'TOPS'    10239 1     21    36    36    1     1     /
'TOPS'    10246 1     21    37    37    1     1     /
'TOPS'    10253 1     21    38    38    1     1     /
'TOPS'    10260 1     21    39    39    1     1     /
'TOPS'    10267 1     21    40    40    1     1     /
'TOPS'    10274 1     21    41    41    1     1     /
'TOPS'    10280 1     21    42    42    1     1     /
'TOPS'    10287 1     21    43    43    1     1     /
```

```
  'TOPS'    10294 1     21    44    44    1     1     /
  'TOPS'    10301 1     21    45    45    1     1     /
  'TOPS'    10308 1     21    46    46    1     1     /
  'TOPS'    10315 1     21    47    47    1     1     /
  'TOPS'    10321 1     21    48    48    1     1     /
  'TOPS'    10328 1     21    49    49    1     1     /
  'TOPS'    10335 1     21    50    50    1     1     /
  'TOPS'    10343 1     21    51    51    1     1     /
  'TOPS'    10352 1     21    52    52    1     1     /
  'TOPS'    10363 1     21    53    53    1     1     /
  'TOPS'    10376 1     21    54    54    1     1     /
  'TOPS'    10391 1     21    55    55    1     1     /
  'TOPS'    10410 1     21    56    56    1     1     /
  'TOPS'    10432 1     21    57    57    1     1     /
  'TOPS'    10459 1     21    58    58    1     1     /
  'TOPS'    10492 1     21    59    59    1     1     /
  'TOPS'    10531 1     21    60    60    1     1     /
  'TOPS'    10577 1     21    61    61    1     1     /
  'TOPS'    10633 1     21    62    62    1     1     /
  'TOPS'    10700 1     21    63    63    1     1     /
  'TOPS'    10781 1     21    64    64    1     1     /
  'TOPS'    10877 1     21    65    65    1     1     /
  'TOPS'    10993 1     21    66    66    1     1     /
  'TOPS'    11132 1     21    67    67    1     1     /
  'TOPS'    11299 1     21    68    68    1     1     /
  'TOPS'    11500 1     21    69    69    1     1     /
  'TOPS'    11740 1     21    70    70    1     1     /
  'TOPS'    12028 1     21    71    71    1     1     /
  'TOPS'    12375 1     21    72    72    1     1     /
  'TOPS'    12790 1     21    73    73    1     1     /
  'TOPS'    13288 1     21    74    74    1     1     /
  'TOPS'    13887 1     21    75    75    1     1     /
  'TOPS'    14604 1     21    76    76    1     1     /
  'TOPS'    15466 1     21    77    77    1     1     /
  'TOPS'    16499 1     21    78    78    1     1     /
  'TOPS'    17740 1     21    79    79    1     1     /
  'TOPS'    19228 1     21    80    80    1     1     /
/

OLDTRAN

INIT

GRIDFILE
2 1 /

-- Specifies what is to be written in the GRID output file
RPTGRID
1 1 1 1 1 0 0 0 /

-- DEBUG
--  0 0 1 0 1 0 1  /
```

```
PROPS
==============================================================

-- Specifies water saturation tables: Water saturation, Water relative
permeability, Oil relative permeability
-- and Oil-Water capillary pressure

SWFN
--Sw  Krw         Pcow
  0.2  0          14.8375
  0.26 0.015      14.244
  0.32 0.0754     13.6505
  0.38 0.104      13.057
  0.44 0.129      12.4635
  0.5  0.149      10.0895
  0.56 0.166      7.7155
  0.62 0.179      5.3415
  0.68 0.189      2.9675
  0.74 0.196      1.7805
  0.8  0.2        0.5935
  1    0.2        0
/

SOF2
-- So       Kro
  0.2       0
  0.26      0.0180
  0.32      0.0500
  0.38      0.0950
  0.44      0.1540
  0.5       0.2290
  0.56      0.3210
  0.62      0.4320
  0.68      0.5610
  0.74      0.7110
  0.8       0.9
/

-- Specifies PVT properties of water:
PVTW
6500  1.03  3.0E-06  .54  0.0 /


-- Specifies PVT properties of the oil: Rs, pressure, Bo and oilvisc
PVDO
-- P   Bo    Uo
 5000 1.313 1.8158
 6000 1.3050      2.0005
 6500 1.3020      2.1000
 7000 1.2990      2.2027
 7500 1.2960      2.3087
 8000 1.2930      2.4179
 8500 1.2900      2.5271
 9000 1.2870      2.6362
 9500 1.2840      2.7454
 10000      1.2810      2.8530
/

RSCONST
-- Rs Pbub
  1    6000  /

-- Specifies surface densities: Oil API: 21; Water spec. gravity: 1.15;
Gas spec. gravity: 0.65

GRAVITY
  21  1.15  0.65  /

-- Specifies rock compressibility: 10E-06 psi -1 @ 6500 psia
ROCK
6500  10E-06 /


REGIONS
==============================================================

-- Specifies the number of saturation regions (only one for this case)
SATNUM
42000*1 /


SOLUTION
==============================================================

--     DATUM  DATUM    WOC    WOC    GOC    GOC    RSVD   RVVD   SOLN
--     DEPTH  PRESS   DEPTH   PCOW  DEPTH   PCOG  TABLE  TABLE   METH
EQUIL
      10000 10000  10550  0   0   0   0   0   10  /

-- Specifies parameters to be written in the SOLUTION section of the
RESTART file: pressure, water saturation
-- gas saturation and oil saturation
RPTSOL
PRESSURE  SWAT  SGAS SOIL FIP /

-- Specifies that RESTART files are to written every timestep
RPTRST
BASIC=2 /

SUMMARY    ============================================================

-- Specifies that a SUMMARY file with neat tables is to be written in
text format
RUNSUM

-- Specifies that the SUMMARY file is to be created as a separate file
in addition from the text file with neat tables
SEPARATE
```

```
-- Specifies that reports are to be written only at the timesteps
sepcified in the DATA file. Avoids reports to
-- be created at chopped timesteps (to avoid excessive data and
clutter).
RPTONLY

-- Specifies that a group of parameters specific to ECLIPSE are going
to be written in the SUMMARY files.
-- ALL

FOIP

FOPR

FOPT

FWPR

FWCT

FPR

/

WBHP
/

WBP5

/
WPI5
/

FWIP

FWPT

FGLR

FGOR

/
SCHEDULE   ==========================================================

-- Specifies what is to written to the SCHEDULE file
RPTSCHED                                    FIELD   16:55 18 APR
86
   1   0   1   0   0   0   2   0   0   0   0   2   0   0   0   0   0
   0   0   0   0   0   0   0   0   0   0   0   0   0   0   0   0   0
   0   0   0   0   0   0   0   0   0   0   0   0   0   0   0   0   /


-- Define well specifications:
```

```
WELSPECS
'P'  'G'    1  1 1*  'OIL'  /

/

COMPDAT
'P       '    1    1   1   25 'OPEN'   0  0  .25 0 0 0 Z /

/

WCONPROD
'P' 'OPEN' 'LRAT' 3* 2000 1* 5000 /
/

WELTARG
'P' BHP 5000 /
/

WECON
P  0  0  .8 /
/

TUNING
1 365  /
/
12 1 100/

TSTEP
100*20

/

END
```

VITA

Name: Kolawole Babajide Ayeni

Permanent Address: 5 Morohunmubo Close, Bodija
Ibadan, Oyo. Nigeria.

Email Address: kbayeni@yahoo.com

Education: Ph.D., Petroleum Engineering
Texas A&M University
College Station, USA, 2008.

M.S., Petroleum Engineering
University of Oklahoma
Norman, OK, USA, 2003.

B.S., Petroleum Engineering
University of Ibadan
Ibadan, Nigeria, 1997.